TITLE PAGE

1.	CONTRACT NO.:	14-08-0001-22031
2.	NAME OF CONTRACTOR:	Woodward-Clyde Consultants
3.	KEY PERSONNEL:	
	Principal Investigators:	Yoshiharu Moriwaki I. M. Idriss
4.	GOVERNMENT TECHNICAL OFFICER:	Karen M. Ward
5.	SHORT TITLE OF WORK:	Evaluation of Ground Failure Susceptibility, Opportunity, and Potential in the Urban Area of Anchorage, Alaska
6.	EFFECTIVE DATE OF CONTRACT:	May 1, 1985
7.	CONTRACT EXPIRATION DATE:	August 31, 1987
8.	AMOUNT OF CONTRACT:	$94,696
9.	DATE REPORT IS SUBMITTED:	September 1987

EVALUATION OF GROUND FAILURE SUSCEPTIBILITY, OPPORTUNITY, AND POTENTIAL IN THE URBAN AREA OF ANCHORAGE, ALASKA

FINAL TECHNICAL REPORT

SEPTEMBER 1987

By

Yoshiharu Moriwaki
I. M. Idriss
Woodward-Clyde Consultants
203 N. Golden Circle Drive
Santa Ana, California 92705

Sponsored by the
U.S. Geological Survey
Contract No. 14-08-0001-22031

TABLE OF CONTENTS

TABLE OF CONTENTS (Continued)

LIST OF TABLES

LIST OF FIGURES

LIST OF FIGURES (Continued)

ACKNOWLEDGEMENTS

We gratefully acknowledge the contributions to this study made by Dr. Randall G. Updike, Alaska Division of Geological and Geophysical Surveys, who not only provided valuable data for this study, but also reviewed a draft of this report. We also acknowledge the contributions made by the following personnel of Woodward-Clyde Consultants for performing various analyses for this study: Mohsen Beikae, Shyn-Shiun Lai, David Salom (who is associated with MARAVEN, Venezuela), and Ernesto E. Vicente. Finally, we acknowledge the typing and preparation of this report by Mrs. Hazel Boyd.

EVALUATION OF GROUND FAILURE SUSCEPTIBILITY, OPPORTUNITY, AND POTENTIAL IN THE URBAN AREA OF ANCHORAGE, ALASKA

1.0 INTRODUCTION

1.1 Objective and Approach

This study was conducted as a part of the U.S. Geological Survey's Earthquake Hazards Reduction Program. The goal of this program is a reduction of earthquake hazards through the incorporation of research findings on these hazards into land-use planning decisions. An important objective of the Earthquake Hazards Reduction Program is assessment of the potential for earthquake-induced ground failure in areas of high seismicity.

The objective of this study is to evaluate potential for earthquake-induced ground failure in the urban area of Anchorage, Alaska. Figure 1-1 shows the approximate boundary of the study area. The near-surface soils in the study area range from lightly overconsolidated clay to dense gravelly soil. The earthquake-induced ground failure is a real concern for this area because, as discussed in Section 2, many well-documented ground failures, such as slides, slumps, and cracks, were observed in this area following the 1964 Alaskan earthquake. Some of these 1964 ground failures in Anchorage are also idicated in Figure 1-1. This 1964 experience and the rapid growth of Anchorage in recent years make this type of study for Anchorage particularly appropriate.

The general approach used in the study was to evaluate the following three items: ground failure susceptibility,

ground failure opportunity, and ground failure potential. Ground failure susceptibility is the relative likelihood that a geologic material would fail and contribute to ground failure during earthquake shaking. From the 1964 experience and results of previous investigations (see Section 1.2), liquefaction and earthquake-induced translatory slides appear to be the two key modes of potential ground failure due to earthquakes in Anchorage. Ground failure opportunity depends on the seismicity of an area and the frequency of occurrence of earthquake ground motions capable of causing failure in susceptible materials. Ground failure susceptibility and ground failure opportunity need to be combined to estimate the ground failure potential of a given area.

The main product of this study is the estimated probabilities of occurrence of translatory slides within the study area and the estimated probabilities of liquefaction associated with major geological units in the study area. The ground failure opportunity data, for example, relationships between peak ground acceleration and return period within the study area, based on probabilistic seismic hazard analyses, form another useful product of the study.

1.2 Previous Investigations

In addition to many past geotechnical and geological investigations addressing relatively small areas within Anchorage, there are several previous investigations addressing larger areas of Anchorage that are closely related to this study. Results of these investigations are briefly summarized in this section.

Following the 1964 Alaska earthquake, four maps were prepared by Schmoll and Dobrovolny: Generalized Geologic

Map of Anchorage and Vicinity, Alaska (1972a); Slope Map of Anchorage and Vicinity, Alaska (1972b); Foundation and Excavation Conditions Map of Anchorage and Vicinity, Alaska (1974); and Slope-Stability Map of Anchorage and Vicinity, Alaska (Dobrovolny and Schmoll, 1974). These maps include the current study area and constitute sources of ground susceptibility data for Anchorage.

The following two recent investigations by Updike also provide sources of ground susceptibility data for Anchorage: Subsurface Structure of the Cohesive Facies of the Bootlegger Cove Formation, Southwest Anchorage, Alaska (Ulery and Updike, 1983); and Engineering Geologic Maps of the Government Hill Area, Anchorage, Alaska (Updike, 1985). There is also a report by Harding-Lawson Associates (1979) that addresses general geotechnical hazards in Anchorage.

A recent investigation for the Municipality of Anchorage by Woodward-Clyde Consultants (1986) titled "Anchorage Seismic Hazard Study" and, to some extent, its follow-up investigation on structural damages and mitigative measures (Woodward-Clyde Consultants, 1987) addressed issues similar to those addressed in this study.

Significant geotechnical data associated with downtown Anchorage are presented in a report by Shannon and Wilson (1964) following the 1964 Alaskan earthquake and in a recent report by Woodward-Clyde Consultants (1982b). These and other similar reports provided geotechnical data associated with the study area, used in this study.

1.3 Organization of the Report

Following this introductory section, Section 2 summarizes examples of ground failure in the Anchorage area observed following the 1964 Alaskan earthquake. Section 3 describes the methodology used in this study to evaluate ground failure susceptibility, opportunity, and potential. Section 4 describes the subsurface conditions in the study area with the emphasis on soils that are susceptible to earthquake-induced failures (ground failure susceptibility). Section 5 addresses the earthquake ground motion (ground failure opportunity) in the study area with an emphasis on the weighting of the results of the probabilistic seismic hazard analyses for liquefaction and for translatory slides. Sections 6 and 7 discuss potential in the study area for liquefaction and translatory slides, respectively. Section 8 presents conclusions of the study and recommendations for future studies, and Section 9 contains a list of the references cited in this report. Appendix A presents discussions on the key seismic sources for the study area, and Appendix B presents geologic cross-sections of the study area.

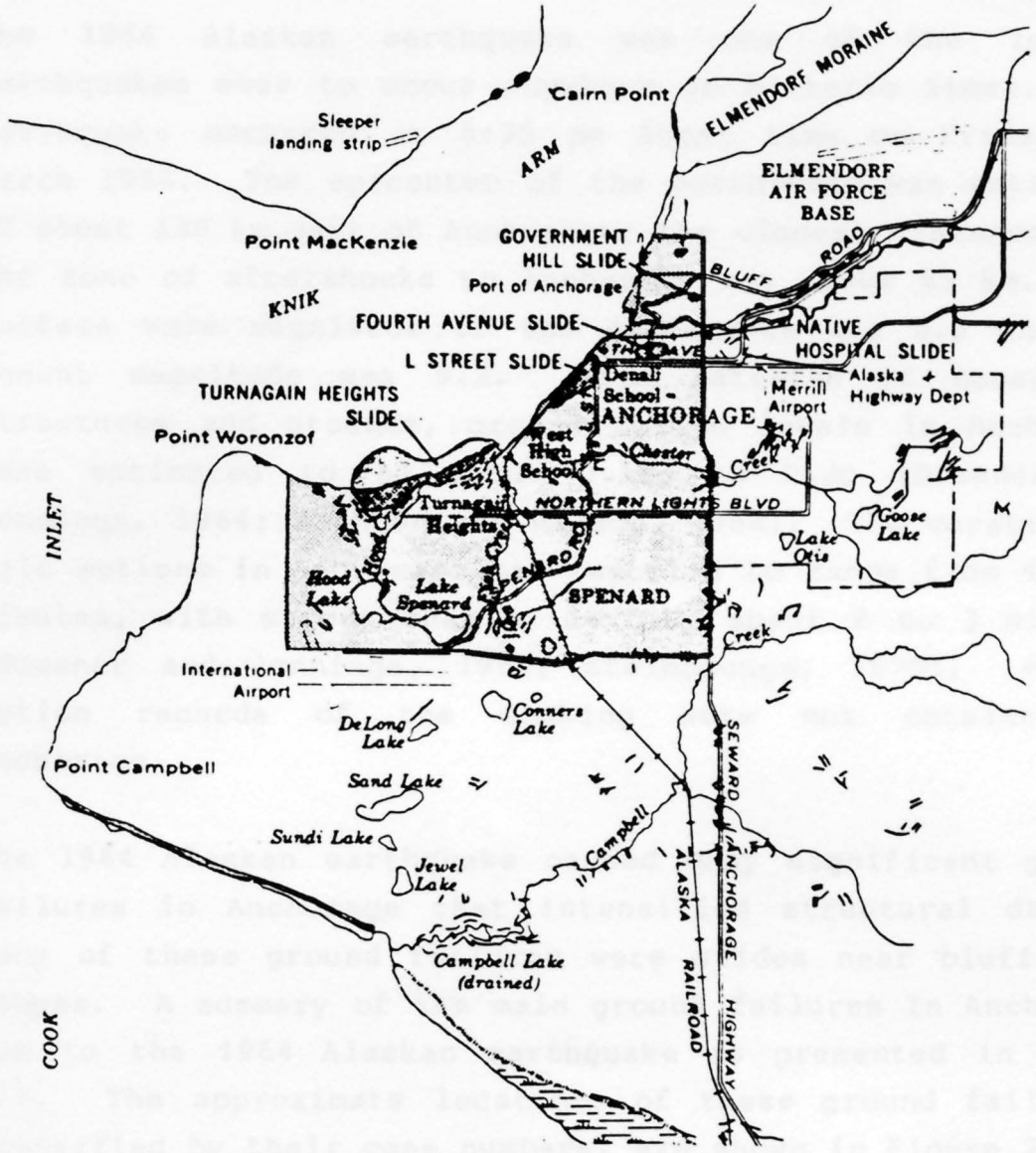

Project GROUND FAILURE POTENTIAL ANCHORAGE, ALASKA Project No. 4196A	APPROXIMATE EXTENT OF STUDY AREA	Fig. 1-1

2.0 GROUND FAILURES IN THE 1964 ALASKAN EARTHQUAKE

The 1964 Alaskan earthquake was one of the largest earthquakes ever to occur anywhere in historic times. The earthquake occurred at 5:35 pm local time on Friday, 27 March 1964. The epicenter of the earthquake was estimated at about 130 km east of Anchorage; the closest distance from the zone of aftershocks to Anchorage was about 65 km. The surface wave magnitude of the earthquake was 8.5 and the moment magnitude was 9.2. From patterns of damage to structures and grounds, ground motion levels in Anchorage were estimated to be about 0.15g to 0.2g (Housner and Jennings, 1964; Shannon and Wilson, 1964). The duration of felt motions in Anchorage was reported to range from 4 to 7 minutes, with strong shaking lasting about 2 to 3 minutes (Housner and Jennings, 1964; Steinbrugge, 1970). Strong motion records of the shaking were not obtained in Anchorage.

The 1964 Alaskan earthquake caused many significant ground failures in Anchorage that intensified structural damage. Many of these ground failures were slides near bluffs and slopes. A summary of the main ground failures in Anchorage due to the 1964 Alaskan earthquake is presented in Table 2-1. The approximate locations of these ground failures, identified by their case numbers, are shown in Figure 2-1.

Based on the data in Table 2-1, the two main modes of observed ground failures appear to be translatory slides and liquefaction. Consequences and manifestations of liquefaction are well-known, but seismically-induced translatory slides are much less known outside of Anchorage. Figure 2-2 shows a schematic illustration of a translatory slide. As can be seen from Figure 2-1,

significant parts of the study area were affected by translatory slides due to the 1964 Alaskan earthquake. Thus, translatory slides caused by earthquakes can be considered as important seismic hazards to Anchorage. On the other hand, when compared to many other cities shaken by large earthquakes, observed evidence for liquefaction under level ground, such as sand boils, was relatively limited.

From Table 2-1 and Figure 2-1, it is clear that the 1964 Alaskan earthquake caused many ground failures in Anchorage. These data indicate that topographical effects, such as the presence of bluffs, are important in evaluating the ground failure potential in Anchorage. An evaluation of potential for seismically-induced ground failures in Anchorage should reflect key features observed in these failures under actual earthquake shaking.

TABLE 2-1 - PERFORMANCE OF SLOPES AND GROUNDS DURING THE 1964 ALASKAN EARTHQUAKE IN THE ANCHORAGE AREA, ALASKA

Case No.	Name and Location	Slope or Site Characteristics	Performance During Earthquake	References
1	Slides along Turnagain Arm, from Point Campbell to Campbell Creek.	A thin cover of wind blown sand, which was probably frozen at the time of the earthquake, and slope wash loosely anchored to the steep (45° plus minus) face of the bluff by over-growth of trees, shrubs, and grasses.	A mat of entire surficial materials slumped downward without rotation a few inches to several feet along the full length (about 4 miles) of the bluff. Locally intense slumping of the shallow materials resulted in a complete exposure of the bluff face below.	Hansen (1965), Long (1973).
2	Slump along Turnagain Arm, southeast of Campbell Creek.	A thin cover of wind blown sand, which was probably frozen at the time of the earthquake, and slope wash loosely anchored to the steep (45° or less) face of the bluff by over-growth of trees, shrubs, and grasses.	Minor or incipient slumping and cracking extended along the bluff from southeast of Campbell Creek to the tracks of the Alaska Railroad near Potter.	Hansen (1965).
3	Potter Hills Slides, along Turnagain Arm, 2-1/2 miles northeast of Potter.	Steep (about 45°) bluff consisting of glacial till underlain by outwash underlain by a sequence of blue clay, silt, and fine sand; the bluff materials abutting against (and probably passing beneath) intertidal silts at the base of the bluff; the bluff saturated at its base and groundwater escaping through the outwash; evidence of ample groundwater at east of the area; history of slope instability.	The slumped area extended about 4000 feet and carried away several hundred feet of tract and right-of-way at two places along the Alaska Railroad; long and narrow fragmented slump blocks rotated backward and broke into many pieces toward the base of the slope; earth and mud flows were observed at some places along the toe; many pressure ridges were observed on the flats below the slides; the sliding was reportedly initiated by failure and flow of the material from the base of the slope; sand was reportedly ejecting from cracks near the slides.	Hansen (1965), McCulloch and Bonilla (1970), Long (1973).

Case No.	Name and Location	Slope or Site Characteristics	Performance During Earthquake	References
4	Slides at Point Woronzof, Knik Arm.	The site underlain by loose unconsolidated sand and gravel, subjected to continuous and vigorous shoreline erosion that undercuts the steep (about 45°) slopes above (the point retreating southward at a mean rate of 2 ft/year).	Three rotational slumps with lengths of about 1500 ft, 500 ft, and 200 ft occurred along the bluff; part of the slump mass disintegrated into a debris avalanche, but most slid down as intact though fractured blocks.	Hansen (1965).
5	Slides along Knik Arm, just south of Cairn Point.	At least 126 ft thick Bootlegger Cove Formation overlain by at least 110 ft thick silty till of the Elmendorf Moraine; the steep slopes (about 45°) subjected to vigorous shoreline erosion and, therefore, history of slope instability and slumping.	Several small rotational landslides mostly involving the Bootlegger Cove Formation were modified by disruption and flow. The largest slide, about 450 ft wide at the beach line, moved out at least 200 ft on to the tidal mudflat, disintegrating into many blocks, and changing into an earthflow at its toe.	Hansen (1965), Miller and Dobrovolny (1959).
6	Northwest Slide, about 1/2 mile northwest of the Government Hill slide.	This layer of outwash (up to 10 ft thick) underlain by the Bootlegger Cove Formation; evidence of history of slides.	An area about 900 ft wide (side to side) and 300 ft long (head to toe) failed in a rotational slide in the Bootlegger Cove Formation; the head dropped by about 20 ft.	Shannon and Wilson (1964).
7	Romig Hill Slide, south side of Chester Creek, about 1/2 mile east of the eastern end of the Turnagain slide.	About 25 ft of probably reworked outwash fill on 30 ft (at the toe) to 80 ft (at the head) of the Bootlegger Cove Formation underlain by dense to very dense glacial till, the slope angle being about 30°, presence of a small pre-earthquake hammock feature at the toe suggestive of pre-earthquake slide perhaps at the time of the "fill placement."	An area about 350 ft wide and 300 ft long moved downward on the order of 2 ft.	Shannon and Wilson (1964), Long (1973).
8	Slide at Third Avenue and Post Road.	Outwash over the Bootlegger Cove Formation, slope edge loaded with the highway embankment; the slide located within a bowl indicative of past slide.	A rotational slump.	Long (1973).

Case No.	Name and Location	Slope or Site Characteristics	Performance During Earthquake	References
9	Slides along the south facing bluff line of Ship Creek between Bluff Road and the tracks of the Alaska Railroad.	Steep (about 45°) bluff about 60 ft high consisting of about 50 ft of outwash underlain by the Bootlegger Cove Formation.	About 1300 ft of bluff gave way in four separate but related slumps involving compound rotational slides of fragmented blocks; the head of the slumps extended back horizontally into the bluff as much as 120 ft; an additional 400 ft of bluff line east and west of the main slide mass cracked and started to slump. At the toe all four slumps bulged out into a chaotic lake of jumbled blocks. Each slump had a length of about 300 ft from crown to toe and passed through the Bootlegger Cove Formation.	Hansen (1965).
10	Fourth Avenue Slide-Downtown Anchorage, approximately between First Avenue and Fourth Avenue and between E Street and Barrow Street.	Relatively dense outwash sand and gravel, ranging 30 to 40 ft thick, underlain by the Bootlegger Cove Formation consisting of upper 20 to 30 ft zone of relatively dense sands and overconsolidated clays and lower zone of lightly overconsolidated clays; the lower zone having pockets of highly sensitive clays and silts, the general geomorphology of the area indicative of history of similar slides.	The slide involved all or part of 14 city blocks in a roughly oval area of about 36 acres. The slide was primarily translatory toward the bluff along Ship Creek. The movement of the slide created one graben west of C Street and two grabens east of C Street. The post-earthquake survey suggested that by the end of the earthquake, another graben had begun to form between Fourth and Fifth Avenues at D and E Streets. Many cracks were observed behind the grabens. Within the grabens that did form, vertical movements of up to 10 feet were measured. Horizontal movements during the slide were measured to be as great as about 19 ft in the soil mass between the bluff and the first graben, as great as about 11 ft between the first and second graben, and generally less than 9 inches behind the second graben. Based on the post-earthquake	Hansen (1965), Shannon and Wilson (1964), WCC (1982b).

Case No.	Name and Location	Slope or Site Characteristics	Performance During Earthquake	References
10 (cont)			investigations, the zone of shearing appears to have been at elevation of about 40 to 50 ft, at or near the interface between a fine sand layer and a lightly overconsolidated clay layer underlying it.	
11	L Street Slide-northwest part of Anchorage, adjacent to Knik Arm.	Relatively dense outwash sand gravel, about 30 ft thick, underlain by the Bootlegger Cove Formation consisting of upper 20 to 30 ft zone of relatively dense sands and overconsolidated clays and lower zone of lightly overconsolidated clays; the lower zone having pockets of highly sensitive clays and silts, the general geomorphology of the area indicative of history of similar slides.	The slide was a translatory slide involving a relatively horizontal, outward movement of a soil block toward the bluff with a graben forming behind the soil block. The slide extended about 4000 ft along the bluff, the width (from the bluff to the graben) of the soil block varied from less than 50 ft to about 250 ft, and the distance between the toe (as represented by the pressure ridges) of the slide to the back of the graben measured as much as about 1200 ft. The maximum measured horizontal displacement of the soil block was about 14 ft toward the bluff (northwest). Relatively few cracks were noted outside the graben. Apparently, there was very little change in elevation within the slide block. Structures on the slide block, thus, suffered little damage from the slide movements. However, the graben areas vertically dropped by as much as about 10 ft. Many buildings and utilities in and along the edge of the graben, thus, were heavily damaged. The shear surface of the slide was probably about 60 to 70 ft from the ground surface.	Hansen (1965), Shannon and Wilson (1964), WCC (1985).

Case No.	Name and Location	Slope or Site Characteristics	Performance During Earthquake	References
12	Native Hospital, or First Avenue, Slide.	Outwash, 40 to 55 ft thick, underlain by the Bootlegger Cove Formation; likely excavation of the slope sometime after 1916; evidence of past multiple slides.	A translatory slide, covering slightly more than 4 acres, was about 650 ft across from flank to flank, and about 350 ft from head to toe. The graben was exceptionally large for the size of the slide; it was about 600 ft long, about 120 ft wide on the average, and about 20 ft deep on the average. The slide moved outward, and tension cracks opened in a fanlike arrangement at the periphery. A large shallow-rooted pressure ridge was about 500 ft long, about 15 ft high, and 40 to 50 ft wide. Lateral slippage of about 17 to 25 ft was estimated at a depth of perhaps 85 to 95 ft or 25 to 35 ft above sea level within the Bootlegger Cove Formation.	Hansen (1965), Shannon and Wilson (1964).
13	Government Hill Slide. South-facing bluff on the north side of Ship Creek.	Outwash, 40 to 55 ft thick, underlain by the Bootlegger Cove Formation; likely excavation of the slope sometime after 1916.	Complex translatory slides occurred involving three somewhat concentric grabens and about 11 acres of land. From flank to flank the slides had a width of 1180 ft; the length from head to toe, in the direction of the slippage was about 600 ft; the head of the slide regressed about 400 ft behind the prequake bluff line. Each graben was about 100 ft across; the outer grabens were deepest, more than 20 ft, the medial graben was 14 to 16 ft deep, and the inner graben average 12 to 14 ft deep. Lataral displacements varied greatly up to about 35 ft southwestward; the toe moved as much as 150 ft, but it was partly by flowage.	Hansen (1965), Shannon and Wilson (1964).

Case No.	Name and Location	Slope or Site Characteristics	Performance During Earthquake	References
14	Turnagain Heights Slide.	Outwash sand of varying thickness (about 20 ft thick at the east end tapering to near zero at the west end) overlying the Bootlegger Cove Formation.	About 130 acres were completely devastated by displacements that broke the ground into countless deranged blocks, collapsed and tilted at all odd angles. The slide extended east-west along the bluff line about 8600 ft; its maximum headward retrogression was about 1200 ft. Maximum lateral slippage exceeded 2000 ft. The ground surface behind the prequake bluff line was lowered by an average of about 35 ft. It was a slide composed of two lobes that merged: West and East Turnagain lobes, each removing about 4300 ft of bluff line. Ground cracking behind the slide was extensive particularly for the East lobe. The depth of probable failure was 15 to 20 ft above sea level or about 60 to 70 ft from the ground surface within the Bootlegger Cove Formation. Translatory motion under gravity was envisioned as the primary mechanism of landsliding.	Hansen (1965), Shannon and Wilson (1974), Seed and Wilson (1967)
15	Ground cracks at various locations shown on the map.	Border areas between natural soils and man-made earthfills.	Ground cracks probably due to differential settlements.	Hansen (1965).
16	Earth Dam impounding Campbell Lake water.		Failure of dam and squirting of muddy water through cracks.	Hansen (1965).

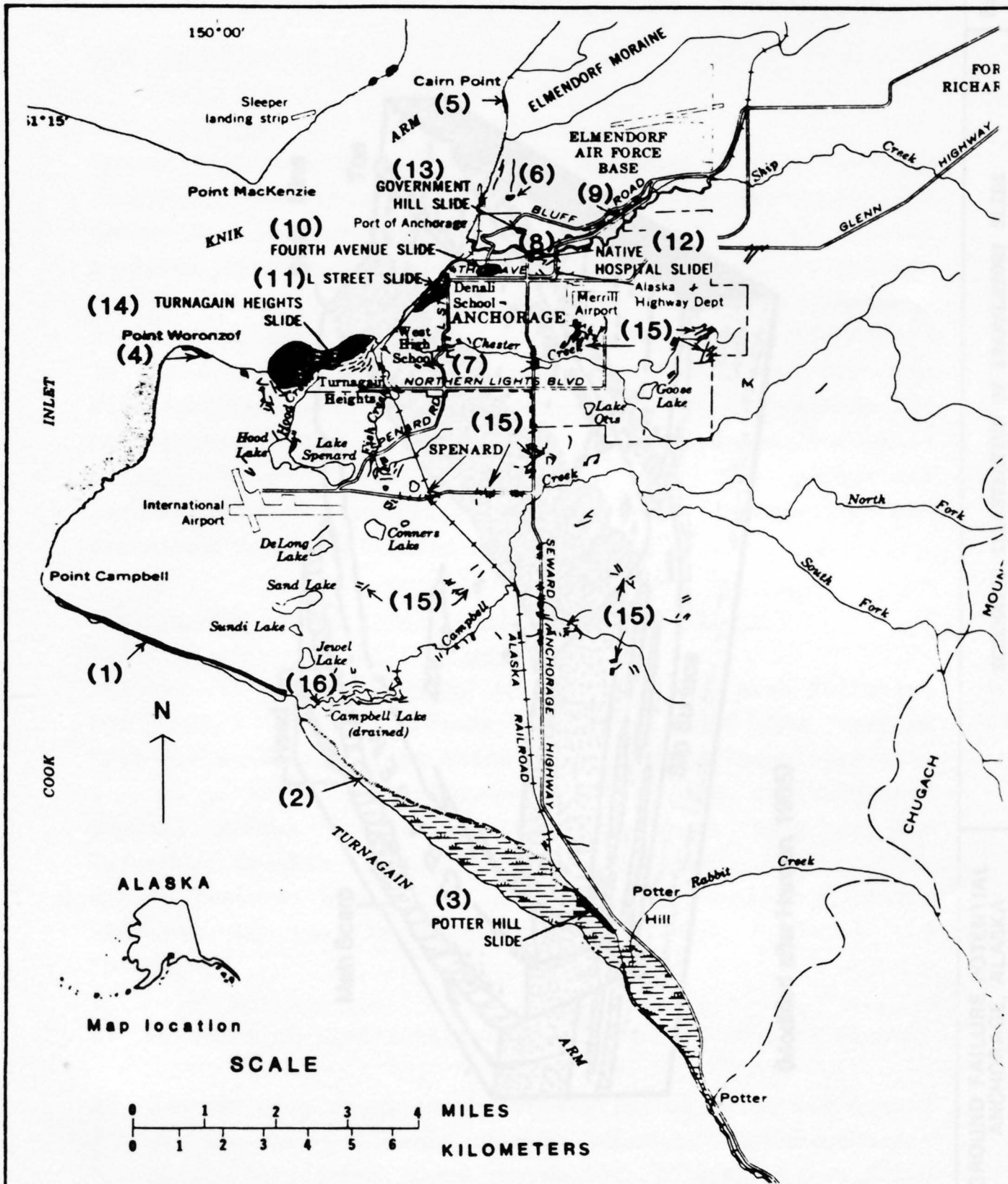

Numbers in parentheses shown above correspond to case numbers used in Table 2-1.

Project GROUND FAILURE POTENTIAL ANCHORAGE, ALASKA Project No. 41966A	GROUND FAILURES IN ANCHORAGE DUE TO 1964 EARTHQUAKE	Fig. 2-1

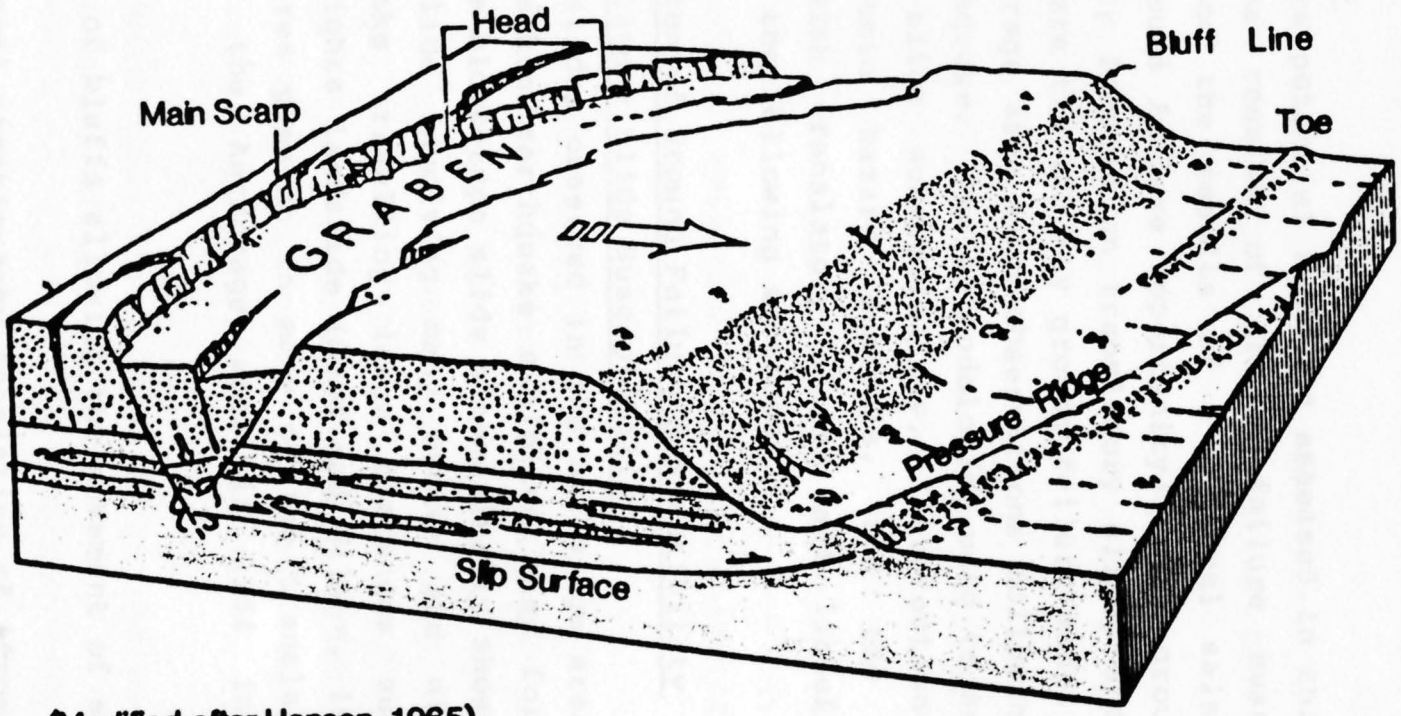

(Modified after Hansen, 1965)

Project: Project No.	GROUND FAILURE POTENTIAL ANCHORAGE, ALASKA 41966A	SCHEMATIC ILLUSTRATION OF TRANSLATORY SLIDE	Fig. 2-2

3.0 METHODOLOGY

3.1 Overview

Ground failure potential has been assessed in this study by combining the results of ground failure susceptibility evaluation and the results of a regional seismic hazard analyses (ground failure opportunity). The ground failure susceptibility focused on translatory slides and liquefaction, which are the two key ground failure modes identified in the Anchorage area from observations following the 1964 Alaskan earthquake. The methodologies used to evaluate the translatory slide susceptibility, liquefaction susceptibility, seismic hazard analysis, and the potentials associated with translatory slides and liquefaction are described in the following sections.

3.2 Evaluation of Ground Failure Susceptibility

3.2.1 Translatory Slide Susceptibility

Translatory slides observed in the Anchorage area following the 1964 Alaskan earthquake exhibited many forms ranging from a single block-type slide schematically shown in Figure 2-2 to a slide involving many broken and disintegrated sliding blocks travelling large distances such as the Turnagain Heights landslide (Seed and Wilson, 1967). Some common features present in many of the translatory slides observed in the Anchorage area in 1964 included the following:

1. Presence of bluffs allowing the movement of soil blocks.

2. General soil stratigraphy consisting of (from the ground surface down) a dense outwash deposit, an overconsolidated Bootlegger Cove formation (clays, sands, and silts), and a slightly overconsolidated Bootlegger Cove

formation (mainly clay with thin layers and lenses of sands and silts).

3. Inferred location of the 1964 slide plane being near the top of the slightly overconsolidated Bootlegger Cove formation.

4. Inferred orientation of the 1964 slide plane being near horizontal.

5. Topographical evidence of similar past slides in the general area.

On the basis of the above observations, areas exhibiting a number of the above features were evaluated and designated in this study as potential areas of seismically-induced ground failure by translatory slide.

3.2.2 Liquefaction Susceptibility

Factors affecting the susceptibility of sandy soil deposits to liquefaction have been addressed in many previous investigations (eg, Seed and Lee, 1966; Seed, 1968; Castro and Poulos, 1977; Seed, 1979). In this study the relative likelihood that a geologic unit consisting of sandy soils would liquefy and contribute to ground failure during seismic shaking was evaluated based on the following:

1. The Standard Penetration Test (SPT) resistance N from available soil borings.

2. The depth of ground water.

3. The age and mode of deposition of the sediments.

As discussed in Section 4.4, the SPT resistance values were corrected for the effect of confining pressure and energy loss in the drive rods (Seed and Idriss, 1982). Because the description of drilling procedures and the presence of fines in each sample were generally incomplete or unavailable, systematic corrections to account for these factors (Seed, et al, 1985) were not applied.

Because the number of SPT data considered to be useable after collection and evaluation was not large, it was decided not to identify different sub-areas within the study area for the evaluation of liquefaction potential. Rather, the selected SPT data were classified according to different general geological units, and the liquefaction potential was evaluated for each set of data, assuming that it was representative of the geological unit.

3.3 Evaluation of Ground Failure Opportunity

The ground failure opportunity was evaluated in this study using a probabilistic seismic hazard analysis. Seismic hazard in this study is defined as the level of peak ground acceleration for a selected value of return period (to be defined later in this section). Seismic hazard at a given site is dependent on the locations and characteristics of the seismic sources of the region and the attenuation of ground motions from the sources to the site. A schematic diagram of a model for probabilistic seismic hazard evaluation is shown in Figure 3-1.

The method for the probabilistic seismic hazard analysis used in this study is described elsewhere (Kulkarni et al, 1979). The method involves obtaining, through a formal mathematical process, the level of a ground motion parameter (eg, acceleration, velocity, spectral ordinates, etc.) that

has a selected probability of being exceeded during a specified time interval. Typically, the annual probability of this level of the ground motion parameter being exceeded is calculated. The inverse of this annual probability is called return period in years. Once the annual probability is obtained, the probability of the level of the ground motion parameter being exceeded over a specified time period can be readily calculated by the following equation:

$$P = 1 - \exp(-\lambda t) \qquad (3\text{-}1)$$

in which P is the probability of the level of the ground motion parameter being exceeded in t years and λ is the annual probability of being exceeded.

The elements of the probabilistic seismic hazard analysis are the following:

1. Defining the location and geometry of earthquake sources relative to the site.

2. Estimating the recurrence of earthquakes of various magnitudes, up to the maximum magnitude, on each source.

3. Selecting an attenuation relationship relating the variation of the ground motion parameter (eg, acceleration, etc.) with distance and magnitude.

A probabilistic seismic hazard evaluation at a site due to a particular source involves convoluting the following three probability functions (eg, Cornell, 1968; Shah et al, 1975; McGuire, 1976; Der-Kiureghian and Ang, 1977; Kulkarni et al, 1979):

1. The probability that an earthquake of a particular magnitude will occur on the source during a specified time interval is calculated using the recurrence rate. This probability function is usually expressed in terms of the mean number of earthquakes, per year, with a given magnitude on this source.

2. The probability that the rupture surface is at a specified distance from the site is assessed by considering both fault geometry and the rupture length (or area) magnitude relationship.

3. The probability that the ground motion parameter from an earthquake of a certain magnitude occurring at a certain distance will exceed a specified level at the site is based on the selected attenuation relationship.

By combining the three probability functions for each source, the annual probability of exceeding a specified level of the ground motion parameter at the site is computed. If there are N sources, then the above process is repeated for each source, and the contributions are added to obtain the total seismic hazard at the site. A relationship between the levels of the ground motion parameter and probability of exceedance is obtained by repeating the computations for several levels of the ground motion parameter. The level corresponding to a specified probability of being exceeded (or return period) is then obtained from the relationship. As stated earlier, the results of the probabilistic seismic hazard analysis are expressed in this study in terms of peak ground acceleration versus return period.

3.4 Evaluation of Ground Failure Potential

The ground failure susceptibility (Section 3.2) and the ground failure opportunity (Section 3.3) are combined to evaluate the ground failure potential. In evaluating the potential for translatory slides and for liquefaction, relationships between the peak ground acceleration and return period developed as described in Section 3.3 should be modified to incorporate the effects of various magnitudes (or durations) first. Next, relationships between peak ground acceleration and the amount of translatory slide movement (or the probability of liquefaction) need to be developed. The relationships between the amount of translatory slide movement (or the probability of liquefaction) and return period can then be developed by combining these two relationships.

3.4.1 Incorporation of Magnitude Contribution for Evaluating Ground Failure Potential

In a typical probabilistic seismic hazard evaluation, equal weights are assigned to all magnitude earthquakes. However, different magnitudes contribute differently at various levels of ground shaking. Different magnitudes can produce identical levels of shaking, but in general the smaller the magnitude the shorter is the duration. Duration has a significant influence on the potential for translatory slide and liquefaction due to earthquake loading conditions. Therefore, it is important that the difference in duration for various magnitude earthquakes be accounted for when the results are to be used for evaluating the potential for ground failure. The simplest and most direct way to accomplish this is to use a weighting scheme that implicitly incorporates the duration of various magnitude earthquakes. Magnitude weighting factors for translatory slide and liquefaction are discussed below. Because magnitude

weighting factors for liquefaction have been in use for some time (Idriss, 1985), they are discussed first.

3.4.1.1 Magnitude Weighting Factors for Evaluating Liquefaction Potential

By correlating the number of cycles to cause liquefaction in sands and silty sands and the estimated average number of cycles associated with various magnitude earthquakes, Seed and Idriss (1982) and Seed et al (1983) developed the following tabulation:

Earthquake Magnitude	Cyclic Stress Ratio Required To Cause Liquefaction Relative To That For m = 7.5
8.5	0.89
7.5	1.00
6.75	1.13
6	1.32
5.25	1.50

The cyclic stress ratio required to cause liquefaction in the above listing is based on: (a) calculating the number of equivalent stress cycles from recorded accelerograms using 0.65 times the peak value to represent an equivalent uniform stress; and (b) normalizing the cyclic test results with respect to 15 cycles, which is considered representative of magnitude 7.5. The choice of m = 7.5 was made because the majority of field data regarding liquefaction of sands and silty sands is for m = about 7.5.

The above tabulation indicates, for example, that the stress level from a magnitude 6 earthquake must be about 32 percent higher than that from a magnitude 7.5 earthquake in order to induce liquefaction in both cases. Since stress is directly

proportional to acceleration, the same ratio can be applied to peak acceleration. Therefore, the inverse of this ratio is representative of the weight of peak acceleration due to magnitude 7.5 earthquake. That is, the weight of m = 6 is 1/1.32 = 0.758 relative to m = 7.5. Similarly, the weight of m = 8.5 is 1/0.89 = 1.124 relative to m = 7.5.

These Magnitude Weighting Factors (MWF), relative to m = 7.5, can be reasonably represented by the following equation (Idriss, 1985):

$$MWF = 0.075\ m^{1.285} \qquad (3\text{-}2)$$

Magnitude weighting factors weighted with respect to other magnitudes can be readily derived by dividing Equation 3-2 by the MWF for that magnitude.

To include these weighting factors directly in the probabilistic seismic hazard analysis discussed in Section 3.3, the attenuation relationship relating the variation of the peak ground acceleration with distance and magnitude is multiplied by Equation 3-2. All the other steps in the analysis remain the same.

3.4.1.2 Magnitude Weighting Factors for Evaluating Potential for Translatory Slides

Magnitude weighting factors were developed in this study for assessing the opportunity and potential for seismically-induced slides. The simplified relationships relating the seismically-induced displacement to the ratio of seismic yield coefficient to peak seismic coefficient (Makdisi and Seed, 1978; Hynes-Griffin and Franklin, 1984) were used for developing this magnitude-weighting scheme. Selected results of the assessment are presented in Section 6.1. The basic methodology is described below.

Previous investigations (eg, Woodward-Clyde Consultants, 1982b, 1985; Idriss, 1985) have shown that at least some of the translatory slides observed in Anchorage due to the 1964 Alaskan earthquake can be evaluated using the Newmark approach (Newmark, 1965). In the Newmark approach, a seismic coefficient k_y, called the yield seismic coefficient and expressed in g's, is computed for a potential slide mass using a series of pseudo-static analyses. The k_y corresponds to a seismic coefficient that results in the computed factor of safety of one. Thus, for seismic coefficient values larger than k_y, a potential slide mass will start to move.

Following the Newmark method, simplified relationships between seismically-induced permanent displacement and k_y/k_{max} for various earthquake magnitudes were developed by various researchers (eg, Makdisi and Seed, 1978; Hynes-Griffin and Franklin, 1984). The k_{max} is the peak seismic coefficient (expressed in g's) acting on the potential slide mass. An example of these relationships by Makdisi and Seed (1978) is shown in Figure 3-2a.

Magnitude weighting factors for the Newmark-type seismically-induced displacement can be obtained from these relationships using a procedure shown in Figure 3-2b and summarized as follows:

1. Select a displacement level (eg, 15 cm in Figure 3-2a).

2. Select consistent values from the available relationships between the displacement and k_y/k_{max} (eg, the lower-bound values in the ranges shown in Figure 3-2a).

3. Tabulate the resulting k_y/k_{max} values for each magnitude.

4. Divide each k_y/k_{max} value by the pre-selected reference k_y/k_{max} designated as $(k_y/k_{max})_{ref}$. The resulting $(k_y/k_{max})/(k_y/k_{max})_{ref}$ values are the magnitude weighting factors for the selected displacement value (eg, in Figures 3-2b $(k_y/k_{max})/(k_y/k_{max})_{ref}$ as the magnitude weighting factors with respect to magnitude 8-1/4 for displacement of 15 cm corresponding to the lower-bounds of the Makdisi and Seed simplified relationships).

These magnitude weighting factors can be used in the probabilistic seismic hazard analysis in exactly the same manner as that discussed for the magnitude weighting factors for liquefaction (Section 3.4.1.1). It should be noted, however, that these weighting factors depend on the selected values of seismically-induced displacement, the selected relationships between the displacement and k_y/k_{max}, and the particular value selected within the ranges in the relationships (eg, lower-bound, upper-bound, etc.). The sensitivity of the magnitude weighting factors to these parameters are discussed in Section 6.1.

3.4.2 Evaluation of Potential for Translatory Slide

The potential for translatory slide in this report is defined by a relationship between the seismically-induced displacement of a slide block and return period for a site of potential translatory slide. This relationship can be obtained from two probabilities: the probability that a level of peak ground acceleration due to earthquakes with a selected magnitude will occur for a specified return period; and the probability that, given that this level of peak

ground acceleration has occurred, it will cause various movements of a potential sliding block at a site. The first probability is discussed in Sections 3.3 and 3.4.1. For simplicity, the second probability is treated in this study as a deterministic relationship between displacement and peak ground acceleration as discussed below.

This deterministic relationship can be developed by computing the seismically-induced displacement of a potential sliding block for various values of peak ground acceleration corresponding to earthquakes of a fixed magnitude (Woodward-Clyde Consultants, 1982b, 1985, 1987; Idriss, 1985).

In Figure 3-3, the soil block shown is assumed to be rigid. Note that in Figure 3-3 when the ground is shaking in the direction away from the bluff, the soil block is free to move in the direction of the bluff as long as the active soil force plus the inertia force on the soil block is greater than the resisting force at the bottom of the soil block.

The active soil force, due to the presence of a graben, in Figure 3-3 is computed as follows:

$$F_{da} = \frac{1}{2} \gamma_t H^2 k_a \qquad (3\text{-}3)$$

where

γ_t = total unit weight of soil
H = height of the soil block
k_a = active soil pressure coefficient (0.33 was used in this study)

As summarized in Figure 3-3, the inertia force on the soil block can be calculated by multiplying the total weight of the soil block by the peak seismic coefficient, k_{max}. In this study, k_{max} is assumed to be equal to the peak ground acceleration.

The resisting force due to soil shear strength acting at the bottom of the soil block in Figure 3-3 can be computed by multiplying the length of the soil block by the average undrained shear strength of the soils involved. As discussed later, the average undrained shear strength of the soil depends on the level and length of shaking and the amount of displacement the soil block has undergone.

Using these three forces, the yield seismic coefficient is calculated as follows:

$$k_y = \frac{F_{rs} - F_{da}}{W} \qquad (3\text{-}4)$$

where

F_{rs} = resisting force due to soil shear strength
F_{da} = driving force due to active soil pressure
W = weight of soil block

Thus, the yield seismic coefficient is that seismic coefficient which, when multiplied by the total weight of the block, gives large enough driving force due to earthquake inertia to make the total driving force equal to the total resisting force.

As discussed in Section 3.4.1.2, once the yield seismic coefficient (k_y) and the maximum seismic coefficient (k_{max})

are known, the displacement of the soil block can be calculated. Makdisi and Seed (1978) have graphically summarized the amount of expected displacement versus k_y/k_{max} for various magnitude earthquakes (Figure 3-2a). Thus, using this graphical summary, it is possible to estimate seismically-induced displacements of a soil block if an earthquake magnitude and k_y/k_{max} are known.

However, the results by Makdisi and Seed cover only up to magnitude 8-1/4 earthquakes. Because it is desirable to utilize in this study the translatory slide data in Anchorage obtained from the 1964 Alaskan earthquake, a moment magnitude 9.2 event, the results of Makdisi and Seed were extrapolated (Woodward-Clyde Consultants, 1982b) to 9 plus earthquakes and expressed as displacement per number of cycles. The resulting relationship is shown in Figure 3-4. Further, based on the relationship between the number of equivalent cycles (NC) and magnitude m presented by Seed and Idriss (1982), the following equation can be obtained by curve fitting and slight extrapolation:

$$NC = 0.24\ e^{0.55m} \qquad (3\text{-}5)$$

The procedure then involves the following steps:

1. Calculate the weight of the soil block and the active force using the given geometry and the unit weight of soils;

2. Calculate the resisting force by multiplying the appropriate undrained shear strength by the length of the soil block;

3. Select a value of the peak seismic coefficient (k_{max});

4. Calculate the yield seismic coefficient (k_y); and

5. Calculate displacement for the number of cycles corresponding to the magnitude of interest (eg, a magnitude of 9.2) using Figure 3-4, Equation 3-5, and a k_y/k_{max} value obtained from Steps 3 and 4.

In calculating the yield seismic coefficient, the value of undrained shear strength used varies depending on the level and length of shaking and the current displacement of the soil block. This is summarized in Figure 3-5. Figure 3-5 reflects the fact that the initial undrained shear strength can change due to cyclic shear strains induced by earthquake loading and/or due to large displacements due to slide movements.

The results of the post-cyclic undrained shear tests, the residual undrained shear strength evaluation, and the lateral deformations in 1964 in the Anchorage area provided the means to construct a relationship between undrained shear strength at the sliding plane and lateral movement at the ground surface shown in Figure 3-5. The entire Anchorage area was subjected to ground shaking during the earthquake. The results of cyclic loading tests on the slightly overconsolidated Bootlegger Cove clay indicated that the maximum reduction in shear strength due to cyclic loading for this clay is about 30 percent (Woodward-Clyde Consultants, 1982b). Therefore, any reduction in undrained shear strength due to shaking alone cannot be any greater than about 30 percent from the peak undrained shear strength. Available data on ground movements due to the 1964 Alaskan earthquake in the Anchorage area (eg, Shannon

and Wilson, 1964) indicated that the amount of lateral movements in Anchorage was, in general, either several feet or less than a few inches (about 1/2 foot or less). Hence, it would seem reasonable to assume that in those areas where the lateral displacement was up to about 1/2 foot, any undrained shear strength reduction was due mainly to earthquake shaking. Thus for lateral displacements of about 1/2 foot, the undrained shear strength should be at least 70 percent of the peak strength. For large lateral displacements of the order of several (or more) feet, the undrained residual strength will be reached. The results of miniature vane tests, direct shear tests, and cone penetration tests indicate that, at these large displacements, the undrained shear strength would be about 30 percent of the peak undrained shear strength (Woodward-Clyde Consultants, 1982b).

3.4.3 Evaluation of Potential for Liquefaction

The liquefaction potential in this report is defined by the probability of liquefaction occurring at a site in a given geological unit in a given time period.

The liquefaction potential is a function of both the opportunity for liquefaction--the occurrence of strong ground shaking (expressed as peak ground acceleration associated with a selected magnitude)--and the susceptibility of the soils to undergo liquefaction due to ground shaking. Liquefaction potential is thus directly related to the seismic hazard at the site and to the characteristics and ground water conditions of the underlying soil deposit.

Thus, the potential for liquefaction is a function of two probabilities: the probability that a level of peak ground

acceleration associated with a selected magnitude event will occur for a specified return period; and the probability that, given that this level of peak ground acceleration has occurred, it will cause liquefaction at the site in a given geological unit. The potential for liquefaction is obtained by convoluting these two probabilities. The first probability is discussed in Sections 3.3 and 3.4.1. A procedure to obtain the second probability is similar to that used in a previous study (Woodward-Clyde Consultants, 1986) and is discussed below.

This second probability can be expressed as follows:

$$P(L|z_k(m_o)) = \sum_{\ell} P(N_{1\ell}) \cdot P(L|z_k(m_o), N_{1\ell}) \qquad (3\text{-}6)$$

where

$P(L|z_k(m_o))$ = Probability that, given a peak ground surface acceleration of z_k weighted with respect to a magnitude m_o is observed at the site, liquefaction occurs.

$P(N_{1\ell})$ = Probability that the soil deposit of interest has a particular value of blow count $N_{1\ell}$.

$P(L\ z_k(m_o), N_{1\ell})$ = Probability to be discussed later.

When K values of $N_{1\ell}$ (ℓ = 1 to K, ie, a total of K SPT blow count data) are available for a soil deposit, the term $P(N_{1\ell})$ can be evaluated using at least two procedures. The first procedure is to use individual data point and assign the same probability to each data point, ie, $P(N_{1\ell}) = 1/k$. This approach was selected for use in this study.

Another approach is to use a single representative value of $N_{1\ell}$ for a given geologic unit at a given site. Methods for selecting this representative $N_{1\ell}$ value were discussed in a previous study (Woodward-Clyde Consultants, 1986).

The term $p(L \mid z_k(m_o), N_{1\ell})$ is obtained from the Seed and Idriss criteria as discussed in the following paragraphs.

The cyclic stress ratio in the soil deposit is related to the peak ground acceleration using the expression (Seed and Idriss, 1971):

$$\frac{\tau}{\sigma'_v} = 0.65 \frac{a_{max}}{g} \frac{\sigma_v}{\sigma'_v} r_d \qquad (3\text{-}7)$$

where:

τ = average cyclic shear stress induced at some depth in the soil deposit by the earthquake ground motion

σ_v = total soil overburden pressure at some depth in the soil deposit

σ'_v = effective soil overburden pressure at some depth in the soil deposit

a_{max} = peak ground acceleration (g's)

g = acceleration of gravity

r_d = depth-dependent reduction factor to account for the deformable nature of soil

0.65 = a factor to obtain the average shear stress, τ, from the maximum shear stress, τ_{max}

The quantification of σ_v' and the ratio σ_v/σ_v' depends on the depth to ground water and the depth to the soil layer for which liquefaction potential is being assessed. Uncertainty in Equation 3-7 was not included in the present analysis.

The liquefaction criteria curves presented in Figure 3-6 represent boundary lines between sites where liquefaction may occur and where liquefaction is not likely to occur as a function of earthquake magnitude, induced cyclic stress ratio (derived from peak acceleration by Equation 3-7) and $N_{1\ell}$ value for the soil deposit. These curves were empirically located by defining the boundary between where liquefaction was observed and was not observed in past earthquakes. In reality, there is uncertainty in the position of the curves as the observational data show: not all sites which fall above the curve experienced liquefaction and a few sites which fall below the curve did experience liquefaction.

The uncertainty in the level of cyclic stress ratio required to cause liquefaction was included in the analysis by defining a probability distribution for the stress ratio at which significant liquefaction would occur in a soil deposit with a specified N_1 value and for a given magnitude earthquake. This distribution was developed by quantifying the engineering judgement of Professor H. B. Seed in a previous study (Woodward-Clyde Consultants, 1986). The resulting probabilistic liquefaction criteria were termed

"modified Seed and Idriss criteria" to distinguish them from the original published Seed and Idriss chart such as the one shown in Figure 3-6.

The median or 50th percentile line for the probability that a given cyclic stress ratio would cause liquefaction during a magnitude 7.5 earthquake from these criteria is shown in Figure 3-7 with a standard deviation of the natural log of stress ratio equal to 0.17. The distribution about the median is lognormal, and the 16th and 84th probability levels as well as the Seed and Idriss original criterion curve for magnitude 7.5 separating sites with and without liquefaction are also shown in Figure 3-7. As can be seen, the Seed and Idriss original criterion curve is essentially coincident with the 16th percentile level of the defined distribution.

Thus, as long as the result of probabilistic seismic hazard analysis weighted with respect to magnitude 7-1/2 are available, the conditional probability function $p(L|z_k(m_o),N_1\ell)$ can be directly evaluated from Figure 3-7 for a given peak acceleration and N_1 blow count with the aid of Equation 3-7. The characterizations of N_1 for the study area are discussed in Section 4.4.

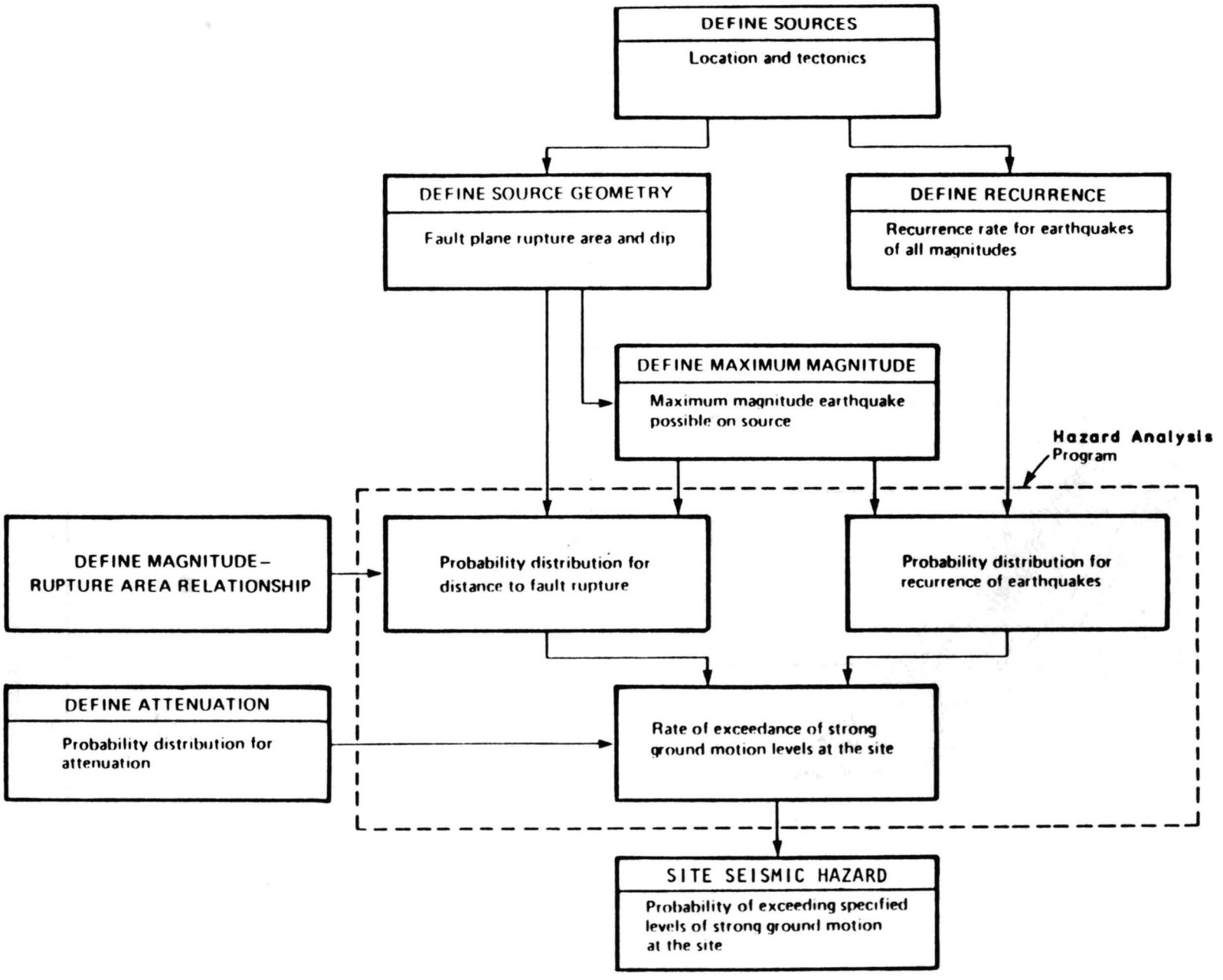

Project: GROUND FAILURE POTENTIAL ANCHORAGE, ALASKA Project No. 41966A	SCHEMATIC DIAGRAM OF MODEL FOR PROBABILISTIC SEISMIC HAZARD EVALUATION	Fig. 3-1

(a) Simplified Displacement Relationship (after Makdisi and Seed, 1978)

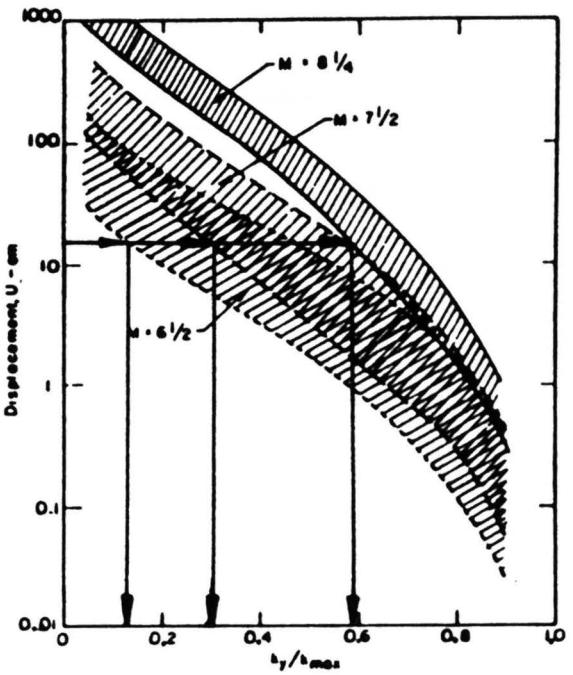

(b) Magnitude Weighting Factors

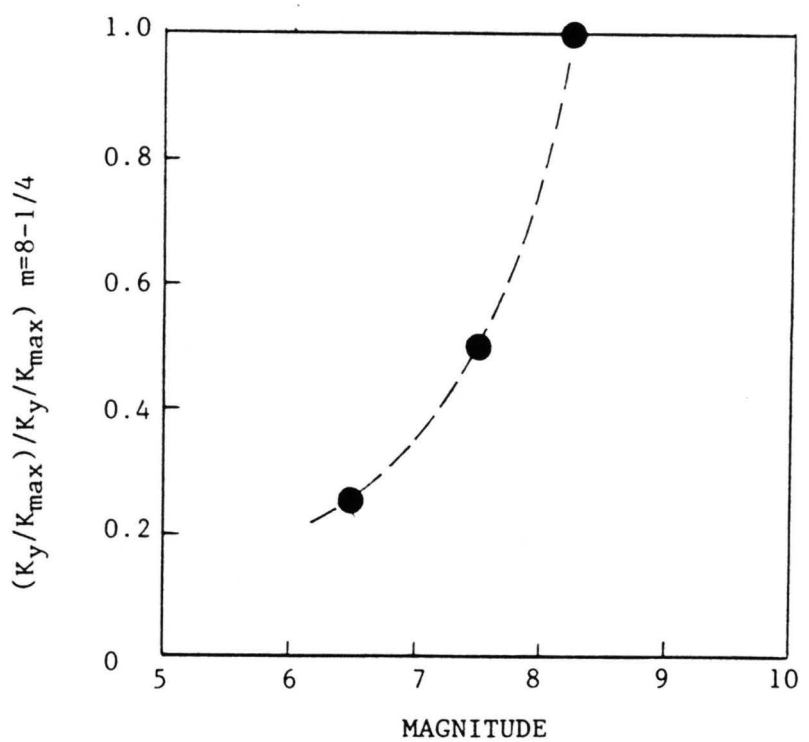

Project GROUND FAILURE POTENTIAL ANCHORAGE, ALASKA Project No. 41966A	MAGNITUDE WEIGHTING FACTORS FOR TRANSLATORY SLIDES	Fig. 3-2

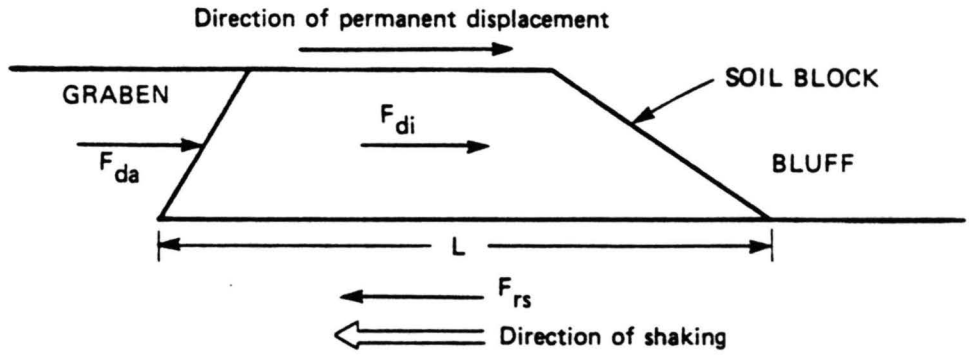

F_{da} = Driving force due to active soil pressure

F_{di} = Driving force due to earthquake inertia

F_{rs} = Resisting force due to soil shear strength

$$F_{di} = k_{max} W$$

where k_{max} = maximum seismic coefficient

W = weight of soil block

$$F_{rs} = S_u L$$

where S_u = average undrained shear strength of soil

L = length of soil block

Yield Seismic Coefficient

$$k_y = \frac{F_{rs} - F_{da}}{W}$$

Project GROUND FAILURE POTENTIAL ANCHORAGE, ALASKA Project No. 41966A	FORCES AND EQUATIONS IN DISPLACEMENT ANALYSIS	Fig. 3-3

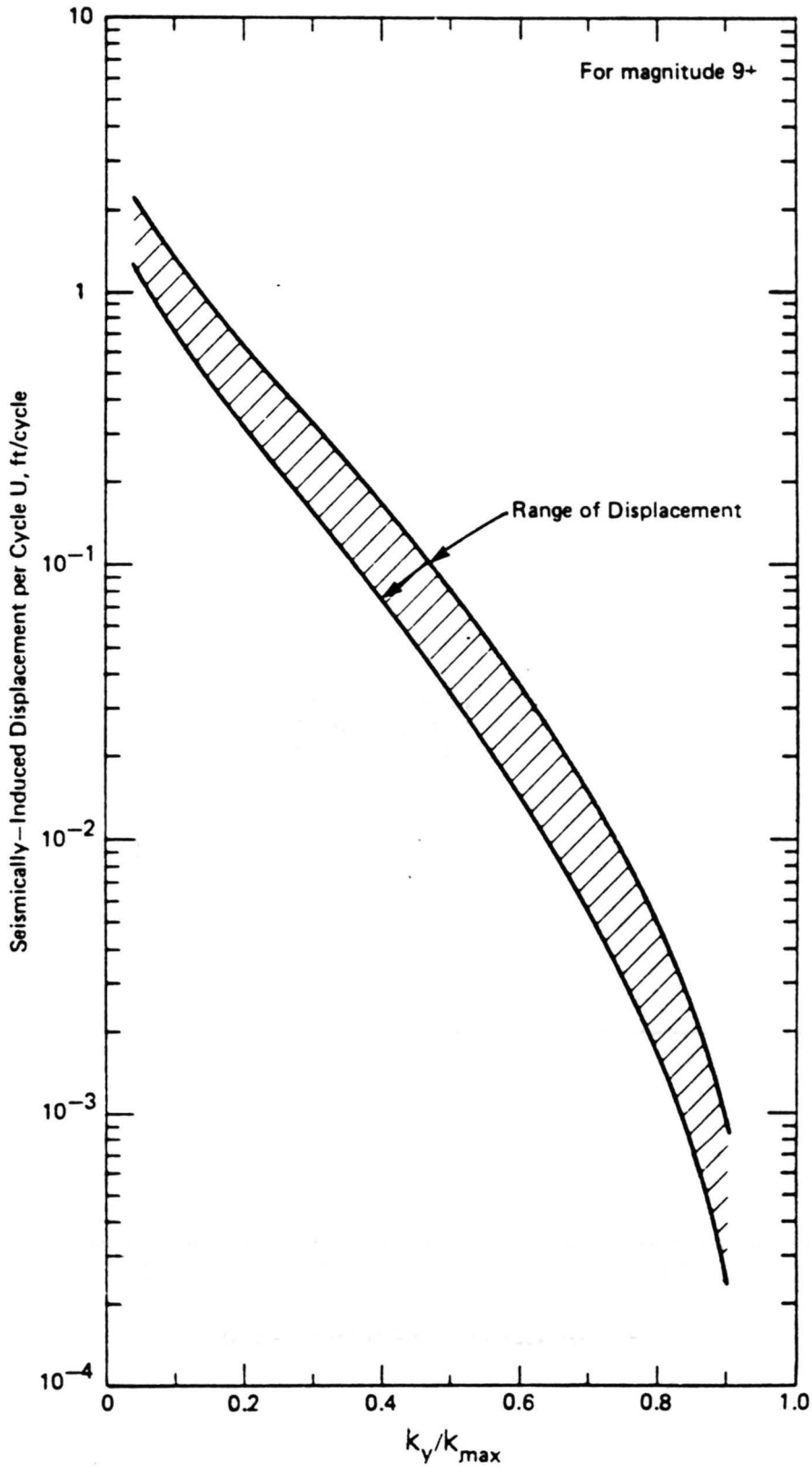

(Woodward-Clyde Consultants, 1982b)

Project GROUND FAILURE POTENTIAL ANCHORAGE, ALASKA Project No. 41966A	SEISMICALLY-INDUCED DISPLACEMENT PER CYCLE FOR MAGNITUDE 9+ EARTHQUAKES	Fig. 3-4

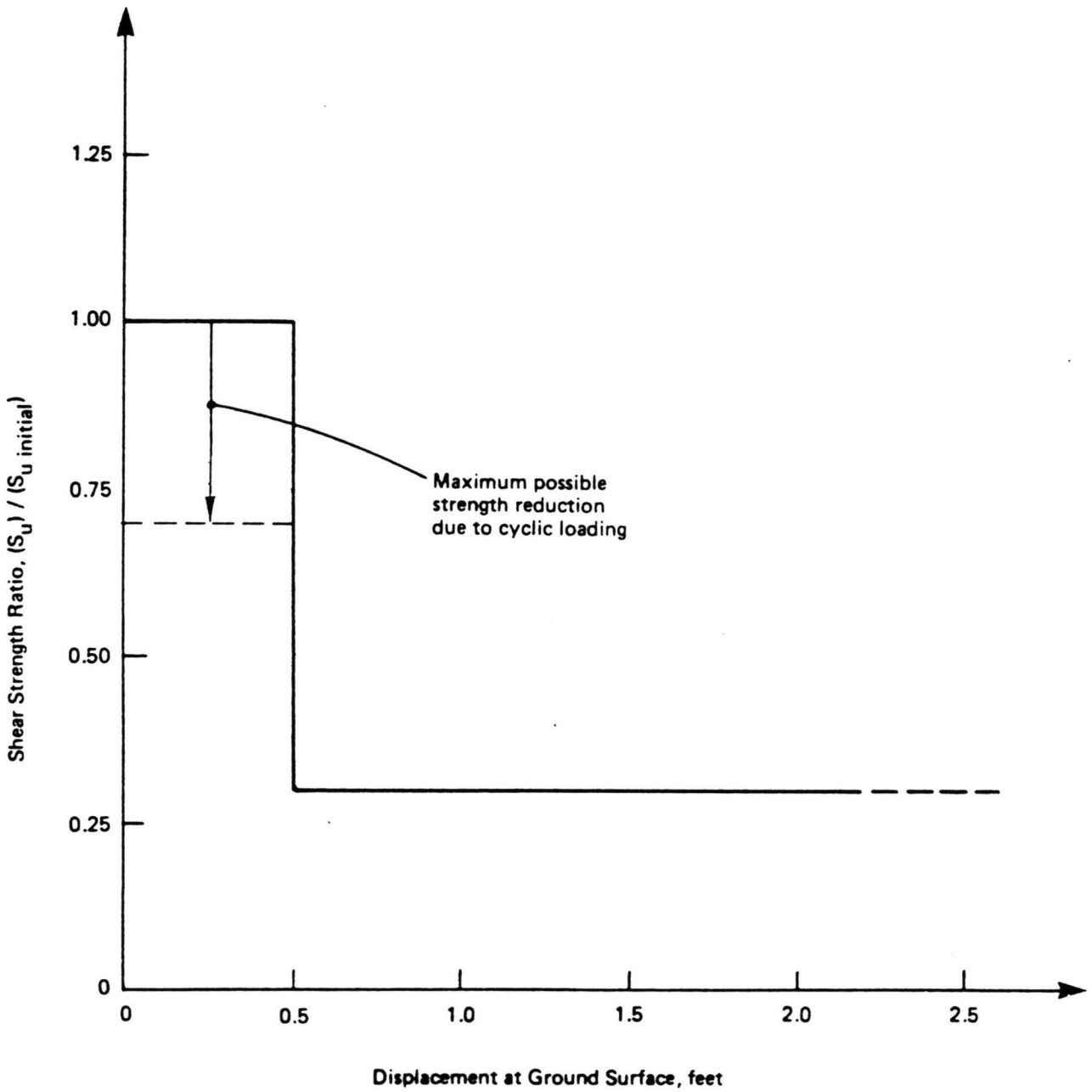

(Woodward-Clyde Consultants, 1982b)

Project GROUND FAILURE POTENTIAL ANCHORAGE, ALASKA Project No. 41966A	IDEALIZED STRENGTH-DISPLACEMENT RELATIONSHIP FOR SLIDING BLOCK	Fig. 3-5

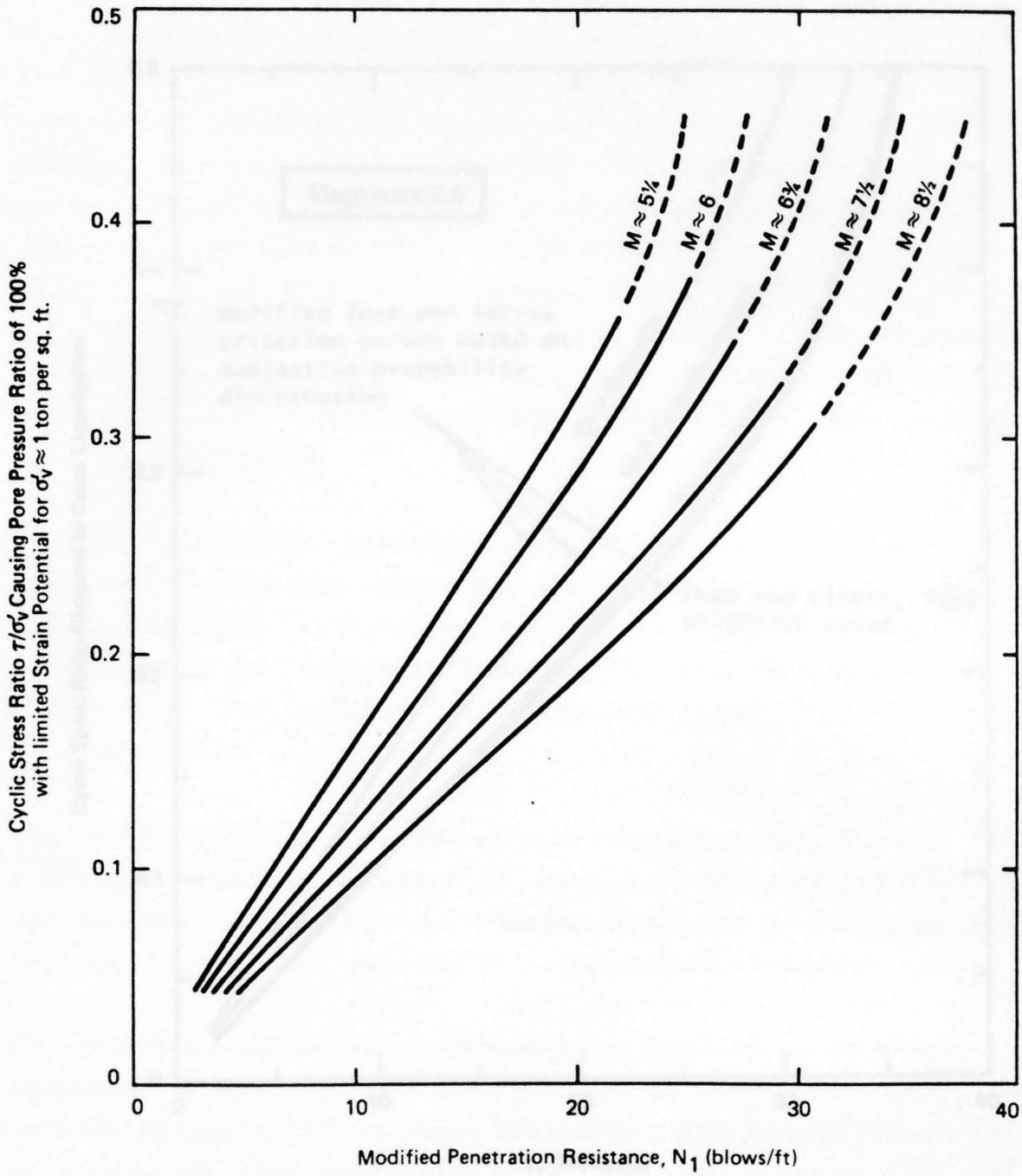

(Seed and Idriss, 1982)

Project GROUND FAILURE POTENTIAL ANCHORAGE, ALASKA Project No. 41966A	CHART FOR EVALUATION OF LIQUEFACTION POTENTIAL	Fig. 3-6

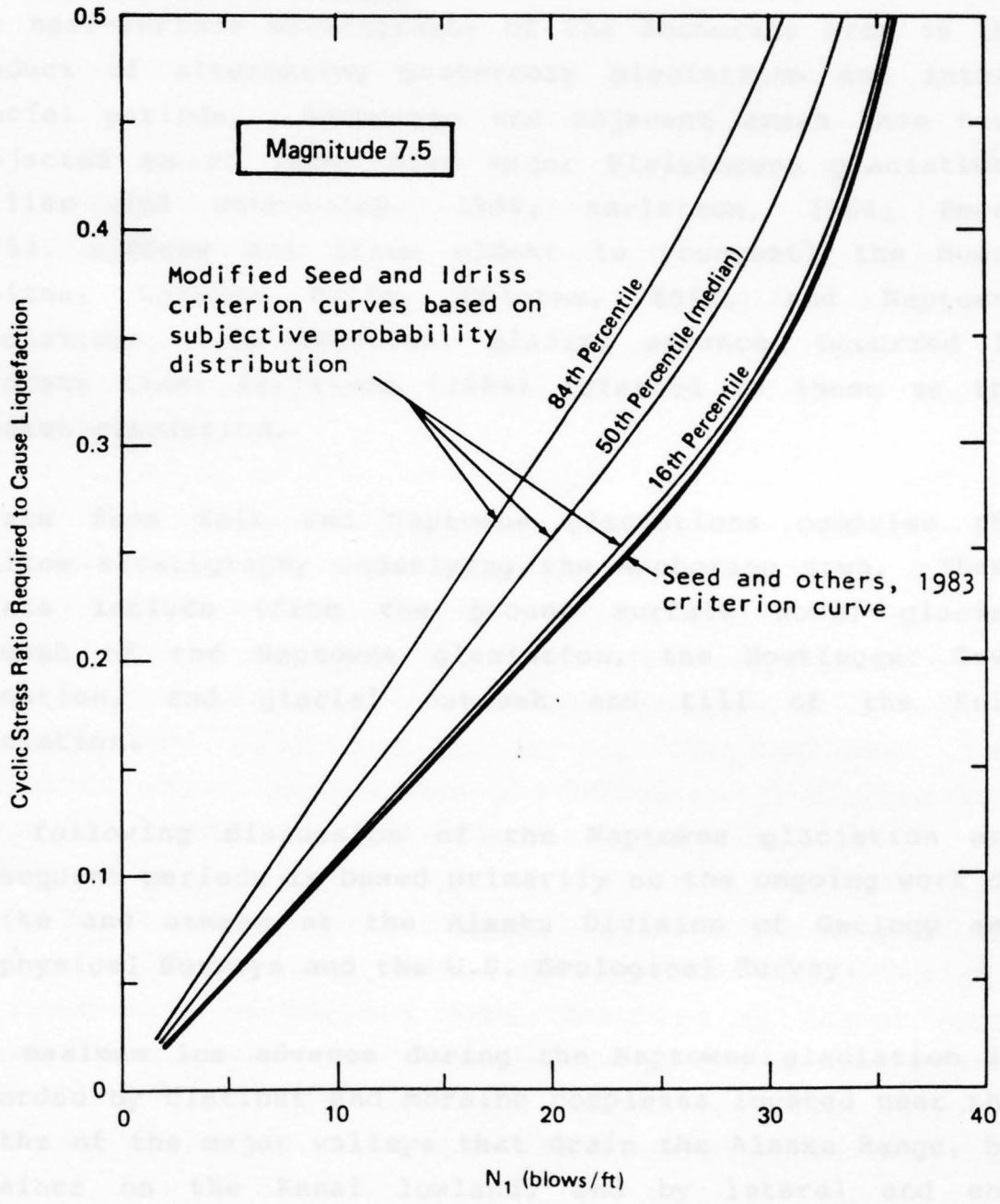

(Woodward-Clyde Consultants, 1986)

Project GROUND FAILURE POTENTIAL ANCHORAGE, ALASKA Project No. 41966A	MODIFIED SEED AND IDRISS LIQUEFACTION CRITERIA	Fig. 3-7

4.0 SUBSURFACE CONDITIONS IN ANCHORAGE

4.1 Geological Background

The near-surface stratigraphy of the Anchorage area is the product of alternating Quaternary glaciations and interglacial periods. Anchorage and adjacent areas have been subjected to at least five major Pleistocene glaciations (Miller and Dobrovolny, 1959; Karlstrom, 1964; Pewe, 1975). These are (from oldest to youngest) the Mount Susitna, Caribou Hills, Eklutna, Knik, and Naptowne glaciations. In addition, glacial advances occurred in Holocene time; Karlstrom (1964) referred to these as the Alaskan glaciation.

Strata from Knik and Naptowne glaciations comprise the shallow stratigraphy underlying the Anchorage area. These strata include (from the ground surface down) glacial outwash of the Naptowne glaciation, the Bootlegger Cove formation, and glacial outwash and till of the Knik glaciation.

The following discussion of the Naptowne glaciation and subsequent periods is based primarily on the ongoing work of Updike and others at the Alaska Division of Geology and Geophysical Surveys and the U.S. Geological Survey.

The maximum ice advance during the Naptowne glaciation is recorded by distinct end moraine complexes located near the mouths of the major valleys that drain the Alaska Range, by moraines on the Kenai lowland, and by lateral and end moraines in the Turnagain and Knik Arms of Cook Inlet. During the early Naptowne glaciation, ice moved into the Anchorage area and till was deposited as ground and lateral moraines. The till is overlain by glaciofluvial sands and

gravels that were deposited as the ice receded from the Anchorage area. This early Naptowne glacial state ended about 34,000 years before present or y.b.p. (Updike, 1982).

Following its withdrawal from the Anchorage area, Naptowne ice readvanced from the northwest into a marine or estuarine body of water. This ice did not reach Anchorage but shed sediments eastward into the Anchorage area. These sediments comprise the Bootlegger Cove formation. This is a revision from the earlier work of Karlstrom (1964), who considered the formation to be of Knik and Naptowne age. The revised age suggests the formation was deposited over a shorter period of time.

In the waning stages of the Naptowne glaciation, ice again readvanced into the Anchorage area, but apparently did not reach downtown Anchorage. The maximum extent of this late Naptowne ice is marked by the Elmendorf Moraine north of the study area. Throughout much of the Anchorage area, outwash deposits were laid down on top of the Bootlegger Cove formation under deltaic and glaciofluvial conditions that prevailed at the end of the Naptowne glaciation.

Following the Naptowne glaciation, glacial advances in the Cook Inlet region have been limited to the mountains that surround the lowland and have consisted of rather small scale fluctuations that extended only up to a few mile beyond present glacier termini. Karlstrom (1964) referred to these Neoglacial advances as the Alaskan glaciation.

Stratigraphic units underlying much of the study area (to a depth of about 150 feet or more) are sediments of Naptowne age. These deposits include the Bootlegger Cove formation and the latest Naptowne outwash.

4.1.1 Bootlegger Cove Formation

The sediments in the Bootlegger Cove formation originated as glacial and glaciofluvial sediments from glacier that lay to the north, south, and west of the study area. Variations in exposed sediment, stream flow velocities, distance from the source areas, as well as variations in depositional environment, produced a sequence of interbedded clay, silt, and sand in the glacial lake. In the Anchorage area the Bootlegger Cove formation was deposited unconformably on early Naptowne till. The Bootlegger Cove formation is considered by Karlstrom (1964), Trainer and Waller (1965), and Updike (1982) to consist of the following three units:

(a) Basal strata deposited in a Naptowne-age proglacial lake at least 18,000 y.b.p.;

(b) Intermediate glacial-marine or estuarine strata deposited about 14,000 y.b.p.; and

(c) Upper freshwater (deltaic) strata deposited in a proglacial lake, apparently more than 8,000 y.b.p.

The intermediate unit is believed by Updike (1982) to be the product of periodic incursions of marine waters into the ice-dammed lake during alternate periods of ice front stagnation and advance. This unit contains clays referred to as "soft clay" and "soft sensitive clay" by Shannon and Wilson (1964). This "soft sensitive clay" has been the subject of a number of studies (eg, Mitchell et al, 1973; Kerr and Drew, 1965) partly because it is considered to have contributed to some of the ground failures observed in Anchorage following the 1964 Alaskan earthquake.

Subsequent to deposition of the intermediate unit of the Bootlegger Cove formation, the upper and deltaic section was deposited in a glacial-lacustrine environment. This environment may have existed intermittently in the Anchorage area due to fluctuation in lake levels in response to changes in the location and height of the glacial ice. Karlstrom (1964) suggested that some of the fluctuations resulted in raising water levels above elevation 80 feet (which is above the present elevation of the Bootlegger Cove formation in downtown Anchorage) while others allowed water levels to drop below elevation 80 feet. Updike (1982) believes that subaerial exposure occurred at the end of the Naptowne glaciation as the glacier receded from the Anchorage area and the lake drained. Regardless of the mechanism, the upper section of the Bootlegger Cove formation was subaerially exposed, locally oxidozed, and weathered prior to deposition of the overlying Naptowne outwash; it is relatively dense or overconsolidated compared to that in the intermediate section.

4.1.2 Naptowne Outwash

Overlying the Bootlegger Cove clay are Naptowne outwash deposits whose thickness in downtown Anchorage is about 30 to 40 feet. This glaciofluvial material was deposited by streams emanating from the retreating glaciers that transported reworked silt, sand, gravel, and cobbles into a large plain referred to as the Anchorage plain. The base of the deposit has a west to east and north to south dip, suggesting that the source area lay to the north and west.

4.2 Bootlegger Cove Formation and Facies in Anchorage Area

In recent years the Bootlegger Cove formation in parts of the Anchorage area have been characterized using facies (Updike and Carpenter, 1985; Updike and Ulery, 1985; Updike,

1982; Ulery and Updike, 1983). Eight geologic facies within the Bootlegger Cove formation have been defined based on their engineering and textural characteristics as follows:

Facies F.I	CLAY, with very minor silt and sand
Facies F.II	SILTY CLAY AND/OR CLAYEY SILT
Facies F.III	SILTY CLAY AND/OR CLAYEY SILT, SENSITIVE
Facies F.IV	SILTY CLAY AND/OR CLAYEY SILT, with thin silt and sand lenses
Facies F.V	SILTY CLAY AND/OR CLAYEY SILT, with random pebbles, cobbles, and boulders
Facies F.VI	SILTY FINE SAND, with silt and clay layers
Facies F.VII	FINE TO MEDIUM SAND, with traces of silt and gravel
Facies F.VIII	SANDY GRAVEL AND GRAVELLY SAND, with discontinuous layers of silt and fine sand.

The mean values or ranges of selected engineering properties associated with these facies as well as those associated with the Naptowne Outwash are summarized in Table 4-1. As can be observed in Table 4-1, F.III consists of slightly overconsolidated Bootlegger Cove clay that corresponded to many of the inferred failure planes in the translatory slides due to the 1964 Alaskan earthquake. Because parts of Anchorage have already been characterized using this facies

system (Ulery and Updike, 1984), an evaluation of the system from a geotechnical engineering point of view was made in this study. The results of this evaluation indicated that while dividing the cohesive part of the Bootlegger Cove formation into five facies may not be necessary from the engineering point of view, the system is useful for characterizing the Bootlegger Cove formation in the study area. For this reason, cross-sections using the facies system were developed for the study area using available data and are presented in Appendix B.

Because the Bootlegger Cove formation is considered to have contained many of the inferred slide planes in the translatory slides in Anchorage due to the 1964 Alaskan earthquake, identifying the extent of this formation in the study area, say at the sea level, may be of some interest. The delineated area of the Bootlegger Cove formation above the sea level is also presented in Appendix B. This data and the cross-sections together with other data were used to identify areas of potential translatory slides in the study area.

4.3 Areas of Potential Translatory Slides

The areas of potential translatory slides were identified based on the following information:

1. Areas of translatory slides due to the 1964 Alaskan earthquake;

2. Areas with topographical evidence of translatory-like slides before the 1964 Alaskan earthquake;

3. Topographic data indicating the presence of bluffs; and

4. Cross-sections and an areal map indicating the extent of the Bootlegger Cove formation above the sea level in the study area, presented in Appendix B.

The resulting areas are identified in Plate 1. In Plate 1 areas designated as Area I represent the areas of potential translatory slides.

4.4 Potentially Liquefiable Geological Units

4.4.1 Geologic Data

Age, mode for deposition, and areal extent of the principal geologic units in the Anchorage area were first identified from available sources (Miller and Dobrovolny, 1959; Schmoll and Dobrovolny, 1972a, 1972b; Updike, 1986). Some of these geologic units were selected for evaluations of liquefaction potential based on considerations of age (Holocene and late Pleistocene), location within the study area, and availability of data; these selected geologic units are described in Table 4-2.

4.4.2 Geotechnical Data

Liquefaction susceptibility assessment based on the proposed Seed and Idriss approach requires evaluation of the Standard Penetration Test (SPT) modified penetration resistance N_1.

About 850 SPT data points were selected for analysis from about 200 selected borings located in eastern parts of the study area (between Wisconsin Street and the Seward Highway, and between the International Airport Road and the Ship Creek). Useable SPT data were not available either from western parts of the study area or from north of the Ship Creek.

The data were selected to include clean and silty sands, gravel-sand mixtures, and non-plastic to slightly plastic silts in various geologic units, at depths not greater than about 60 feet.

These SPT data were obtained by various organizations in the last 22 years, using various drilling procedures. Raw SPT blow counts N were corrected to account for the effect of confining pressure and energy loss in the drive rods using the following equation (Seed and Idriss, 1982):

$$N_1 = C_n \; C_Z \; N \qquad (4\text{-}1)$$

where

C_N = correction factor for confining pressure

C_Z = 0.75 for samples shallower than 10 feet and
1.00 otherwise.

The total unit weight of the soil above and below the ground water table was assumed in these calculations to be 125 pcf. Only the data obtained with the SPT sampler and hammer were selected in this study. Description of drilling procedures and percent of fines in each sample were generally not complete or available. Therefore, corrections to account for these factors, as suggested by Seed et al (1985) were not applied. The effect of not correcting for drilling procedures is considered to be relatively minor. However, the effect of not correcting for fines content in general results in conservative values of SPT data.

4.4.3 Modified Penetration Resistance Results

Values of N_1 were computed for all selected SPT values. Basic statistics for the selected geologic units are summarized in Table 4-3. Histograms showing the actual distribution of N_1 for each of the selected geologic units are shown in Figures 4-1 through 4-3.

4.4.4 Ground Water Depth

Depth to ground water was obtained from available exploratory borings. Reported ground water depths, used in the analyses, were generally shallower than 20 to 30 feet. The SPT data associated with soil samples above the ground water table were not considered in the liquefaction susceptibility evaluation.

TABLE 4-1

SELECTED ENGINEERING PROPERTIES ASSOCIATED WITH NAPTOWNE OUTWASH AND FACIES OF BOOTLEGGER COVE FORMATION

Geologic Unit/ Formation	Geologic Age and Sediment Process	Facies	Soil Classif. (USCS)	Description	Mean Grain Size (mm)	Mean Moisture Content (%)	Atterberg Limits (Mean Values) PL (%)	LL (%)	PI (%)	Mean LI	SPT Data N	N_1	CPT Data q_c (tsf)	f_s (tsf)	FR (%)	OCR	Mean Unconf. Compr. Strength	Mean Sensit. Ratio
Naptowne Outwash	Very Latest Pleistocene Glaciofluvial Sediment		GP, SP	Moderately Dense Packed							40-60		300-500	1-4				
Bootlegger Cove Formation (BCF)	Deposited in Ice-Marginal Glacio-Lacustrine Basin During Late Pleistocene Time	Cohesive Facies of the BCF																
		I	CL	With very minor silt and sand	0.0014	30	23	39	16	0.4	40-60						1.7	9
		II	CL,ML		0.004	28	22	37	15	0.4			<25	<1	2-4	3-4	1.5	3
		III	CL,ML	Sensitive	0.004	30	22	28	6	1.1			<15	<0.4	<2	1.2-1.5	0.9	20
		IV	CL,ML	With silty fine sand lenses	0.015	28	20	35	15	0.5			15-35	1-2	3-7	3-4	1.1	6
		V	CL,ML	With random stones	0.006	28	22	37	15	0.4			25-35	0.5-2	3-7	2	1.9	4
		Non-Cohesive Facies of the BCF																
		IV	SM	With silt and clay layers	0.15	25	NP*				40-60	23-65	25-50	1-4	<2		1.3	--
		VII	SP, SW	With traces of silt/gravel	0.37	29	NP*				40-60	23-65	>100	<2	<1		--	--

NP* = Non-Plastic

TABLE 4-2

GEOLOGIC UNITS SELECTED FOR EVALUATION OF LIQUEFACTION POTENTIAL

Geologic Unit	Form of Deposition	Age	Soil Type
Alluvium (Q_{al})	Fluvial sediments	Holocene	Sand and gravel
Naptowne Outwash (Q_o)	Glacio-fluvial sediments	Very latest Pleistocene; Naptowne glaciation	Sand and gravel with occasional, thin layers of silt and/or surface peat bed.
Bootlegger Cove Formation (Q_{bc})	Ice-marginal glacio-lacustrine basin	Late Pleistocene, 10,000-18,000 years B.P.; Naptowne glaciation	Sand and gravel at Point Woronzof grading to stratified clay, silt, and sand in the downtown area

TABLE 4-3

STATISTICS OF THE MODIFIED PENETRATION RESISTANCE (N_1) FOR SELECTED GEOLOGIC UNITS

	Alluvium Qal	Naptowne Outwash Qo	Bootlegger Cove Formation Qbc
No. Obs.	32	238	580
Mean	62	61	43
Median	69	57	39
Std. Dev.	19	27	22
Coef. Var.	0.31	0.45	0.50
NUMBER OF SAMPLES PER SOIL TYPE (mostly based on reported visual classification)			
ML	3	8	221
SM	17	26	178
SP-SM,SW-SM	1	33	37
Other Soil Types	11 (34%)	171 (72%)	144 (25%)

Material : Q_{al}

Number of SPT Values : 32

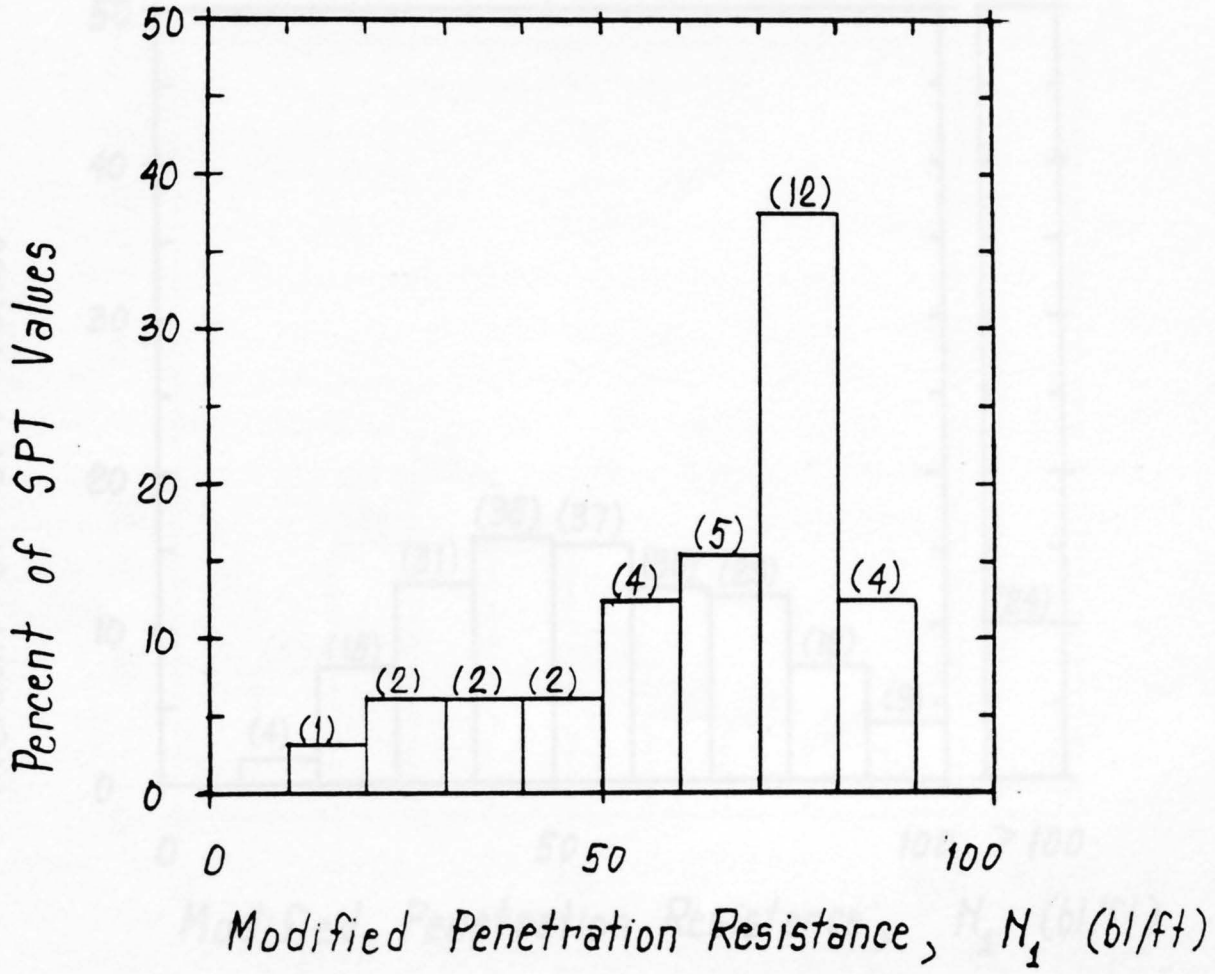

* Number of data points

Project GROUND FAILURE POTENTIAL ANCHORAGE, ALASKA Project No. 41966A	HISTOGRAM OF N_1 FOR ALLUVIUM	Fig. 4-1

Material : Q_o

Number of SPT Values : 238

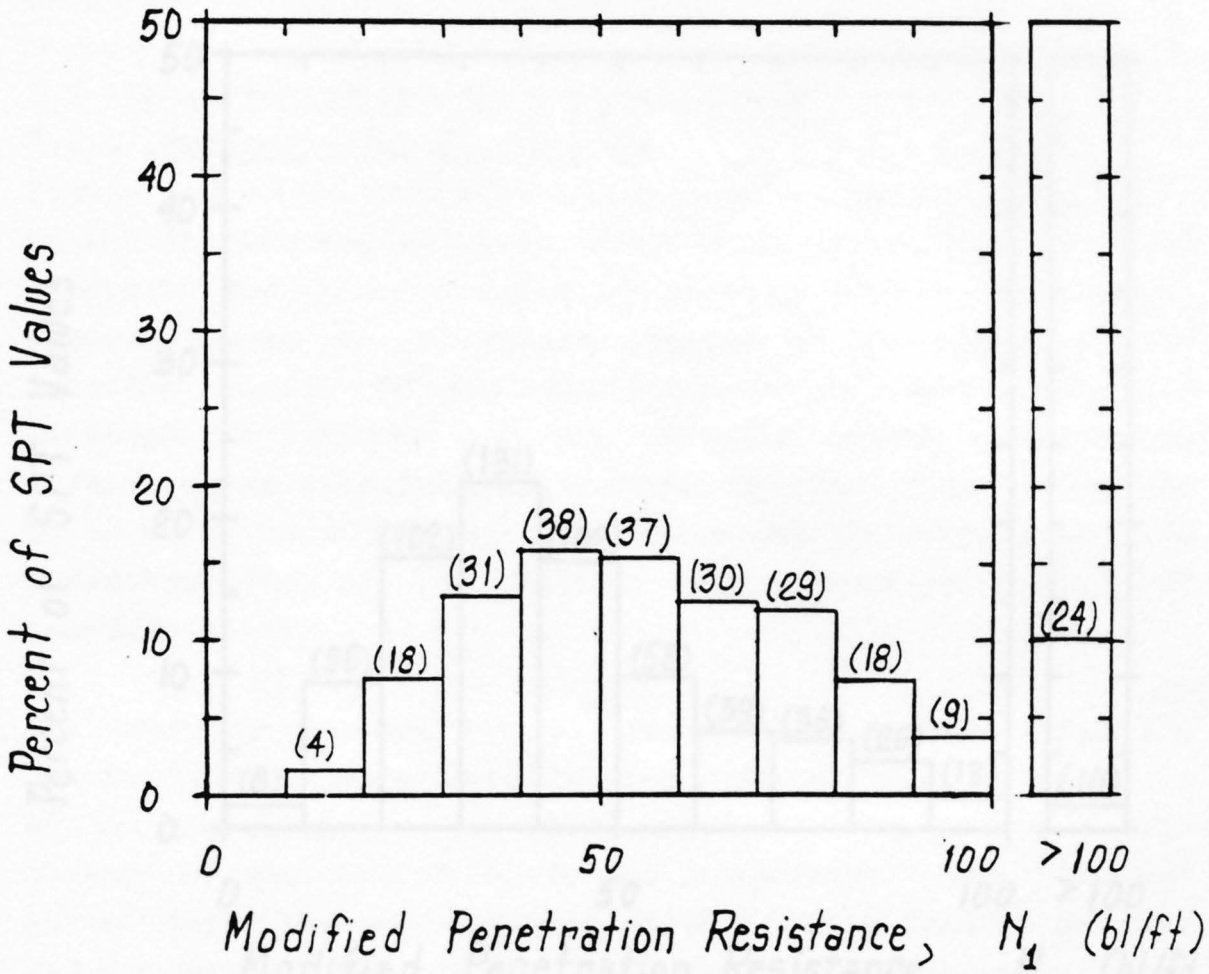

* Number of data points

Project GROUND FAILURE POTENTIAL ANCHORAGE, ALASKA Project No. 41966A	HISTOGRAM OF N_1 FOR NAPTOWNE OUTWASH	Fig. 4-2

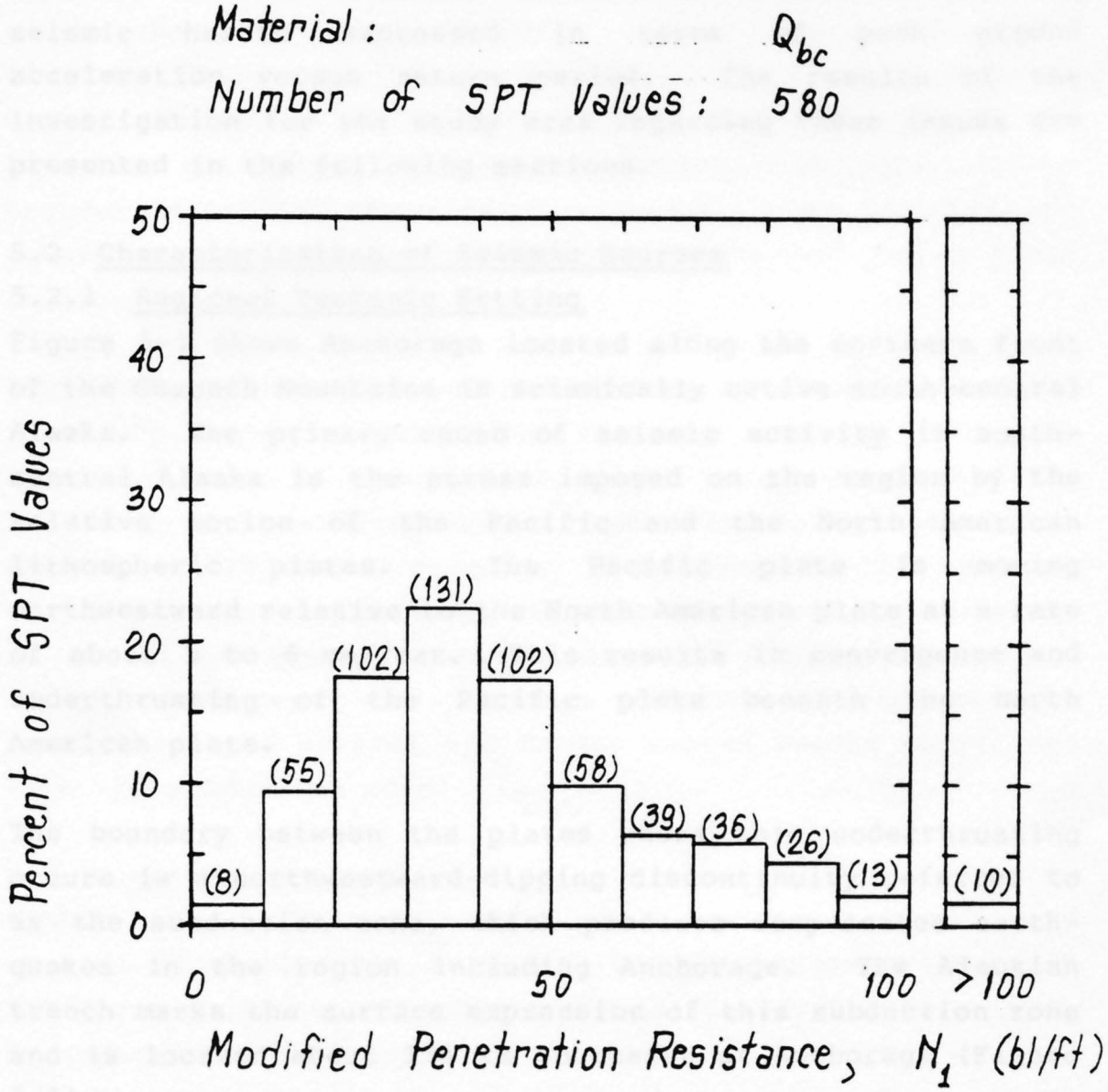

* Number of data points

Project GROUND FAILURE POTENTIAL ANCHORAGE, ALASKA Project No. 41966A	HISTOGRAM OF N_1 FOR BOOTLEGGER COVE FORMATION	Fig. 4-3

5.0 POTENTIAL EARTHQUAKE GROUND MOTIONS IN ANCHORAGE

5.1 Overview

An assessment of potential earthquake ground motions using probabilistic seismic hazard analyses involves characterization of seismic sources, attenuation relationships, and seismic hazard expressed in terms of peak ground acceleration versus return period. The results of the investigation for the study area regarding these issues are presented in the following sections.

5.2 Characterization of Seismic Sources

5.2.1 Regional Tectonic Setting

Figure 5-1 shows Anchorage located along the northern front of the Chugach Mountains in seismically active south-central Alaska. The primary cause of seismic activity in south-central Alaska is the stress imposed on the region by the relative motion of the Pacific and the North American lithospheric plates. The Pacific plate is moving northwestward relative to the North American plate at a rate of about 5 to 6 cm/year. This results in convergence and underthrusting of the Pacific plate beneath the North American plate.

The boundary between the plates where this underthrusting occurs is a northwestward-dipping discontinuity referred to as the subduction zone, which produces deep-seated earthquakes in the region including Anchorage. The Aleutian trench marks the surface expression of this subduction zone and is located about 330 km southeast of Anchorage (Figure 5-1).

Geologic evidence indicates that subduction has progressively shifted from its ancient position at the

Border Ranges fault, southeastward to its present position (MacKevett and Plafker, 1974; Tysdal and Case, 1979). This southeastward shift apparently resulted from the process of scraping off blocks of the oceanic sediments that were lying on top of the lower subducting plate and accreting these materials onto the leading edge of the overriding crustal plate (MacKevett and Plafker, 1974; Tysdal and Case, 1979). These accreted sediments are presently seen as highly deformed and faulted rocks located throughout the Chugach and Kenai Mountains (Magoon et al, 1976). Boundaries between these large accreted blocks of crust are suture zones, such as the Border Ranges and Eagle River faults.

The active convergence and underthrusting along the subduction zone imparts compressive stresses into the overlying crust resulting in deformation, which is expressed as folds and high-angle reverse and thrust faults. Those upper crustal faults that are active in response to the compressional stresses imposed by the subduction zone are referred to as shallow crustal seismic sources. The seismic hazard of the Anchorage area is thus related to both shallow crustal seismic sources and deeper seated events associated with the subduction zone.

5.2.2 Seismic Sources

Within the Anchorage region, four seismic sources are considered to have the potential for earthquakes that could produce significant ground motions in the study area. These sources are as follows:

- Shallow Crustal Seismic Sources
  - The Castle Mountain Fault
  - The Border Ranges Fault Zone

° Subduction Zone Seismic Sources

The Megathrust (Interplate) Zone

The Benioff (Intraplate) Zone

The seismic hazard evaluation in the study area requires the location and geometry of these sources with respect to the study area and the seismicity of these sources. Figures 5-1 and 5-2 show the location of these sources and the study area. Table 5-1 summarizes an idealized geometry and location of these sources for probabilistic seismic hazard analyses. The seismicity of each source was characterized by source definition parameters including maximum magnitude and rate of seismicity. Table 5-1 also summarizes the values of these parameters used in the probabilistic seismic hazard analyses.

All seismic source parameters used in the analysis were fixed except for the distance to the Border Ranges fault. This distance varies from about 10 to 20 km within the study area. Therefore, the probabilistic seismic hazard analyses in this study were performed using both 10 km and 20 km for the distance to this fault.

Further details of these and related seismic sources are presented in Appendix A.

5.3 Attenuation Relationship

Ideally, the most appropriate attenuation relationship for the seismic hazard analysis of a region should be based on ground motion data recorded in that region. Such data are very limited for the Anchorage area. Therefore, attenuation relationships derived based on data recorded mostly in California were examined, and two attenuation relationships (Idriss, 1985) corresponding to deep soil sites and soft

soil sites were selected to complete the seismic hazard analyses for this study. While it is recognized that attenuation relationships in the Anchorage area may be somewhat different from those based mainly on Californian data (eg, Jacob and Mori, 1984), there appears to be insufficient data to reach firm conclusions based on local data alone. A detailed examination of attenuation relationships for Anchorage was not a part of the scope in this study.

For deep soil sites, the following equation was used for the median (50-percentile) peak ground acceleration in this study:

$$\ln a = \ln \alpha(m) - \beta(m) \ln (R + 20)$$

where m is local magnitude for $m < 6$ and surface wave magnitude for $m \geq 6$. The distance R is the closest distance to the source for $m \geq 6$ and the hypocentral distance for $m < 6$. The values of $\alpha(m)$ and $\beta(m)$ as well as a standard error term (lognormal) S.E.(m) are functions of magnitude m as follows:

m	$\alpha(m)$	$\beta(m)$	S.E.(m)
4.5	189	2.22	0.70
5	195	2.13	0.58
5.5	147	1.97	0.48
6	98	1.79	0.42
6.5	61.6	1.60	0.38
7	37.2	1.41	0.35
7.5	22	1.22	0.35
8	13.7	1.05	0.35
8.5	8.4	0.88	0.35

Similarly, for soft soil sites, the following equation is used in this study:

$$\ln a = \ln \alpha(m) - \beta(m) \ln (R + 20)$$

with

m	$\alpha(m)$	$\beta(m)$	S.E.(m)
4.5	52.7	1.82	0.70
5	53	1.74	0.58
5.5	43.7	1.62	0.48
6	31.1	1.47	0.42
6.5	20.9	1.31	0.38
7	14.2	1.16	0.35
7.5	9.1	1.00	0.35
8	6.2	0.86	0.35
8.5	4.1	0.72	0.35

The above attenuation relationships are based on the results by Idriss et al (1982) and Woodward-Clyde Consultants (1979) modified to account for the possible variation of peak horizontal acceleration with site conditions (Idriss, 1985; Seed and Idriss, 1982).

5.4 Results of Probabilistic Seismic Hazard Analyses

Figures 5-3a and 5-3b show the results of probabilistic seismic hazard analysis in terms of peak ground acceleration versus return period corresponding to 10 km and 20 km to the Border Ranges fault, respectively, for the parts of the study area that can be characterized as deep soil sites. Figures 5-4a and 5-4b similarly show the results for the parts of the study area that can be characterized as soft soil sites. These figures also show the contributions to the total seismic hazards provided by each source. The results presented in Figures 5-3 and 5-4 are based on assigning equal weight to all magnitudes (see Section 3.4 for discussion of magnitude weighting factors).

TABLE 5-1

SEISMIC SOURCES

Fault Name	Fault Classification	Approximate Distance To Site Km	Approximate Fault Length Km	Estimated Maximum Earthquake	a*	b*
Megathrust	Subduction	65	1,400	9.5	1.782	0.7
Benioff	Subduction	45	1,400	7.5	3.089	0.9
Border Ranges	Reverse	10	500	7.5	3.153	0.85
Castle Mountain	Right-Lateral Strike-Slip and Reverse	40	475	7.5	3.852	0.85

*Note: These are parameters in the Gutenberg-Richter recurrence relationship.

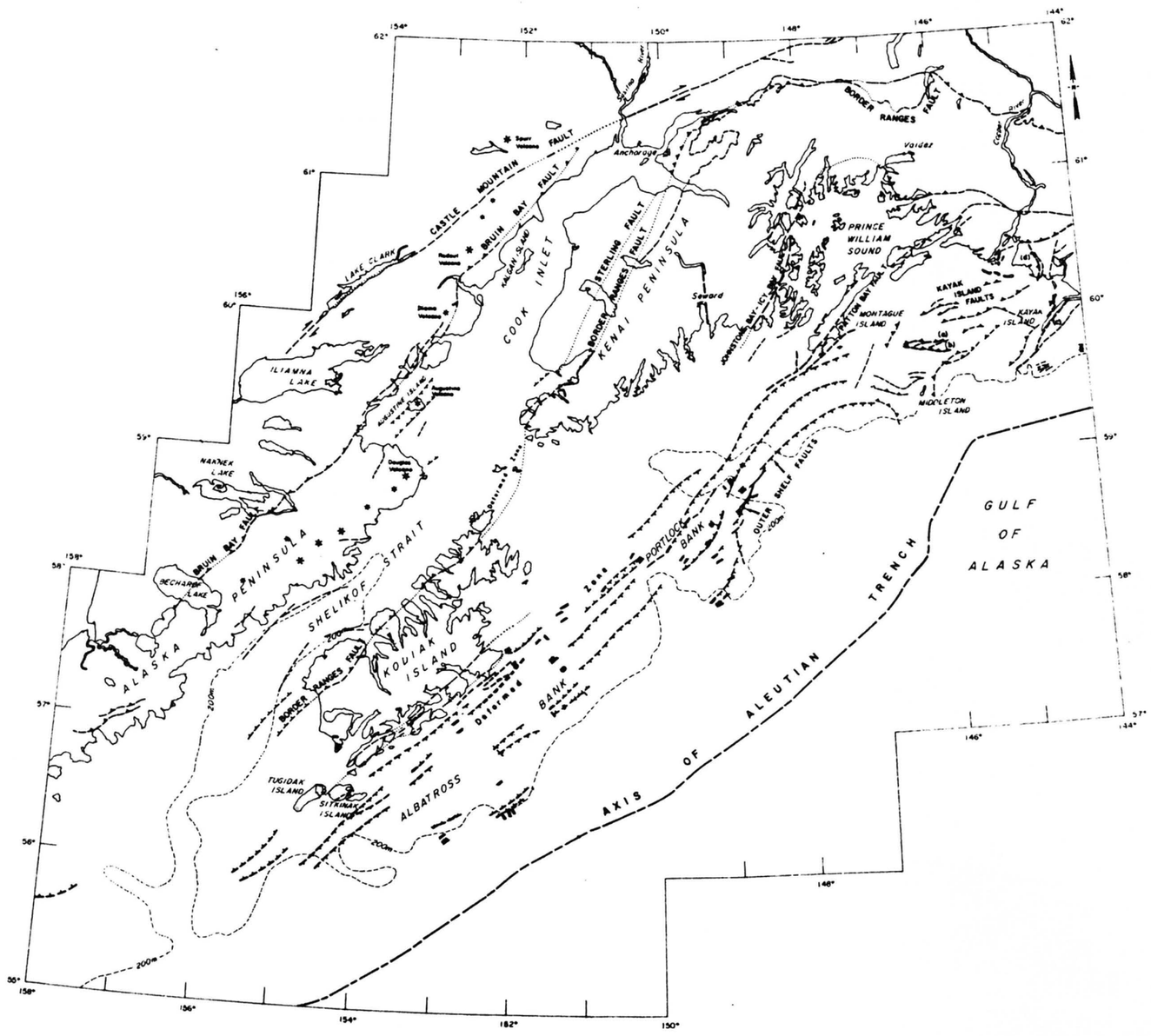

EXPLANATION

Active Faults

- Fault, dashed where approximately located, dotted where concealed or questionable. Hachures indicate relatively down dropped side of fault.
- Thrust Fault, dashed where approximately located, dotted where concealed or questionable. Barbs indicate relatively upthrown side of fault.
- Strike-Slip Fault, dashed where approximately located, dotted where concealed or questionable. Arrows indicate relative displacement.
- Submarine surface fault or scarp recognized from geophysical data. Hachures on downthrown side of fault.
- Lineament, inferred for this study to be an earthquake-producing structure.

Inactive Faults

- Fault, dashed where approximately located, dotted where concealed or questionable. Hachures indicate relatively down dropped side of fault.
- Thrust Fault, dashed where approximately located, dotted where concealed or questionable. Barbs indicate relatively upthrown side of fault.
- Strike-Slip Fault, dashed where approximately located, dotted where concealed or questionable. Arrows indicate relative displacement.
- Submarine surface fault or scarp recognized from geophysical data. Hachures on downthrown side.

* Volcanic Centers
Quaternary volcanic center, vent or cone.

Line of cross-section.

NOTES:

Active Fault – A subaerial or submarine fault that breaks or is inferred to break Holocene or unconsolidated sediments (Holocene young but without any age determination) or a submarine fault is exposed on the sea floor.

Inactive Fault – A subaerial or submarine fault that does not break Holocene nor unconsolidated sediments (Holocene young but without any age determination) nor is it exposed on the sea floor.

Base Map Compiled from World Aeronautical Charts.

25 0 25 50 Nautical Miles
25 0 25 50 100 Kilometers
25 0 25 50 Statute Miles

Woodward-Clyde Consultants

REGIONAL SEISMIC SOURCE MAP

Project No. 41966A

GROUND FAILURE POTENTIAL
ANCHORAGE, ALASKA

Fig. 5-1

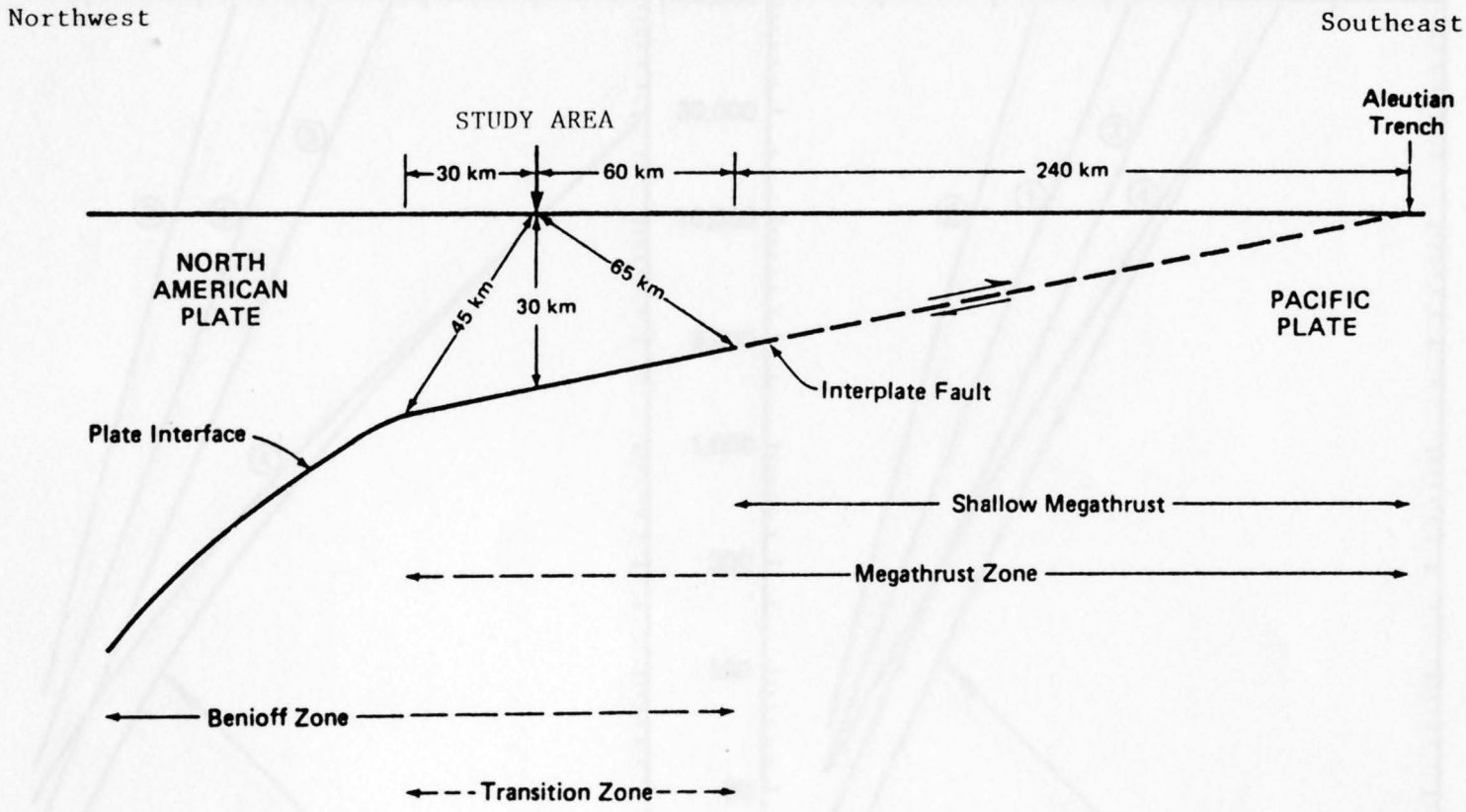

Project: GROUND FAILURE POTENTIAL ANCHORAGE, ALASKA Project No. 41966A	SCHEMATIC CROSS-SECTION SHOWING SUBDUCTION ZONE SOURCES	Fig. 5-2

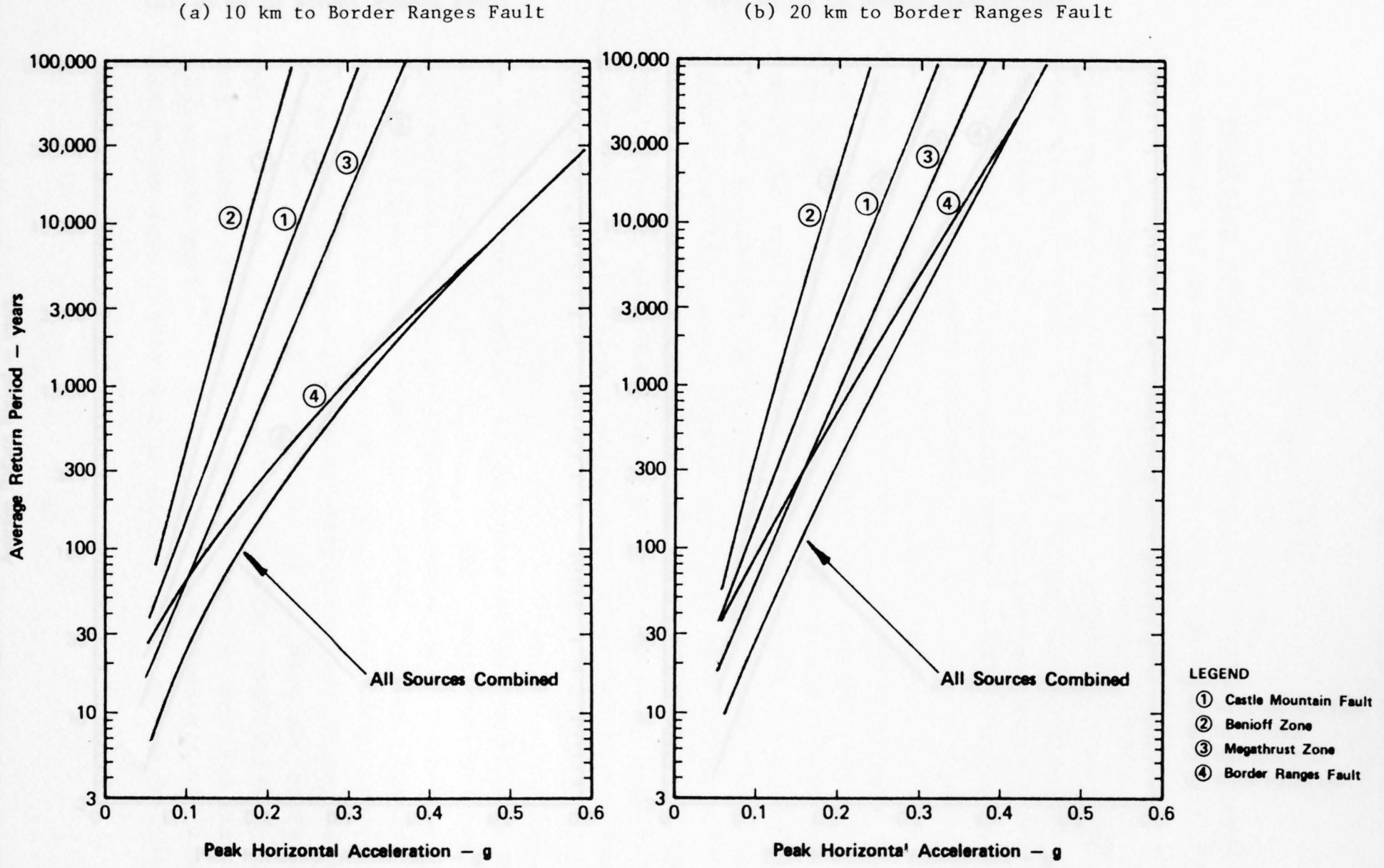

Project: Project No.	GROUND FAILURE POTENTIAL ANCHORAGE, ALASKA 41966A	UNWEIGHTED RESULTS OF PROBABILISTIC SEISMIC HAZARD ANALYSES FOR DEEP SOIL SITES	Fig. 5-3

(a) 10 km to Border Ranges Fault

(b) 20 km to Border Ranges Fault

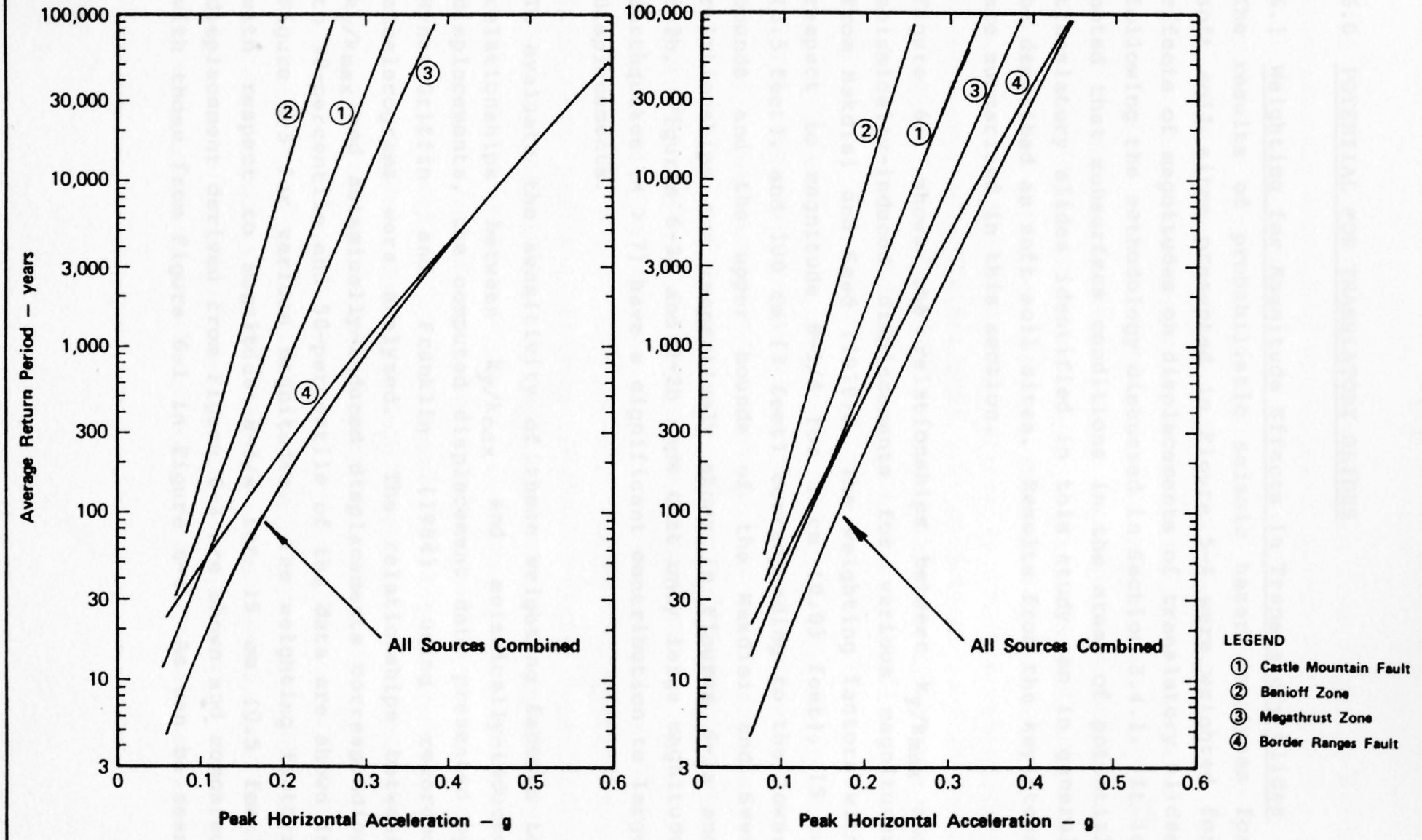

Project: Project No.	GROUND FAILURE POTENTIAL ANCHORAGE, ALASKA 41966A	UNWEIGHTED RESULTS OF PROBABILISTIC SEISMIC HAZARD ANALYSES FOR SOFT SOIL SITES	Fig. 5-4

6.0 POTENTIAL FOR TRANSLATORY SLIDES

6.1 Weighting for Magnitude Effects in Translatory Slides

The results of probabilistic seismic hazard analyses for soft soil sites presented in Figure 5-4 were weighted for effects of magnitudes on displacements of translatory slides following the methodology discussed in Section 3.4.1. It is noted that subsurface conditions in the areas of potential translatory slides identified in this study can in general be described as soft soil sites. Results from the key steps are summarized in this section.

Figure 6-1 shows the relationships between k_y/k_{max} and seismically-induced displacements for various magnitudes from Makdisi and Seed (1978). The weighting factors with respect to magnitude 8-1/4 for 1 cm (0.03 feet), 15 cm (0.5 feet), and 100 cm (3 feet) corresponding to the lower bounds and the upper bounds of the Makdisi and Seed relationships are respectively shown in Figures 6-2a and 6-2b. Figures 6-2a and 6-2b show that only large magnitude earthquakes (M > 7) have a significant contribution to large displacements.

To evaluate the sensitivity of these weighting factors to relationships between k_y/k_{max} and seismically-induced displacements, the computed displacement data presented by Hynes-Griffin and Franklin (1984) using recorded accelerograms were analyzed. The relationships between k_y/k_{max} and seismically-induced displacements corresponding to 90-percentile and 50-percentile of the data are shown in Figure 6-3 for various magnitudes. The weighting factors with respect to magnitude 8-1/4 for 15 cm (0.5 feet) displacement derived from Figure 6-3 are shown and compared with those from Figure 6-1 in Figure 6-4. As can be seen

from Figure 6-4, the weighting factors from Figure 6-3 are approximately bounded by those from Figure 6-1.

Because the relationships by Makdisi and Seed shown in Figure 6-1 are more appropriate for deep and soft soil sites in the study area compared to those based on the data by Hynes-Griffin and Franklin shown in Figure 6-3, magnitude weighting factors developed using the Makdisi-Seed displacements were used in this study. It is noted that the Makdisi-Seed relationships were developed by using response results of earth structures excited by input accelerograms (Makdisi and Seed, 1978); thus, the conditions used in their development are considered to be similar to those expected at areas of potential translatory slides identified in this study.

The relationships by Makdisi and Seed shown in Figure 6-1 go only up to magnitude 8-1/4. However, for the study area the relationships up to magnitude about 9-1/2 are required because the 1964 Alaskan earthquake had a moment magnitude of 9.2 and the maximum magnitude associated with the megathrust is 9-1/2 (Section 5). Using the extrapolated data from previous studies (Woodward-Clyde Consultants, 1982b; Idriss, 1985), the Makdisi-Seed displacements were augmented to magnitude 9-1/2. The resulting weighting factors with respect to a reference magnitude of 9-1/2 for 1 cm (0.03 feet), 15 cm (0.5 feet), and 100 cm (3 feet) are shown in Figures 6-5a and 6-5b from the lower bound and upper bound relationships, respectively.

The results of probabilistic seismic hazard analyses for soft soil sites at 10 km from the Border Ranges fault were weighted for magnitude contributions corresponding to 15 cm displacement using the lower bound (Figure 6-5a) and upper

bound (Figure 6-5b) weighting factors. The results using the lower bound and upper bound factors are shown in Figures 6-6a and 6-6b, respectively.

Because the results using the upper bound weighting factors shown in Figure 6-5b are more conservative, the results of probabilistic seismic hazard analyses (for soft soil sites at 10 km from the Border Ranges fault) were weighted for magnitude contributions corresponding to various displacements using the upper bound factors for this study. The results are shown in Figures 6-7a, 6-7b, and 6-7c for displacements of 1 cm (0.03 feet), 15 cm (0.5 feet), and 100 cm (3 feet), respectively. For increasing amount of seismically-induced displacement, the gradual reduction in the contribution by the Border Ranges fault (as well as the Castle Mountain fault and the Benioff zone) and the gradual increase in the contribution by the Megathrust zone are quite apparent in Figures 6-7a, 6-7b, and 6-7c. As can be seen in Figure 6-7c, the Megathrust zone completely dominates the total hazard for a seismically-induced displacement of 100 cm (3 feet).

6.2 k_{max} - Displacement Relationships

As discussed in Section 3.4.2, in addition to the weighted results of seismic hazard analyses, relationships between peak ground acceleration and seismically-induced permanent displacement for potential slide blocks of interest are needed in the evaluation. Because the site-by-site development of these relationships would not be possible for this study, a general relationship shown below was developed for magnitude 9-1/2 events using a generic translatory sliding block schematically shown in Figure 6-8. The sliding block shown in Figure 6-8 are considered to represent reasonably conservative conditions for the study area.

K_{max}	Range of Computed Displacement (feet)
0.14	0.05 to 0.14
0.16	0.17 to 0.47
0.18	8.3 to 15
0.20	15 to 28
0.30	31 to 57

Computed K_y = 0.128

In developing this relationship, the following equation (Idriss, 1985) was used with an overconsolidation ratio (OCR) of 1.2 to estimate the initial undrained shear resistance (Su) along the bottom sliding plane of the block.

$$Su/\sigma_{vo}' = 0.19\ (OCR)^{0.78} \qquad (6\text{-}1)$$

where σ_{vo}' is the effective overburden pressure along thew bottom sliding plane.

6.3 Potential for Translatory Slides

The results shown in Figures 6-7a, 6-7b, and 6-7c were combined with the results shown in Section 6.2 to produce relationships between seismically-induced displacement and return period shown in Figure 6-9. Because of the sensitivity of the displacement on the acceleration levels, the movements beyond 100 cm (3 feet) should be considered as large for a regional evaluation such as this study. The relationship shown in Figure 6-9 is considered to be applicable for the entire area designated as Area I in Plate I. Specific studies should be made to refine the likelihood of seismically-induced permanent displacements at a specific site for important structures particularly if the site is considered to be better than that indicated by Figure 6-9 or if the site, such as the Turnagain Heights area, has a known history of very large translatory slides.

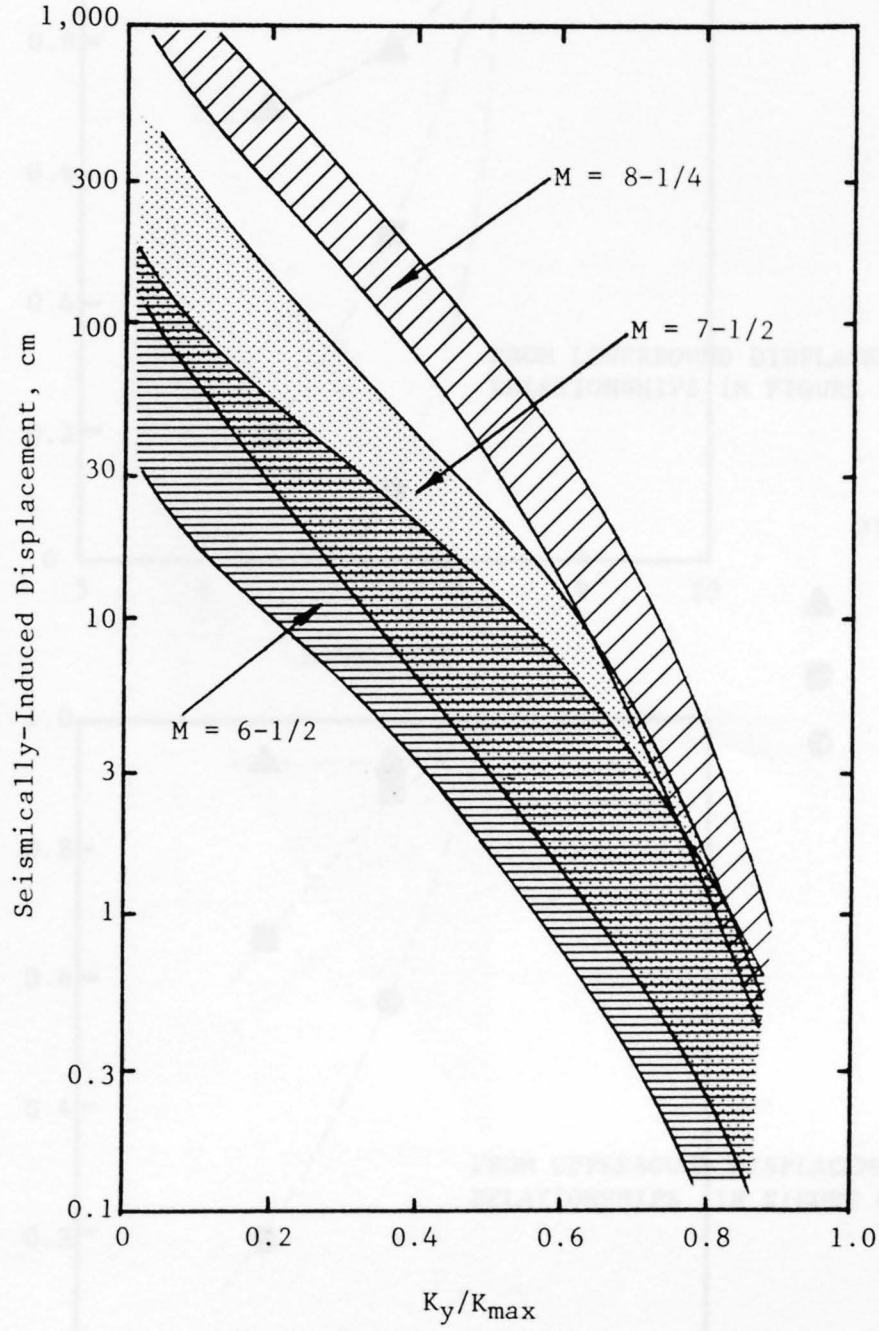

(Makdisi and Seed, 1978)

Project GROUND FAILURE POTENTIAL ANCHORAGE, ALASKA Project No. 41966A	CHART FOR SEISMICALLY-INDUCED PERMANENT DISPLACEMENT - MAKDISI AND SEED	Fig. 6-1

(a)

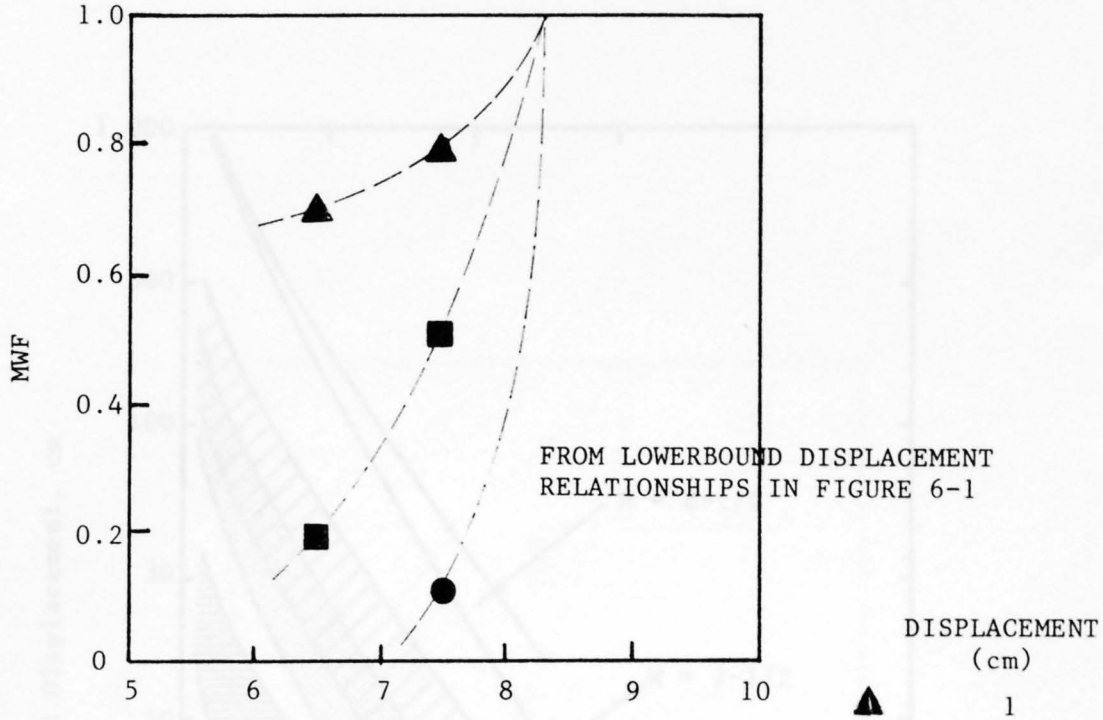

(b)

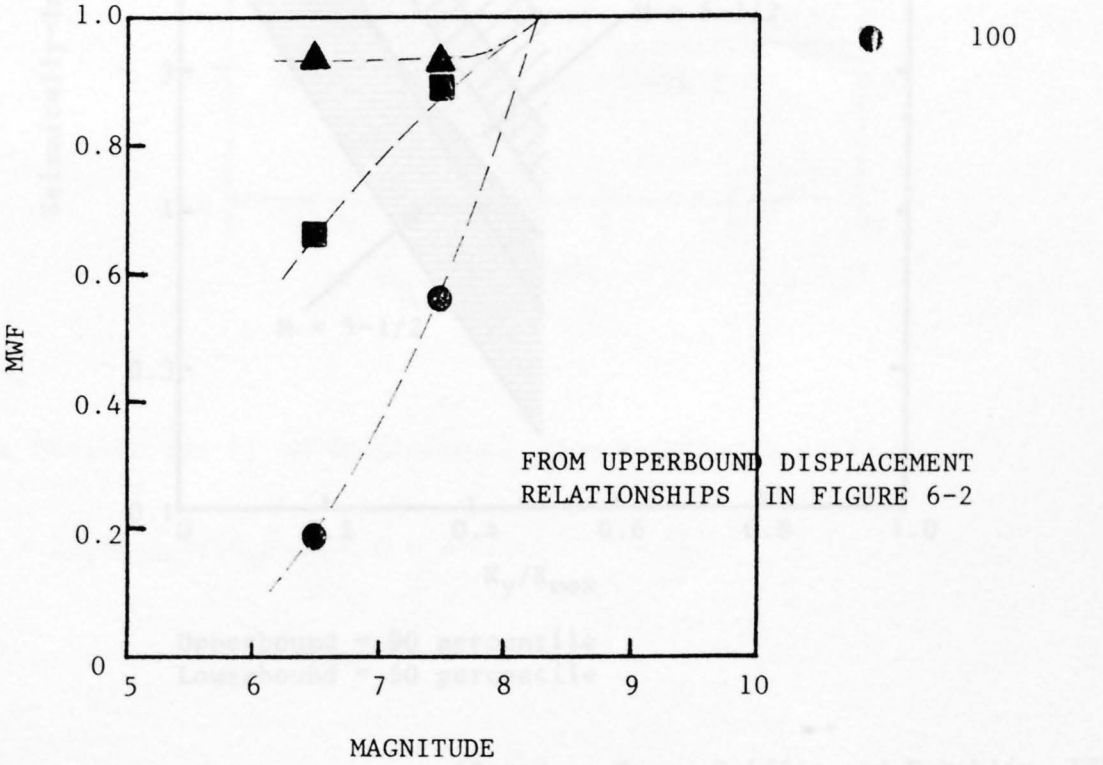

MWF = Magnitude Weighting Factors = $(K_y/K_{max})/(K_y/K_{max})$ m = 8-1/4

Project GROUND FAILURE POTENTIAL ANCHORAGE, ALASKA Project No. 41966A	MAGNITUDE WEIGHTING FACTORS FROM MAKDISI AND SEED DISPLACEMENT RELATIONSHIPS	Fig. 6-2

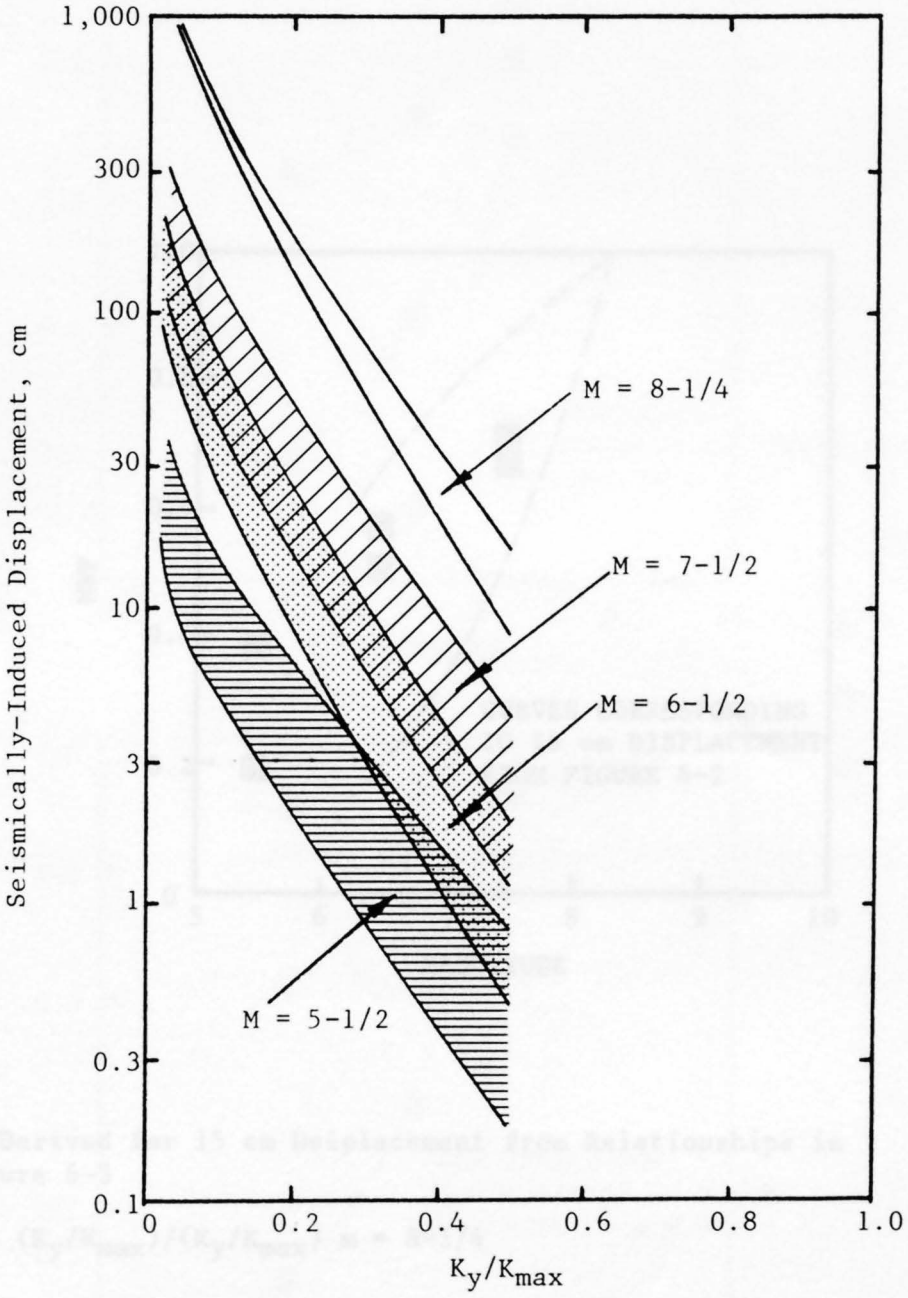

Upperbound = 90 percentile
Lowerbound = 50 percentile

(Based on Hynes-Griffin and Franklin, 1984)

Project GROUND FAILURE POTENTIAL ANCHORAGE, ALASKA Project No. 41966A	CHART FOR SEISMICALLY-INDUCED PERMANENT DISPLACEMENT BASED ON HYNES-GRIFFIN AND FRANKLIN	Fig. 6-3

WOODWARD-CLYDE CONSULTANTS

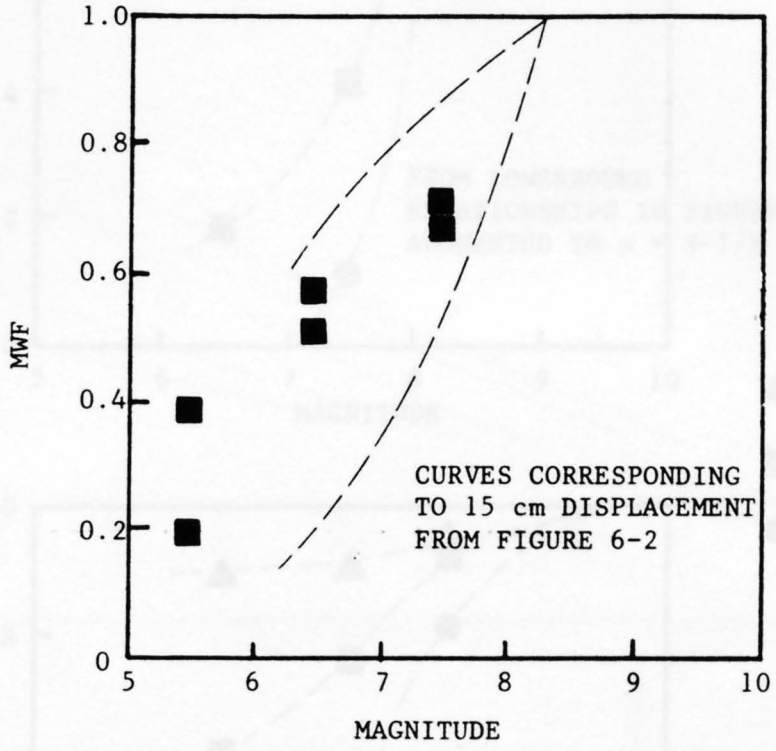

Data Derived for 15 cm Dsiplacement from Relationships in Figure 6-3

MWF = $(K_y/K_{max})/(K_y/K_{max})$ m = 8-1/4

Project GROUND FAILURE POTENTIAL ANCHORAGE, ALASKA Project No. 41966A	COMPARISON OF MAGNITUDE WEIGHTING FACTORS FOR TRANSLATORY SLIDES	Fig. 6-4

(a)

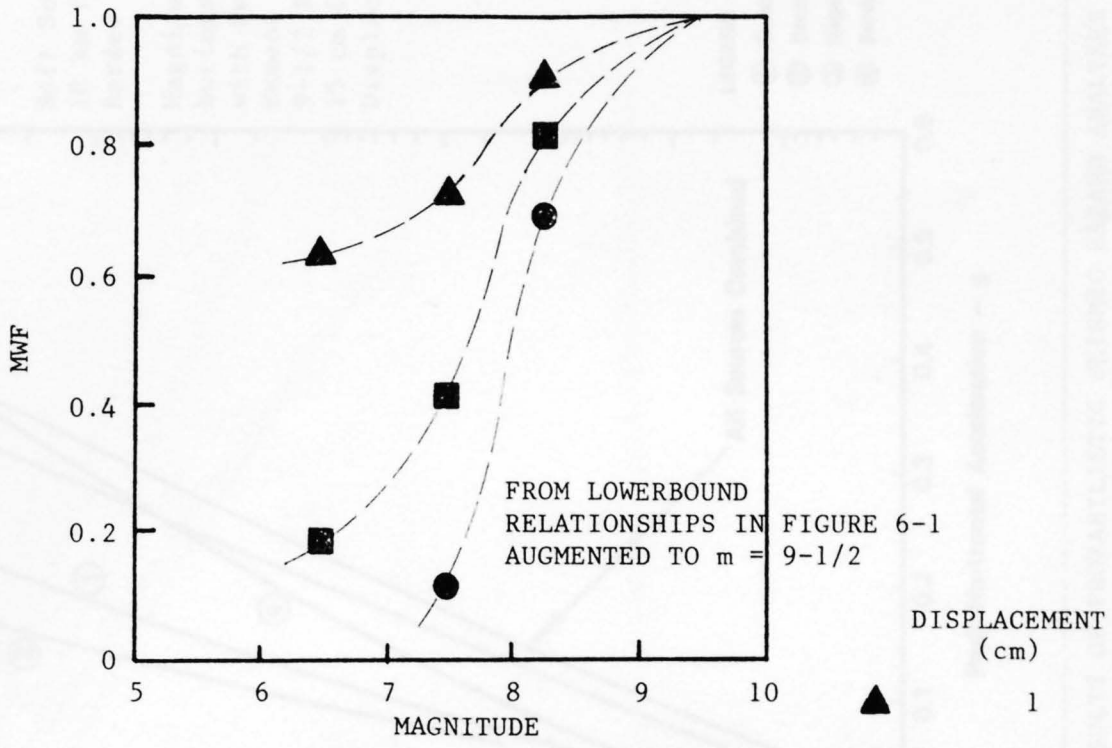

(b)

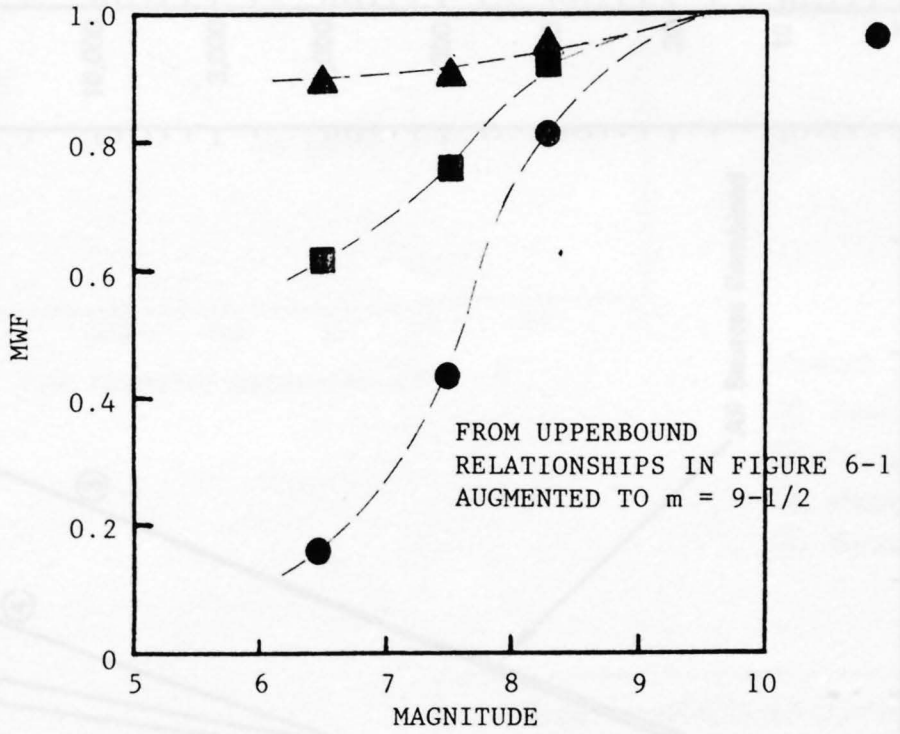

$MWF = (K_y/K_{max})/(K_y/K_{max})\ m = 9\text{-}1/2$

Project GROUND FAILURE POTENTIAL ANCHORAGE, ALASKA Project No. 41966A	MAGNITUDE WEIGHTING FACTORS FOR TRANSLATORY SLIDES ANCHORED TO M = 9-1/2	Fig. 6-5

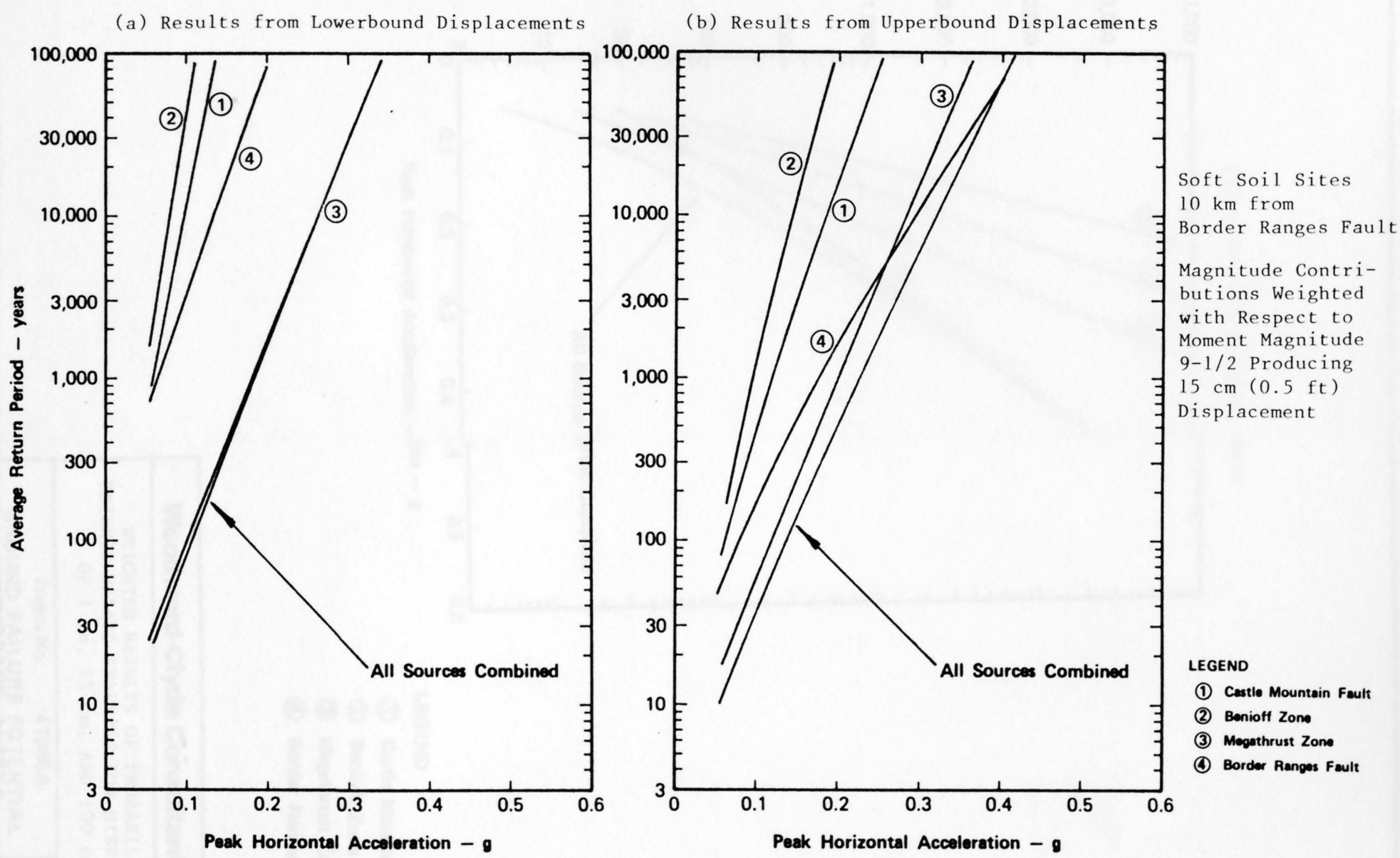

Project: Project No.	GROUND FAILURE POTENTIAL ANCHORAGE, ALASKA 41966A	WEIGHTED RESULTS OF PROBABILISTIC SEISMIC HAZARD ANALYSES COMPARISON OF LOWERBOUND AND UPPERBOUND RESULTS	Fig. 6-6

(a) 1 cm Displacement

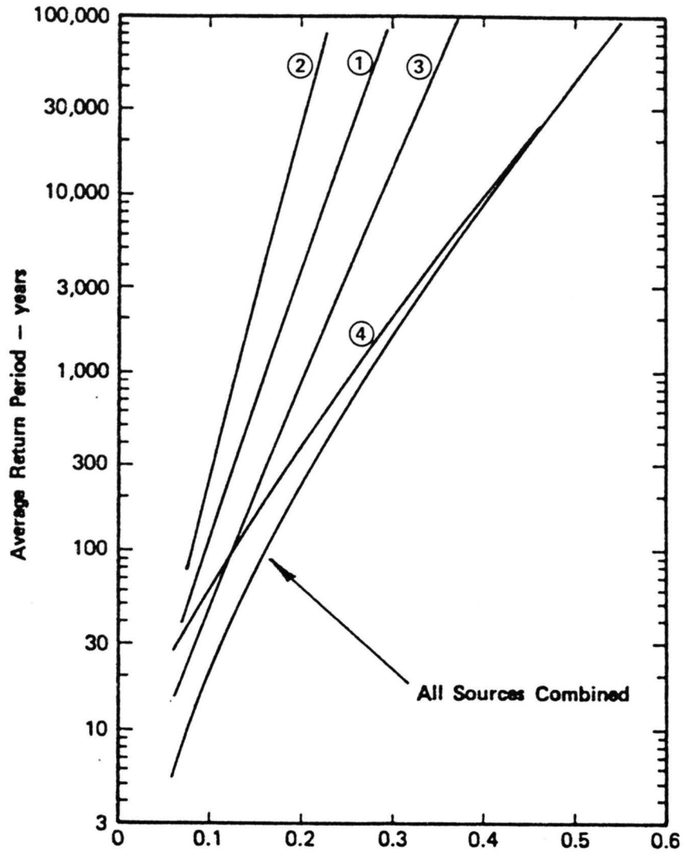

(b) 15 cm Displacement

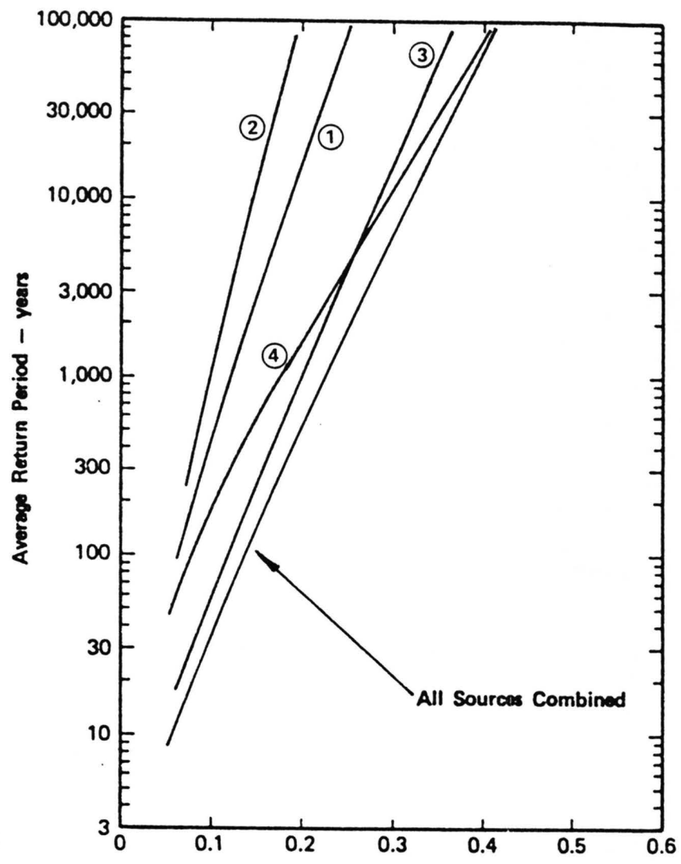

(c) 100 cm Displacement

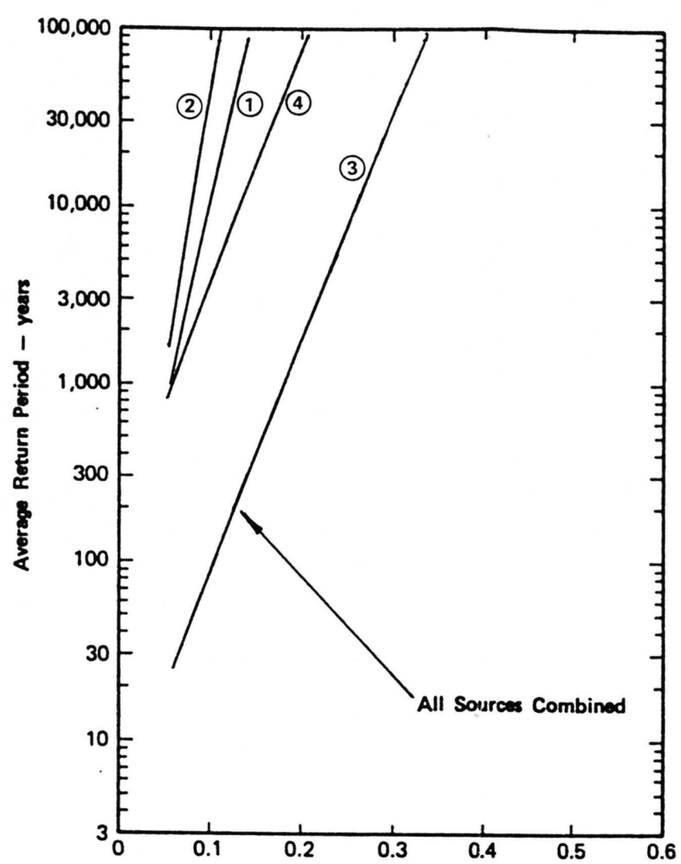

LEGEND

① Castle Mountain Fault
② Benioff Zone
③ Megathrust Zone
④ Border Ranges Fault

Soft Soil Sites
10 km to Border Ranges Fault

Magnitude Contributions
Weighted with Respect to
Moment Magnitude 9-1/2
Producing Indicated
Displacements Using
Upperbound Values

Woodward-Clyde Consultants

WEIGHTED RESULTS OF PROBABILISTIC SEISMIC HAZARD ANALYSES FOR DISPLACEMENTS OF 1 cm, 15 cm, AND 100 cm

Project No. 41966A

GROUND FAILURE POTENTIAL
ANCHORAGE, ALASKA

Fig. 6-7

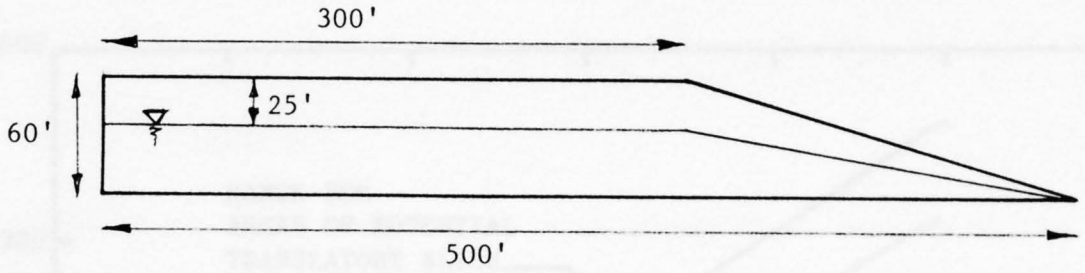

Values Used in Analyses:

Average γ_t = 120 pcf (average total unit weight)

$Su = 0.19\ (OCR)^{0.78}\sigma_{vo}'$ (undrained shear strength)

$K_a = 0.33$ (coefficient of active earth pressure)

Project GROUND FAILURE POTENTIAL ANCHORAGE, ALASKA Project No. 41966A	SLIDING BLOCK USED IN TRANSLATORY SLIDE COMPUTATIONS	Fig. 6-8

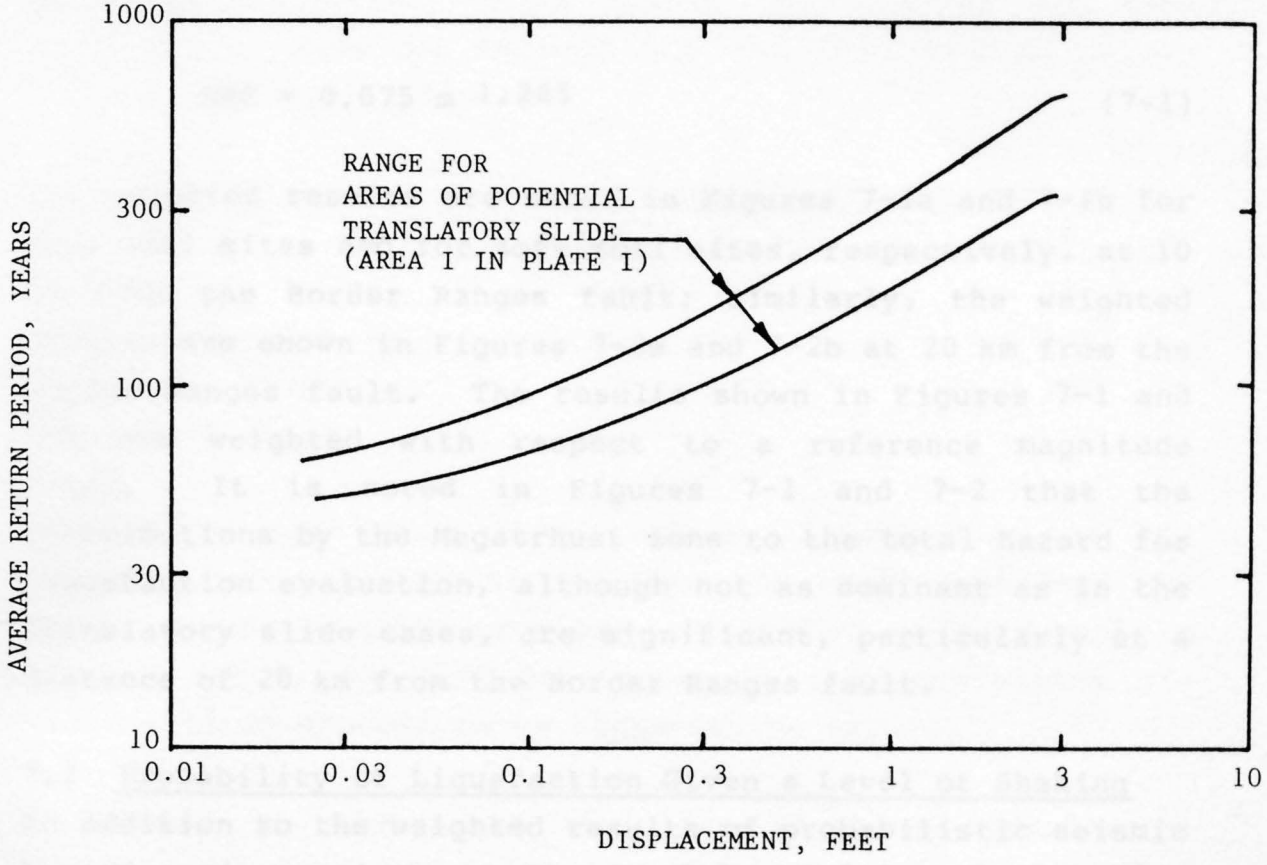

Project GROUND FAILURE POTENTIAL ANCHORAGE, ALASKA Project No. 41966A	TRANSLATORY SLIDING POTENTIAL	Fig. 6-9

7.0 POTENTIAL FOR LIQUEFACTION

7.1 Weighting for Magnitude Effects in Liquefaction

The results of probabilistic seismic hazard analyses for deep soil sites and for soft soil sites presented in Figures 5-3 and 5-4 were weighted for effects of magnitudes on liquefaction (Section 3.4.1) using the following magnitude weighting factors (Idriss, 1985) with a reference magnitude of 7-1/2:

$$MWF = 0.075\ m^{1.285} \qquad (7\text{-}1)$$

The weighted results are shown in Figures 7-1a and 7-1b for deep soil sites and for soft soil sites, respectively, at 10 km from the Border Ranges fault; similarly, the weighted results are shown in Figures 7-2a and 7-2b at 20 km from the Border Ranges fault. The results shown in Figures 7-1 and 7-2 are weighted with respect to a reference magnitude 7-1/2. It is noted in Figures 7-1 and 7-2 that the contributions by the Megatrhust zone to the total hazard for liquefaction evaluation, although not as dominant as in the translatory slide cases, are significant, particularly at a distance of 20 km from the Border Ranges fault.

7.2 Probability of Liquefaction Given a Level of Shaking

In addition to the weighted results of probabilistic seismic hazard analyses shown in Figures 7-1 and 7-2, relationships between probability of liquefaction (given a peak ground acceleration from a magnitude 7-1/2 event) and peak ground acceleration are required for evaluation of liquefaction potential (Section 3.4.3). Such relationships for the selected geological units are shown in Table 7-1.

7.3 Liquefaction Potential

The appropriate results in Figures 7-1 and 7-2 are combined with those in Table 7-1 to develop the relationships between liquefaction potential and return period for the selected geological units. The resulting relationships can be integrated to obtain probability of liquefaction associated with the selected geological units for a one-year or any other period. Such computations for deep soil sites at 10 km from the Border Ranges fault, representing the most conservative case in Figures 7-1 and 7-2, result in the following probabilities:

	Probability of Liquefaction	
	One-Year Period	100-Year Period
Alluvium (Q_{al})	9×10^{-5}	9×10^{-3}
Naptowne Outwash (Q_o)	7×10^{-5}	7×10^{-3}
Bootlegger Cove Formation (Q_{bc})	9×10^{-4}	9×10^{-2}

As can be seen from these values, liquefaction of the selected sandy geological units in the study area does not appear to be a major problem. Note that as discussed in Section 4.4.2, the SPT data used in this evaluation are considered in general to be conservative values.

It should be emphasized that the above observation is general and applicable for the selected geological units. The geology in the Anchorage area indicates that wide local variations in soil properties are likely. Thus, for example, loose sandy zones could be locally present in parts of the study area. These local zones should have much higher liquefaction potential than the numbers calculated for the above selected geological units would indicate. Furthermore, large number of ground cracks caused by the

1964 Alaskan earthquake should not be forgotten. It is quite possible that near-surface soil deposits in the study area under significant earthquake shaking would be more prone to fissuring due to seismically-induced ground deformations than to extensive liquefaction. The amount of ground deformation may be enhanced by increase in excess pore water pressures caused by the earthquake shaking.

TABLE 7-1

CONDITIONAL PROBABILITY OF LIQUEFACTION

Geological Unit	Number of SPT Data	Conditional Probability of Liquefaction Given Following Peak Ground Acceleration Value		
		0.1 g	0.2 g	0.3 g
Alluvium (Q_{al})	32	0.11×10^{-9}	0.12×10^{-2}	0.25×10^{-1}
Naptowne Outwash (Q_o)	238	0.14×10^{-9}	0.83×10^{-3}	0.19×10^{-1}
Bootlegger Cove Formation (Q_{bc})	580	0.45×10^{-2}	0.25×10^{-1}	0.89×10^{-1}

Note:

The above probability values were computed for magnitude 7-1/2 using the relationships in Figure 3-7.

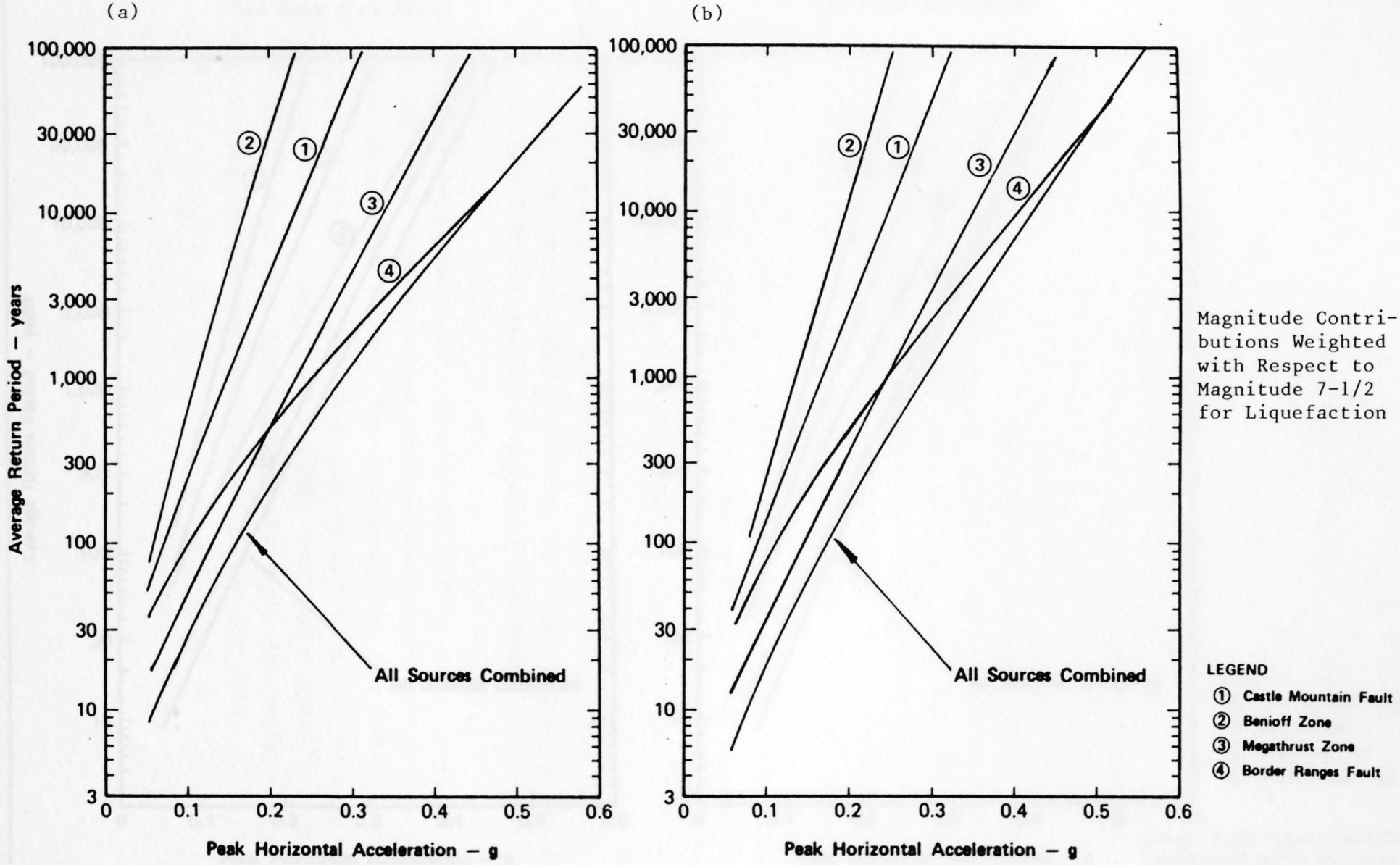

Project: Project No.	GROUND FAILURE POTENTIAL ANCHORAGE, ALASKA 41966A	WEIGHTED RESULTS OF PROBABILISTIC SEISMIC HAZARD ANALYSES 10 km TO BORDER RANGES FAULT	Fig. 7-1

(a) Deep Soil Sites

(b) Soft Soil Sites

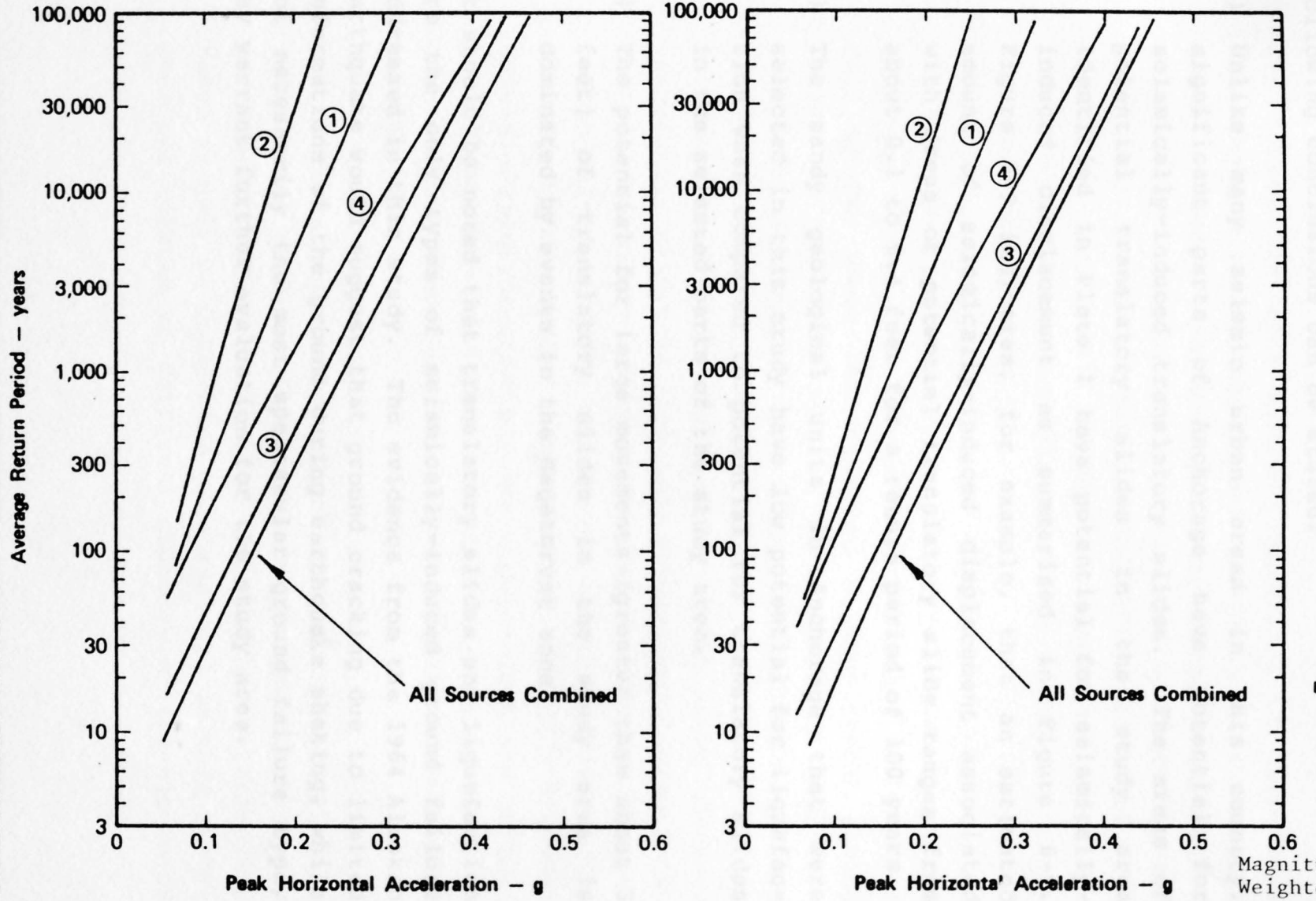

Magnitude Contributions Weighted with Respect to Magnitude 7-1/2 for Liquefaction

Project: GROUND FAILURE POTENTIAL ANCHORAGE, ALASKA Project No. 41966A	WEIGHTED RESULTS OF PROBABILISTIC SEISMIC HAZARD ANALYSES 20 km TO BORDER RANGES FAULT	Fig. 7-2

8.0 CONCLUSIONS AND RECOMMENDATIONS FOR FURTHER STUDIES

From the results of the study presented in this report, the following conclusions can be stated:

1) Unlike many seismic urban areas in this country, significant parts of Anchorage have potential for seismically-induced translatory slides. The areas of potential translatory slides in the study area identified in Plate I have potential for seismically-induced displacement as summarized in Figure 6-9. Figure 6-9 indicates, for example, that an estimated amount of seismically-induced displacement associated with areas of potential translatory slide ranges from about 0.1 to 0.4 feet for a return period of 100 years.

2) The sandy geological units in Anchorage that were selected in this study have low potential for liquefaction when compared to potential for translatory slides in the selected parts of the study area.

3) The potential for large movements (greater than about 3 feet) of translatory slides in the study area is dominated by events in the Megathrust zone.

It should be noted that translatory slides and liquefaction are the only types of seismically-induced ground failure addressed in this study. The evidence from the 1964 Alaskan earthquake would suggest that ground cracking due to limited deformations of the ground during earthquake shaking, while not necessarily the most spectacular ground failure type, may warrant further evaluation for the study area.

Based on the above conclusions and the results of this study, the following recommendations for further studies are made:

1) The effects of more accurate modelling of recurrence associated with the Megathrust zone should be investigated. Because the potential for large movements of translatory slides in the study area is dominated by the Megathrust zone, a better characterization of the Megathrust zone should improve the understanding of the likelihood of large translatory slide movements in the Anchorage area.

2) The relationships between seismically-induced displacement and k_y/k_{max} for areas of translatory slides (as well as for areas that resulted in significant ground cracks in the 1964 Alaskan earthquake) in Anchorage should be developed. The relationships used in this study were an augmented version of relationships developed by Makdisi and Seed for earth dams. Because translatory slides in Anchorage involve earth structures that are somewhat different from earth dams and because the undrained shearing resistance along the base of the sliding block changes with shaking and displacement, specific relationships between displacement and k_y/k_{max} should be developed for the Anchorage area with an emphasis on displacements due to magnitude nine plus earthquakes.

3) The effects of attenuation on the potential for translatory slides and liquefaction in Anchorage should be investigated. Because an attenuation relationship based largely on California data was used in this study, possible effects of different attenuation relationships

that may be more appropriate for the Anchorage area should be investigated with an emphasis on the attenuation of earthquake motions from the Megathrust zone.

4) The mechanism of translatory slides in the Anchorage area should be investigated further. In particular, the main factors affecting the dimensions and details of translatory slides should be evaluated. For example, the main reasons for the difference between the 1964 L-Street slide (a single block, moving up to about 14 feet with a graben behind it) and the 1964 Turnagain Heights slide (many disintegrated blocks, moving hundreds of feet) should be evaluated for a better planning of land use in the Anchorage area.

Finally, it is noted that this study is intended to provide a regional characterization of the seismic hazard and the likelihood of translatory slides and liquefaction in susceptible soils in the Anchorage urban area. Results of the study are not intended to be used in place of site-specific evaluations. At any specific site, the likelihood of translatory slides and liquefaction could vary significantly from the results presented herein due to variation in the soil characteristics, depth to ground water, and geometry.

9.0 REFERENCES

Abe, K. (1975) "Reliable Estimation of the Seismic Moment of Large Earthquakes", Journal of Physics of the Earth, v. 23, 381-390.

Bruhn, R. L. (1979) "Holocene Displacement Measured by Trenching the Castle Mountain Fault near Houston, Alaska", Alaska Division of Geologic and Geophysical Surveys, Geology Department 61, 1-4.

Castro, G., and Poulos, S. J. (1977) "Factors Affecting Liquefaction and Cyclic Mobility", Journal of the Geotechnical Engineering Division, ASCE, v. 103, no. GT6, 501-506.

Cornell, C. A. (1968) "Engineering Seismic Risk Analysis", Bulletin of the Seismological Society of America, v. 58, no. 5, 1583-1606.

Davies, J. N. and House, L. (1979) "Aleutian Subduction Zone Seismicity, Volcano-Trench Separation, and Their Relation to the Great Thrust-Type Earthquakes", Journal of Geophysical Research, v. 84, 4583-4591.

Davison, F. C. and Scholz, C. H. (1985) "A Moment Magnitude Scale", Journal of Geophysical Research, v. 84, 2348-2350.

Der-Kiureghian, A. and Ang, A. H.-S. (1977) "A Fault-Rupture Model for Seismic Risk Analysis", Bulletin of the Seismological Society of America, v. 67, no. 4, 1173-1194.

Detterman R. L., Plafker, G., Judson, T., Tysdal, R. G., and Pavoni, N. (1974) "Surface Geology and Holocene Breaks Along the Susitna Segment of the Castle Mountain Fault, Alaska", U.S. Geological Survey Miscellaneous Field Studies Map, MF-618, Scale 1:24,000, 1 sheet.

Detterman, R. L., Plafker, G., Tysdal, R. G., and Hudson, T. (1976) "Geology of Surface Features Along Part of the Talkeetna Segment of the Castle Mountain-Caribou Fault System, Alaska", U.S. Geological Survey Miscellaneous Field Studies Map, MF-738, Scale 1:63,360, 1 sheet.

Dickinson, W. R. and Seeley, D. R. (1979) "Structure and Stratigraphy of Fore-Arc Regions", Bulletin of the American Association of Petroleum Geologists, v. 63, no. 1, 2-31.

Dobrovolny, E. and Schmoll, H. R. (1974) "Slope-Stability Map of Anchorage and Vicinity, Alaska", U.S. Geological Survey Map I-787-E.

Evans, C. D., Buck, E., Buffler, R., Fisk, G., Forbes, R., and Parker, W. (1972) "The Cook Inlet Environment: A Background Study of Available Knowledge", University of Alaska, Resource and Science Service Center, Alaska Sea Grant Program, Anchorage, Alaska.

Grantz, A. (1966) "Strike-Slip Faults in Alaska", U.S. Geological Survey Open Field Report, 82 p.

Hanks, T. C. and Kanamori, H. (1979) "A Moment Magnitude Scale", Journal of Geophysical Research, v. 82, 2981-2987.

Hansen, W. R. (1965) "Effects of the Earthquake of March 27, 1964 at Anchorage, Alaska; The Alaska Earthquake, March 27, 1964, Effects on Communities", U.S. Geological Survey Professional Paper, 542-A p.

Harding-Lawson Associates (1979) "Geotechnical Hazards Assessment, Municipality of Anchorage, Anchorage, Alaska", report prepared for Municipality of Anchorage, Alaska.

Housner, G. W. and Jennings, P. C. (1964) "Generation of Artificial Earthquakes", ASCE, Journal of Engineering Mechanics Division, v. 90, 113-150.

Hynes-Griffin, M. E. and Franklin, A. G. (1984) "Rationalizing the Seismic Coefficient Method", Miscellaneous Paper GL-84-13, Department of the Army, Waterways Experiment Station, Corps of Engineers.

Idriss, I. M. (1985) "Evaluating Seismic Risk in Engineering Practice", Proceedings, XI International Conference on Soil Mechanics and Foundation Engineering, v. I, 255-320, San Francisco, California, August.

Idriss, I. M., Sadigh, K., and Power, M. S. (1982) "Dependence of Peak Horizontal Accelerations and Velocities on Earthquake Magnitude at Close Distances to the Source", Paper presented at the Special Session on Ground Motion Parameters, Seismological Society of America Annual Meeting, Anaheim, California, April.

Jacobs, K. H. and Mori, J. (1984) "Strong Motions in Alaska-Type Subduction Zone Environment", Proceedings of the Eight World Conference on Earthquake Engineering, v. II, San Francisco, California.

Kanamori, H. (1977) "The Energy Release in Great Earthquakes", Journal of Geophysical Research, v. 82, 1073-1096.

Karlstrom, T. V. (1964) "Quaternary Geology of the Kenai Lowland and Glacial History of the Cook Inlet Region, Alaska", U.S. Geological Survey Professional Paper 443, 69 p.

Kawakatsu, H. and Seno, T. (1983) "Triple Seismic Zone and the Regional Variation of Seismicity Along the Northern Honshu Arc", Journal of Geophysical Research, v. 88, 4215-4230.

Kelley, J. (1981) personal communication.

Kerr, P. F. and Drew, I. M. (1965) "Quick Clay Movements, Anchorage, Alaska", A Preliminary Report, Air Force Cambridge Research Laboratories Scientific Reports (AFCRL-66-78), Bedford, MA, USAF, Office of Aerospace Research.

Kulkarni, R. B., Sadigh, K., and Idriss, I. M. (1979) "Probabilistic Evaluation of Seismic Exposure", Proceedings, Second U.S. National Conference on Earthquake Engineering, Stanford, California, 90-98.

Lahr, J. and Stevens, C. (1982) personal communication, Seismologists, U.S. Geological Survey, Menlo Park.

Lahr, J. C., Page, R. A., and Fogleman, K. A. (1985) "The 1984 Sutton Earthquake--New Evidence for Activity of the Castle Mountain Fault (Abst.)", Seismological Society of America Annual Meetings Program with Abstracts.

Long, E. L. (1973) "Earth Slides and Related Phenomena", The Great Alaska Earthquake of 1964, National Academy of Science, 644-773.

MacKevett, E. M. and Plafker, G. (1974) "The Border Ranges Fault in South-Central Alaska", U.S. Geological Survey, Journal Research, v. 2, 323-329.

Magoon, L. B., Adkinson, W. L., and Egbert, R. M. (1976) "Map Showing Geology Wildcat Wells Tertiary Plant Fossil Locations, K-Ar Age Dates and Petroleum Operations, Cook Inlet Area, Alaska", U.S. Geological Survey Map I-1019, scale 1:250,000.

Makdisi, F. I. and Seed, H. B. (1978) "Simplified Procedure for Estimating Dam and Embankment Earthquake-Induced Deformations", Journal of the Geotechnical Engineering Division, ASCE, v. 104, no. GT7, 849-867.

McCulloch, D. S. and Bonilla, M. G. (1970) "Effects of the Earthquake of March 27, 1964, on the Alaska Railroad", U.S. Geological Survey Professional Paper 545-D, D1-D161.

McGuire, R. K. (1976) "FORTRAN Computer Program for Seismic Risk Analysis", U.S. Geological Survey, Open-File Report 76-67.

Miller, R. D. and Dobrovolny, E. (1959) "Surficial Geology of Anchorage and Vicinity, Alaska", U.S. Geological Survey Bulletin 1093, 128 p.

Mitchell, J. K., Houston, W. N., and Yamane, G. (1973) "Sensitivity and Geotechnical Properties of Bootlegger Cove Clay", National Academy of Sciences, The Great Alaska Earthquake of 1964, Engineering, 157-178.

Newmark, N. M. (1965) "Effects of Earthquakes on Dams and Embankments", Geotechnique, v. 5, no. 2, June.

Page, R. A. (1968) "Aftershocks and Microaftershocks of the Great Alaska Earthquake of 1964", Bulletin of the Seismological Society of America, v. 58, 1131-1168.

Page, R. A. and Lahr, J. (1971) "Measurements for Fault Slip on the Denali, Fairweather and Castle Mountain Faults, Alaska", Journal of Geophysical Research, v. 76, 8543-8544.

Pewe, T. L. (1975) "Quaternary Geology of Alaska", U.S. Geological Survey Professional Paper 835, 145 p.

Schmoll, H. R. and Dobrovolny, E. (1972a) "Generalized Geologic Map of Anchorage and Vicinity, Alaska", U.S. Geological Survey Map I-787-A.

Schmoll, H. R. and Dobrovolny, E. (1972b) "Slope Map of Anchorage and Vicinity, Alaska", U.S. Geological Survey Map I-787-B.

Schmoll, H. R. and Dobrovolny, E. (1974) "Foundation and Excavation Conditions, Map of Alaska and Vicinity, Alaska", U.S. Geological Survey Map I-787-D.

Seed, H. B. (1968) "Landslides During Earthquakes Due to Soil Liquefaction", Journal of the Soil Mechanics and Foundations Division, ASCE, v. 94, no. SM5, 1055-1122.

Seed, H. B. (1979) "Soil Liquefaction and Cyclic Mobility Evaluation for Level Ground During Earthquakes", Journal of the Geotechnical Engineering Division, ASCE, v. 105, no. GT2, 201-255.

Seed, H. B. and Lee, K. L. (1966) "Liquefaction of Saturated Sands During Cyclic Loading", Journal of the Soil Mechanics and Foundations Division, ASCE, v. 92, no. SM6, 105-134.

Seed, H. B. and Idriss, I. M. (1971) "Simplified Procedure for Evaluating Soil Liquefaction Potential", Journal of the Soil Mechanics and Foundations Division, ASCE, v. 97, no. SM9, 1249-1273.

Seed, H. B. and Idriss, I. M. (1982) "Ground Motions and Soil Liquefaction During Earthquakes", Monograph Series No. 5, Earthquake Engineering Research Institute, Berkeley, California, December.

Seed, H. B. and Wilson S. D. (1967) "The Turnagain Heights Landslide, Anchorage, Alaska", Journal of the Soil Mechanics and Foundation Division, ASCE, v. 93, no. SM$, July, 325-353.

Seed, H. B., Idriss, I. M., and Arango, I. (1983) "Evaluation of Liquefaction Potential Using Field Performance Data", Journal of Geotechnical Engineering, ASCE, v. 109, no. 3, 458-482.

Seed, H. B., Tokimatsu, K., Harder, L. F., and Chung, R. M. (1985) "Influence of SPT Procedures in Soil Liquefaction Resistance Evaluations", Journal of Geotechnical Engineering, v. 111, no. 12, December.

Seno, T., Shimazaki, K., Somerville, P., Sudo, K., and Eguchi, T. (1980) "Rupture Process of the Miyagi-Oki, Japan, Earthquake of June 12, 1978", Physics of the Earth and Planetary Interiors, v. 23, 39-61.

Shah, H. C., Mortgat, C. P., Kiremedjian, A. S., and Zsutty, T. C. (1975) "A Study of Seismic Risk for Nicaragua, Part I", The John A. Blume Earthquake Engineering Center, Technical Report No. 11, Department of Civil Engineering, Stanford University.

Shannon and Wilson (1964) "Report on Anchorage Area Soil Studies, Alaska", Report prepared for the U.S. Army Engineer District, Anchorage, Alaska, Contract No. DA-95-507-CIVENG-64-18.

Steinbrugge, K. V. (1970) "Earthquake Engineering", Robert L. Wiegel, Editor, Prentice-Hall, 167-226.

Sykes, L. R. and Quittmeyer, R. C. (1981) "Repeat Times of Great Earthquakes along Simple Plate Boundaries", in Simpson, D. W., and Richards, P. G., eds., 1981, Maurice Ewing Series No. 4, Earthquake Prediction and International Review: Washington, D.C., American Geophysical Union, 217-246.

Trainer, F. W. and Waller, R. M. (1965) "Subsurface Stratigraphy of Glacial Drift at Anchorage, Alaska", U.S. Geological Survey Professional Paper 525-D, D167-D174.

Tysdal, R. G. and Case, J. E. (1979) "Geologic Maps of the Seward and Blying Sand Quadrangles, Alaska", U.S. Geological Survey Map I-1150, scale 1:250,000, with text.

Ulery, C. A. and Updike, R. G. (1983) "Subsurface Structure of the Cohesive Facies of the Bootlegger Cove Formation in Southwest Anchorage, Alaska", Alaska Division of Geological and Geophysical Surveys Professional Report 84, 5 p., scale 1:15,840, 3 sheets.

Updike, R. G. (1982) personal communication, Geologist, State of Alaska, Division of Geological and Geophysical Surveys.

Updike, R. G. (1984) personal communication, Geologist, State of Alaska, Division of Geological and Geophysical Surveys.

Updike, R. G. (1985) personal communication, Geologist, State of Alaska, Division of Geological and Geophysical Surveys.

Updike, R. G. (1985) "Engineering Geologic Maps, Government Hill Area, Anchorage, Alaska", U.S. Geological Survey I-Series Map, I-1610.

Updike, R. G. (1986) personal communication, Geologist, State of Alaska, Division of Geological and Geophysical Surveys.

Updike, R. G. and Carpenter, B. A. (1985) "Engineering Geology of the Government Hill Area, Anchorage, Alaska", U.S. Geological Survey Bulletin 1588, in press.

Updike, R. G. and Ulery, C. A. (1983) "Preliminary Geologic Map of the Anchorage B-6 NW (Eklutna Lake) Quadrangle, Alaska", Alaska Division of Geological and Geophysical Surveys, Report of Investigations 83-8, 2 plates.

Updike, R. G. and Ulery, C. A. (1985) "Engineering Geologic Map and Cross Sections, Southwest Anchorage, Alaska", Alaska Division of Geological and Geophysical Surveys Professional Report 89.

Wesnousky, S. G., Scholz, C. H., Shimazaki, K., and Masuda, T. (1983) "Earthquake Frequency Distribution and the Mechanics of Faulting", Journal of Geophysical Research, v. 88, no. B11, 9331-9340.

Woodward-Clyde Consultants (1979) "Report of the Evaluation of Maximum Earthquake and Site Ground Motion Parameters Associated with the Offshore Zone of Deformation, San Onofre Nuclear Generating Station", prepared for Southern California Edison.

Woodward-Clyde Consultants (1981) "Report on the Bradley Lake Hydroelectric Project Design Earthquake Study", submitted to the Department of Army, Alaska District, Corps of Engineers, Anchorage, Alaska.

Woodward-Clyde Consultants (1982a) "Final Report on Seismic Studies for Susitna Hydroelectric Project", report prepared for Acres American, Inc., Buffalo, New York.

Woodward-Clyde Consultants (1982b) "Anchorage Office Complex, Geotechnical Investigation, Anchorage, Alaska, Volumes I-III", report prepared for Alaska Department of Transportation and Public Facilities, Central Region, Design and Construction, Anchorage, Alaska.

Woodward-Clyde Consultants (1985) "A Re-evaluation of the 1964 "L" Street Slide", report prepared for Headquarter Materials, Public Facilities, Alaska Department of Transportation, Anchorage, Alaska.

Woodward-Clyde Consultants (1986) "Anchorage Seismic Hazard Study", report prepared for Municipality of Anchorage, 16 May 1986.

Woodward-Clyde Consultants (1987) "Seismic Risk Study - Technical Report" report in preparation for Municipality of Anchorage.

ZONE I

ZONE I

ZONE I

ZONE I

ZONE OF POTENTIAL TRANSLATORY SLIDE

0 1 2 KILOMETERS

0 1 2 MILES

The zones shown in this map reflect only the general and average trend of potential for estimated seismic ground damage. Local variation of the subsurface conditions likely will have very significant effects on the actual seismic ground performance in a given area.

Woodward-Clyde Consultants

ZONES OF POTENTIAL TRANSLATORY SLIDES

GROUND FAILURE POTENTIAL
ANCHORAGE, ALASKA

JOB NO. 4190A

APPROVAL

CONSULTING ENGINEERS, GEOLOGISTS AND ENVIRONMENTAL SCIENTISTS

DATE: SEPTEMBER 1987 | PLATE 1

APPENDIX A

SEISMIC SOURCES

APPENDIX A
SEISMIC SOURCES

The following sections describe the known characteristics of the seismic sources that are considered significant to the seismic ground motions in the Anchorage area. As discussed in Section 5.2 of the main text, the sources can be divided into shallow (crustal) sources and deep sources associated with the subduction zone.

A.1 Shallow (Crustal) Seismic Sources

A.1.1 Castle Mountain Fault

The Castle Mountain fault is a right-lateral strike-slip and reverse fault about 475 km long. As can be seen in Figure A-1, it is trending east-northeast/west-southwest subparallel to the northwest shore of Cook Inlet (Woodward-Clyde Consultants, 1982a). The fault is located about 40 km northwest of the downtown Anchorage area at its closest approach. Displacement along the fault initiated about the end of Mesozoic time (Grantz, 1966), approximately 60 to 70 million years before present (m.y.b.p.). Evidence of Holocene (11,000 y.b.p.) displacement is observed only along the 80 km long western segment of the fault in the Susitna lowland (Detterman et al, 1974, 1976). It is noted that a recent earthquake (14 August 1984) having M = 5.4 was shown by Lahr et al (1985) to be directly associated with the Castle Mountain fault.

Although there is no documented evidence for displacement along the Castle Mountain fault during historical time, the maximum earthquake magnitude may be estimated from available seismological and geological data. A magnitude M_S=7.0 earthquake occurred in the vicinity of the Castle Mountain

fault west of Anchorage in 1933. Due to poor accuracy in epicenter location at that time, it is not known if the earthquake was related to the Castle Mountain fault and no investigations of surface displacement were reported (Page and Lahr, 1971). Thus, the available seismological data constrain the magnitude of the largest historical earthquake that could have been associated with the Castle Mountain fault to magnitude M_S=7.0.

The available geologic and seismological data provide a basis for constraining the estimate of the maximum earthquake magnitude through the use of various empirical relationships that have been developed between fault characteristics and earthquake magnitude. The maximum earthquake magnitude for the Castle Mountain fault is estimated by considering its maximum surface rupture length, total length, fault area, and displacement per event. The total length of the Castle Mountain fault is about 475 km and evidence for Holocene displacement is present along about 80 km of its length across the Susitna lowland (Evans et al, 1972). The maximum strike-slip displacement of Holocene deposits has been reported as 2.4 m (Bruhn, 1979) and 7 m (Detterman et al, 1974).

On the basis of these parameters and empirical relationships, the maximum earthquake magnitude for the fault is judged to be 7-1/2.

Based on the displacement and estimated ages of the displaced deposits reported by Detterman et al (1974) and Bruhn (1979), Woodward-Clyde Consultants (1982a) estimated the rate of strike-slip displacement on the Castle Mountain fault to be from 1.3 to 10 mm/year. Assuming an average slip rate of about 5 mm/year, the average recurrence

interval for a magnitude M_S=7-1/2 (maximum earthquake) was estimated to be about 235 years on the Castle Mountain fault (Woodward-Clyde Consultants, 1982a). The recurrence relationship for the Castle Mountain fault used in this study is shown in Figure A-2.

A.1.2 Border Ranges Fault

MacKevett and Plafker (1974) mapped the Border Ranges fault as a north-dipping reverse fault that juxtaposes upper Paleozoic and lower Mesozoic rocks on the north over upper Mesozoic and Tertiary rocks on the south. They reported that the fault can be traced for more than 1,000 km northeast from Kodiak Island, across the Kenai Peninsula, along the northeast and northern front of the Chugach Mountains and eastward to the St. Elias Mountains (Figure A-1).

The Border Ranges fault is interpreted to be an ancient subduction zone that developed near the close of the Mesozoic time or in early Tertiary time (MacKevett and Plafker, 1974). Tectonic activity of the Border Ranges fault diminished since the Mesozoic as crust accreted to the continent and the active subduction zone migrated southeastward to its present location in the Aleutian trench. Magoon et al (1976) have mapped the fault's main trace in the northeastern part of the Anchorage area. The location of the fault for this study was based on recent studies by Updike (1985).

In the Kenai Peninsula and Anchorage areas, the Border Ranges fault is largely covered by surficial deposits and its location is not well defined. MacKevett and Plafker (1974) and Magoon et al (1976) have mapped the Kenai Mountains adjacent to the Kenai lowlands as the lower plate on the southeast side of the Border Ranges fault. However,

the fault has not been specifically identified in the Kenai lowlands. The northwest front of the Kenai Mountains forms an abrupt topographic lineament that extends from northeast of Anchorage nearly the length of the Kenai Peninsula. This lineament has been interpreted to coincide with the Border Ranges fault and the striking linearity and pronounced geomorphic expression of this feature is suggestive of late Cenozoic activity. However, no displacements of Quaternary sediments along the trace of the Border Ranges fault are reported in the literature, although no detailed investigations have been made of the Border Ranges fault's activity or earthquake potential.

Studies of the microseismicity in the southern Kenai Peninsula area show a diffuse zone of seismicity along the Border Ranges fault. However, no well-defined spatial association between the microseismicity and the Border Ranges fault has been established (Woodward-Clyde Consultants, 1981).

Among inconclusive geomorphic and seismological evidence that is suggestive of more recent activity, geologic mapping in the southern Kenai Peninsula by John Kelley (1981) also suggests a reactivation by more youthful faulting along a portion of the ancient Border Ranges suture zone. Such a reactivation would be consistent with the faulted basin margins and fore-arc tectonic model of the area as presented by Dickinson and Seeley (1979). If the Border Ranges fault has been reactivated, it may be analogous to the Castle Mountain-Bruin Bay system bounding the northwest side of Cook Inlet.

The geologic studies being conducted to the northeast of Anchorage by Updike and Ulery (1983) have provided evidence

for probable Holocene displacement on a fault closely associated with the Border Ranges and Eagle River faults. The field relationships for this fault (the Twin Peaks fault) suggest normal faulting along a northwest-dipping fault. So far, the studies have not been able to confirm regional continuity of the normal fault with either the Border Ranges fault or the Eagle River fault, but they do suggest the presence of youthful faulting northeast of the Anchorage area. It is not clear how normal faulting along the northeasterly trend of the Border Ranges fault would fit into the regional tectonic framework. Continuing studies may provide more definitive evidence concerning the extent and nature of this youthful faulting.

At present, few data are available to assess the earthquake potential of the Border Ranges fault and the available evidence does not appear to be conclusive. Because of the large uncertainty in the recency of displacement, the Border Ranges fault is conservatively assumed for this analysis to be capable of generating significant earthquakes.

Adequate data are also not available to definitely estimate the maximum earthquake magnitude on the fault. However, if it is hypothesized that the Border Ranges fault is part of the same tectonic system as the Castle Mountain fault, then a similar maximum magnitude may be considered. Based on the assumption that the Border Ranges fault is active, a conservative maximum earthquake magnitude of M_S=7-1/2 is estimated for the fault.

Earthquake recurrence is also conservatively estimated in this analysis due to the lack of adequate seismic or geologic data. As discussed previously, late Quaternary displacements have not been reported along the Border Ranges

fault. The Holocene deposits that are displaced in the area studied by Updike (1984) to the northeast of the site may be several thousand to as young as several hundred years old. If these displacements are conservatively assumed to be along the Border Ranges fault, then the recurrence interval for the fault is estimated for the present study to be approximately 500 years. In our judgement, the apparent lack of Holocene displacement along the major portion of the Border Ranges fault indicates that 500 years is a very conservative recurrence interval estimate. We have selected this recurrence interval for the maximum earthquake for the purpose of evaluating the seismic ground motions in the Anchorage area. The recurrence relationship used for the Border Ranges fault used in this study is presented in Figure A-2.

A.1.3 Eagle River Fault

The Eagle River fault (Figure A-1), like the Border Ranges fault, is an ancient Mesozoic, north-dipping thrust fault. The very sinuous trace of the Eagle River fault seen in Figure A-1 results from its generally shallow northward dip. No evidence for Quaternary activity along the fault has been reported in the literature. Unlike the Border Ranges fault, the Eagle River fault does not have a marked geomorphic expression. This suggests that the fault has not been active during at least Holocene time and probably during late Quaternary time. The Eagle River fault also does not appear to have a clear spatial association with microseismicity (Woodward-Clyde Consultants, 1981).

However, because of its fault length (>100 km), close association with the Border Ranges fault, and the present active tectonic setting of the region, considerable uncertainty exists regarding the activity of the Eagle River

fault. The observations presented above suggest that the fault is not active and should not be considered a potential seismic source. The proximity of the Eagle River fault to the Border Ranges fault and the similarity in the sense of displacement suggest that if the Eagle River fault were active within the present tectonic regime, its role may be similar to that assumed for the Border Ranges fault. Therefore, for the purposes of the probabilistic seismic hazard analysis, the Eagle River and Border Ranges faults are considered to be part of the same fault zone. For conservatism, the closest approach, maximum earthquake magnitude and recurrence for this fault zone are assumed to be those of the Border Ranges fault.

A.2 Subduction Zone Seismic Sources

Seismic sources within the subduction zone are defined using the seismicity of the subduction zone. Figure A-3 shows a plot of seismicity for the period October 1971 through March 1982 (Lahr and Stevens, 1982), and the location of the cross-sectional profile normal to the subduction zone shown in Figure A-4. The location of the plate interface, interpreted from the seismicity, is shown in Figure A-4. The subduction zone shown in Figure A-4 contains at least two distinct seismic regions. The shallow region of the plate interface, which has a shallow dip, is characterized by the periodic occurrence of great earthquakes. This region is termed the megathrust zone in this report. At greater depths, the more steeply dipping region of the plate interface is aseismic. However, earthquakes having moderate magnitudes occur randomly in time within the deeper portion of the subducted slab. This region is termed the Benioff zone.

The transition between the megathrust zone and the Benioff zone has not been clearly delineated in most subduction zones. Davies and House (1979) propose three criteria for choosing the boundary between the two zones. Thes criteria are the presence of a bend in the subducted plate, the transition of earthquakes mechanisms from interplate to intraplate, and the change from periodic great earthquakes on the megathrust to the uniform seismicity of the Benioff zone.

The change in bend in the subducted plate is indicated in Figure A-4. It appears that the transition in earthquake mechanisms and seismicity is not confined to this location, but is distributed over an interval of the subducting plate that extends updip. This interval is termed the transition zone, and its updip boundary is delineated by the inferred limit of rupture of the 1964 earthquake. The seismicity of the transition zone may consist of components of both interplate faulting on the plate interface and intraplate faulting within the subducted plate, corresponding to the characteristics of the megathrust and Benioff zones, respectively. The three source regions (megathrust, transition, and Benioff) within the subduction zone are shown schematically in Figure A-5.

Megathrust Zone

The subduction zone in south-central Alaska was ruptured by an earthquake of energy magnitude M_w 9.2 in 1964. This earthquake is the second largest earthquake that has been known to occur, and its size is close to the maximum earthquake for this subduction zone.

The maximum magnitudes of megathrust earthquakes are most reliably estimated from upper bound estimates of fault

rupture area. Using the relationship of Abe (1975) between seismic moment and rupture area, and relating seismic moment and M_W using the relation of Hanks and Kanamori (1979), we obtain the relation:

$$M_W = \log A + 4$$

where A is the fault rupture area in km^2.

This relation between rupture area and magnitude provides a magnitude estimate for the 1964 earthquake that is close to the observed value. The length of the zone that ruptured (measured along the Alaska trench axis) is approximately 750 km (Sykes and Quittmeyer, 1981). The width that ruptured (measured in the downdip direction) has been variously estimated from 200 km (Sykes and Quittmeyer, 1981) to 360 km (Davies and House, 1979). The width of the aftershock zone (Page, 1968) appears to increase from approximately 200 km in the southwest to approximately 350 km in the northwest. Beneath Anchorage, the width of the shallow megathrust zone appears to be 240 km (Figure A-4), which we take to be an average estimate of the width of the shallow megathrust in Alaska. Using the relation between fault area and magnitude, we estimate a magnitude of 9.3, which agrees well with the observed value of 9.2 (Kanamori, 1977).

In order to estimate the maximum magnitude on the megathrust, we allow the dimensions of the rupture zone to increase to maximum plausible values. Allowing the rupture to extend into the transition zone gives a fault width of 330 km (Figure A-4) and a magnitude of 9.4. Based on this result, a magnitude of 9.5 is judged to be a reasonable estimate for the largest megathrust earthquakes in Alaska. There is only one global precedent for an earthquake of this magnitude, which is the 1960 Chile earthquake.

The Alaska-Aleutian subduction zone experiences a high rate of seismic activity, as indicated by its seismicity during the past century (Figure A-6). This figure shows events of magnitude 7.4 and greater, and is believed to be complete above this magnitude for the period since 1900. All of these events are assumed to have occurred on the megathrust zone. A recurrence relation derived from these events is shown in Figure A-7. Recurrence is expressed as the number of events exceeding a given magnitude per 100 years per 1,000 km^2 of ground surface area.

The recurrence relation shown in Figure A-7 has the form of the Gutenberg-Richter relationship:

$$\log_{10} N(M) = a - bM$$

where N(M) is the number of events in a given time interval with magnitude greater than M, and a and b are constrants. A relation of this form appears to be an acceptable fit to the seismicity data for the entire Alaska-Aleutian megathrust zone, as shown in Figure A-7. Davison and Scholz (1985) also found that the seismicity of the entire Alaskan-Aleutian megathrust zone for the period 1899-1984 is consistent with a Gutenberg-Richter recurrence relation.

This consistency with the b-value recurrence model is not observed in the historical seismicity, however, if segments of the megathrust (eg, the Alaska zone that ruptured in 1964) are examined (Davison and Scholz, 1985). The observed recurrence relations for segments are found to be consistent with the characteristic earthquake model in whch the slip on a fault is dominated by large events (eg, Wesnousky et al, 1983). In this model, the recurrence of large events is underestimated if the recurrence of smaller events is

extrapolated to larger magnitudes using the b-value model. Conversely, the recurrence of smaller events is overestimated if the recurrence of larger events is extrapolated to smaller magnitudes using the b-value model.

In a probabilistic seismic hazard analysis, the use of a characteristic earthquake recurrence model generally results in lower estimates of seismic hazard. Accordingly, it would not be appropriate to use the characteristic model unless it were strongly supported by empirical data. There are several aspects relating to earthquake recurrence in the Alaskan subduction zone that suggest caution. First, the period of observation of seismicity does not span a complete seismic cycle, whereas ideally we need observation of several cycles in order to have confidence in our interpretation. This limitation in seismicity data may be partly overcome by examining the behavior of subduction zones in a global sense, and then applying common recurrence characteristics of subduction zones to the Alaska zone. Until the past few years, it was widely believed that a characteristic earthquake recurrence model generally holds in subduction zones. According to this model, each segment of a subduction zone experiences repeated occurrence of large earthquakes having approximately equal sizes and recurrence intervals. However, in the past few years, several examples have been identified in which this model did not hold. The most recent of these is the M_w 7.9 earthquake of May 1986 which occurred in the central Aleutian arc. It occurred on part of the rupture zone of the much larger (M_w 9.1) earthquake of 1957. According to the characteristic recurrence model, no large earthquakes would be expected on this zone for several centuries until the repeat of the very large 1957 event. To the extent that the Alaskan and Aleutian arcs are contiguous, it seems

prudent to allow for the possibility of a similar kind of earthquake recurrence in the Alaskan subduction zone. This may be accomplished by using the b-value recurrence model of Figure A-7 rather than the chracteristic recurrence model. Recurrence may not be precisely described by the b-value model, but this model provides a convenient representation in the absence of more detailed information.

Benioff Zone

The maximum magnitude of the Benioff zone is estimated to be M_W 7.5, based on a study of global Benioff zone seismicity (Woodward-Clyde Consultants, 1982a).

The seismicity of the Benioff zone beneath lower Cook Inlet during the past 80 years is shown in Figure A-8. In contrast to the seismicity of the megathrust zone, the Benioff zone is characterized by earthquakes that occur randomly in time. There is not indication that these earthquakes have characteristic sizes, and their recurrence is well described by the b-value model. A recurrence relation based on this seismicity is shown in Figure A-7. The relation is defined in the magnitude range 5 to 7.5, and is expressed as the number of events exceeding a given magnitude per 100 years per 1,000 km^2 of ground surface area.

Transition Zone

The transition zone is the region that lies between the megathrust zone and the Benioff zone (Figures A-4 and A-5). In south central Alaska, it has a width of about 100 km and underlies lower Cook Inlet and the Kenai Peninsula. Beneath Anchorage, it is about 30 km deep and is the region of the subduction zone that is closest to Anchorage.

The seismicity characteristics of the transition zone are currently not well understood. It can be seen from Figure A-4 that in Alaska, the transition zone experiences intraplate earthquakes that appear to be a shallow continuation of the Benioff zone. However, it is not known whether the transition zone also experiences interplate earthquakes on the down-dip continuation of the megathrust zone.

In other subduction zones, large interplate earthquakes have occurred in the transition zone. A well-studied example is the M_w 7.5 Miyagi-oki earthquake (Seno et al, 1980; Kawakatsu and Seno, 1983). Earthquakes of this kind appear to occur about every 40 years in the region of Miyagi-oki. In the Alaskan-Aleutian subduction zone, the M_s 7.5 earthquake of 1948 beneath the Shumagin Islands (Figure 5-6) may have occurred on the transition zone, based on its landward location and greater depth compared with the megathrust zone seismicity. Also, the M = 7.3 earthquake of 1903 beneath Shelikoff Strait (Figure A-8) may have occurred in the transition zone.

Based on these observations, it seems appropriate to take the seismic potential of the transition zone into account. The intraplate seismicity of the transition zone could be represented by extending the Benioff zone to include the transition zone.

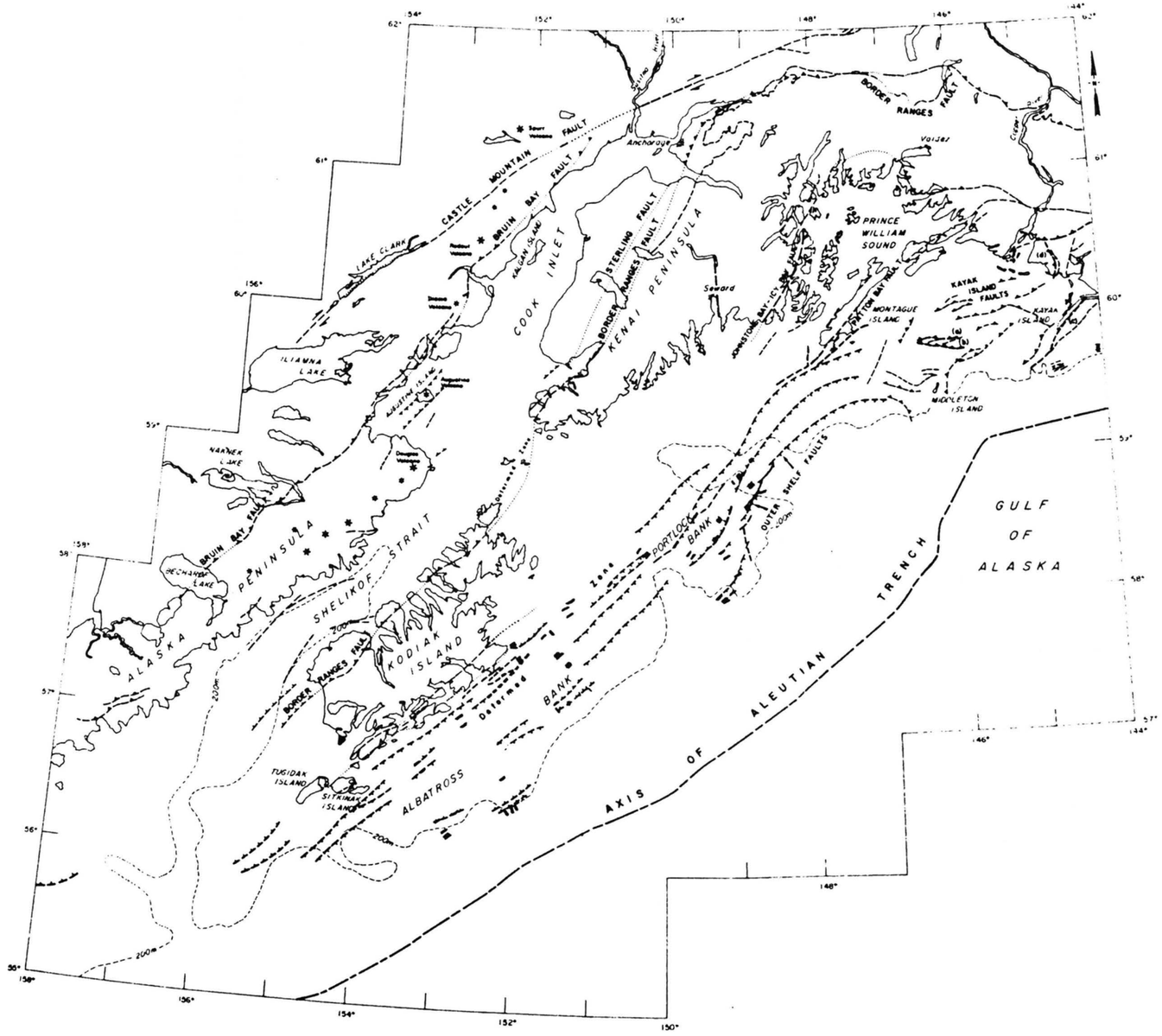

EXPLANATION

Active Faults

- Fault, dashed where approximately located, dotted where concealed or questionable. Hachures indicate relatively down dropped side of fault.
- Thrust Fault, dashed where approximately located, dotted where concealed or questionable. Barbs indicate relatively upthrown side of fault.
- Strike-Slip Fault, dashed where approximately located, dotted where concealed or questionable. Arrows indicate relative displacement.
- Submarine surface fault or scarp recognized from geophysical data. Hachures on downthrown side of fault.
- Lineament, inferred for this study to be an earthquake-producing structure.

Inactive Faults

- Fault, dashed where approximately located, dotted where concealed or questionable. Hachures indicate relatively down dropped side of fault.
- Thrust Fault, dashed where approximately located, dotted where concealed or questionable. Barbs indicate relatively upthrown side of fault.
- Strike-Slip Fault, dashed where approximately located, dotted where concealed or questionable. Arrows indicate relative displacement.
- Submarine surface fault or scarp recognized from geophysical data. Hachures on downthrown side

* Volcanic Centers
Quaternary volcanic center, vent or zone.

Line of cross-section.

NOTES:

Active Fault – A subaerial or submarine fault that breaks or is inferred to break Holocene or unconsolidated sediments (Holocene young but without any age determination) or is submarine fault is exposed on the sea floor.

Inactive Fault – A subaerial or submarine fault that does not break Holocene nor unconsolidated sediments (Holocene young but without any age determination) nor is it exposed on the sea floor.

Base Map Compiled from World Aeronautical Charts.

25 0 25 50 Nautical Miles
25 0 25 50 100 Kilometers
25 0 25 50 Statute Miles

Woodward-Clyde Consultants

REGIONAL SEISMIC SOURCE MAP

Project No. 41966A

GROUND FAILURE POTENTIAL
ANCHORAGE, ALASKA

Fig. A-1

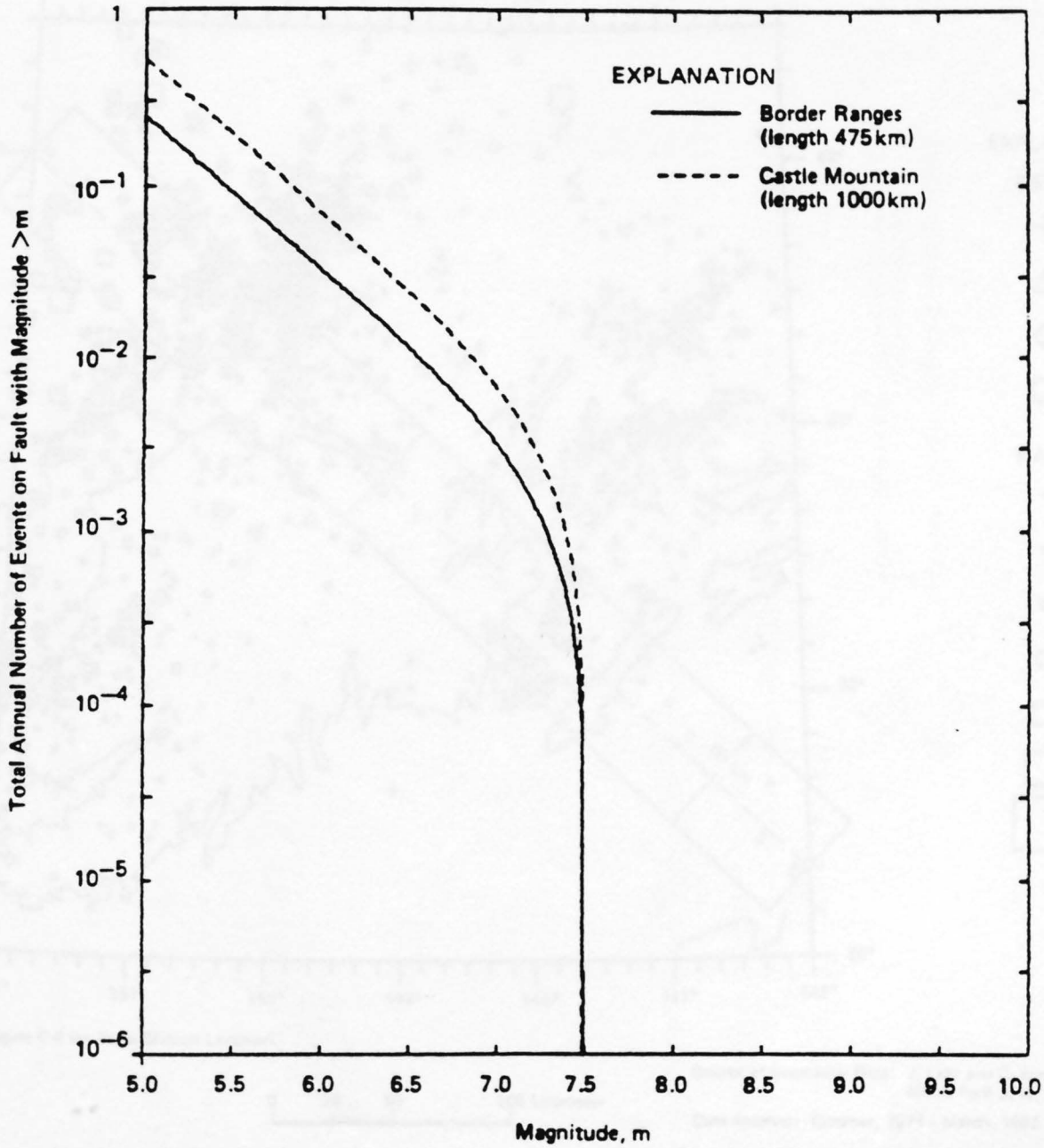

Project GROUND FAILURE POTENTIAL ANCHORAGE, ALASKA Project No. 41966A	RECURRENCE RELATIONSHIPS FOR CRUSTAL FAULTS	Fig. A-2

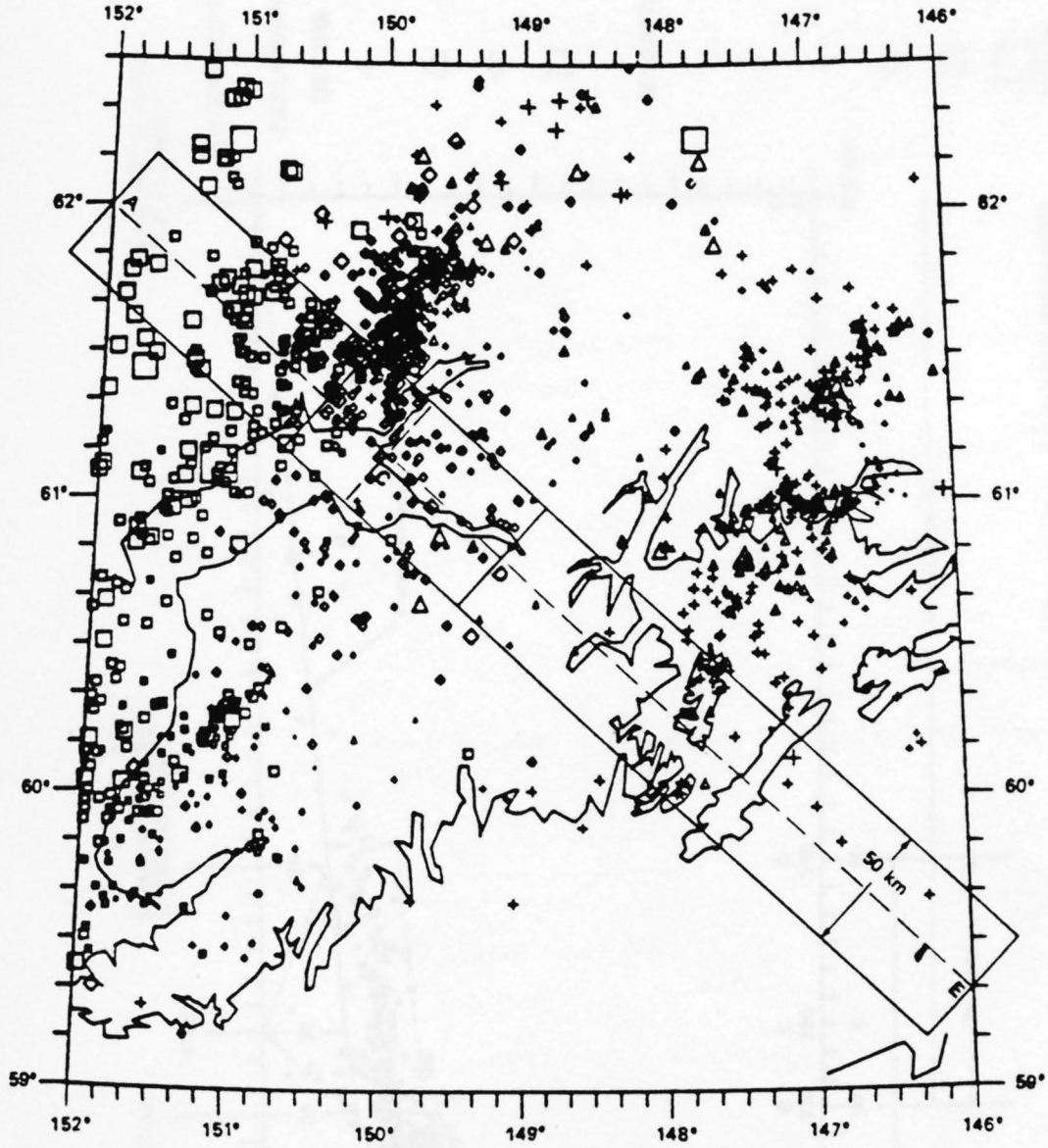

EXPLANATION

DEPTHS

+ 0.0+

△ 22.0+

◇ 32.0+

□ 50.0+

MAGNITUDES

. 0.0+

• 1.0+

▫ 2.0+

□ 3.0+

□ 4.0+

□ 5.0+

□ 6.0+

See Figure C-4 for Cross Section Location.

0 25 50 100 kilometer

Source of Seismicity Data: J. Lahr and C. Stevens USGS, Menlo Park June, 1982

Data Interval: October, 1971 - March, 1982 (incomplete)

Project GROUND FAILURE POTENTIAL ANCHORAGE, ALASKA Project No. 41966A	LOCATION MAP FOR SUBDUCTION ZONE CROSS SECTION	Fig. A-3

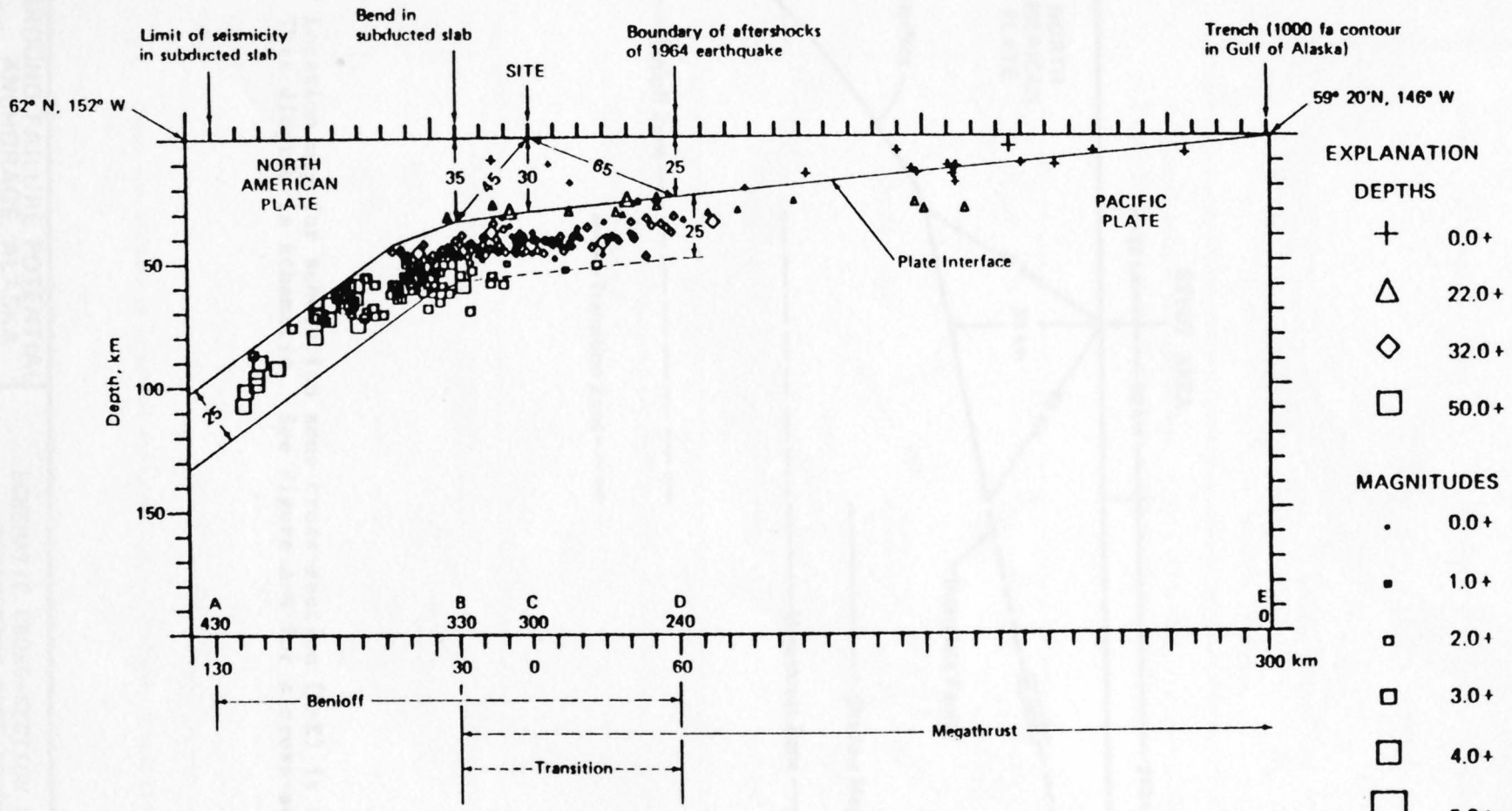

Note: All distances in km
No vertical exaggeration
See Figure C-3 for map view

Source of Seismicity Data: J. Lahr and C. Stevens USGS, Menlo Park June, 1982

Data Interval: October, 1971 - March, 1982 (incomplete)

Project: GROUND FAILURE POTENTIAL ANCHORAGE, ALASKA	CROSS SECTIONAL GEOMETRY OF SUBDUCTION ZONE SOURCES	Fig. A-4
Project No. 41966A		

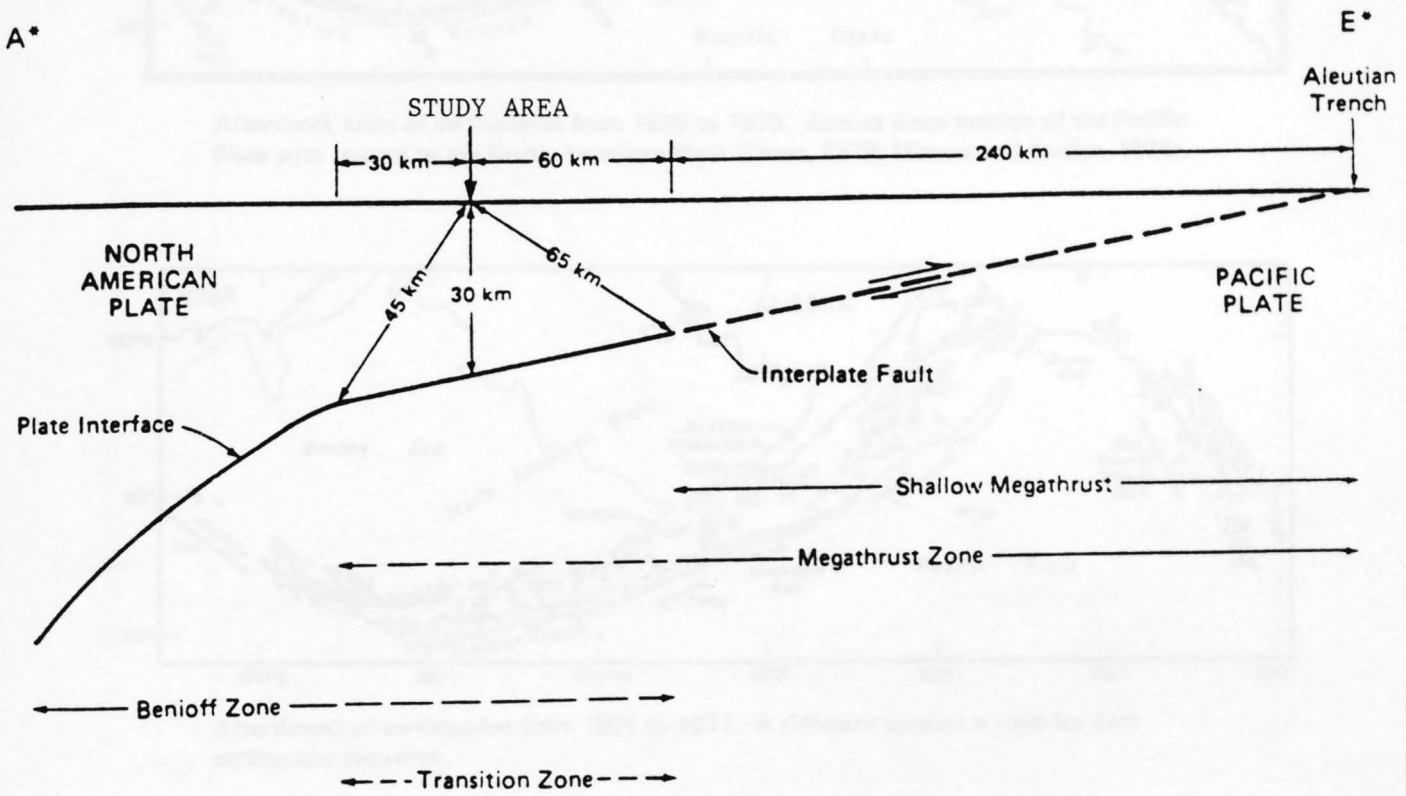

* Location map for subduction zone cross-section (A-E) is shown in Figure A-3. This diagram is schematic. See Figure A-4 for a cross-section drawn to scale.

Project GROUND FAILURE POTENTIAL ANCHORAGE, ALASKA Project No. 41966A	SCHEMATIC CROSS-SECTION SHOWING SUBDUCTION ZONE SOURCES	Fig. A-5

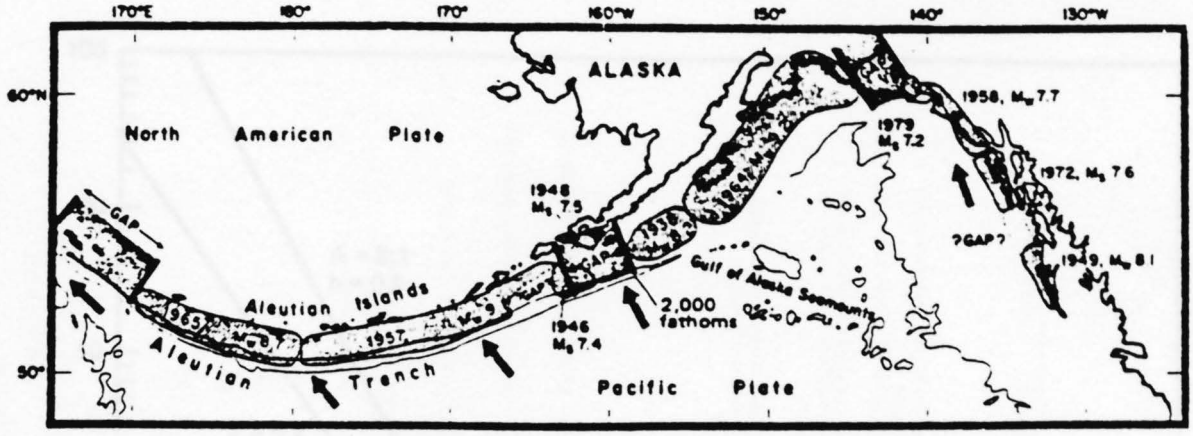

Aftershock areas of earthquakes from 1938 to 1979. Arrows show motion of the Pacific Plate with respect to the North American Plate (Chase, 1978; Minster and Jordan, 1978).

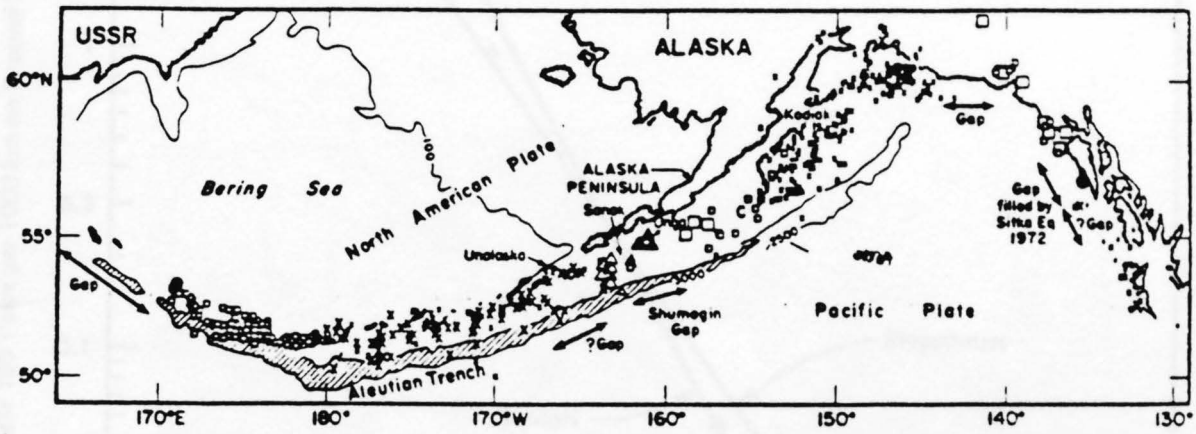

Aftershocks of earthquakes from 1925 to 1971. A different symbol is used for each earthquake sequence.

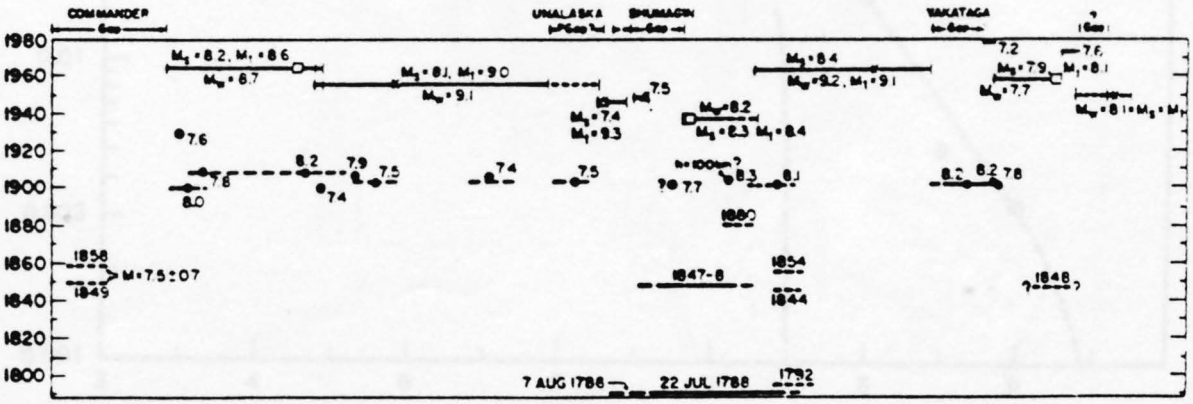

Space-time diagram of epicenters and lengths of rupture zones, shown dashed where less certain.

After Davies et al, 1981

Project GROUND FAILURE POTENTIAL ANCHORAGE, ALASKA Project No. 41966A	RUPTURE ZONES OF MAGNITUDE 7.4 AND GREATER EARTHQUAKES IN THE ALASKAN AND ALEUTIAN SUBDUCTION ZONE	Fig. A-6

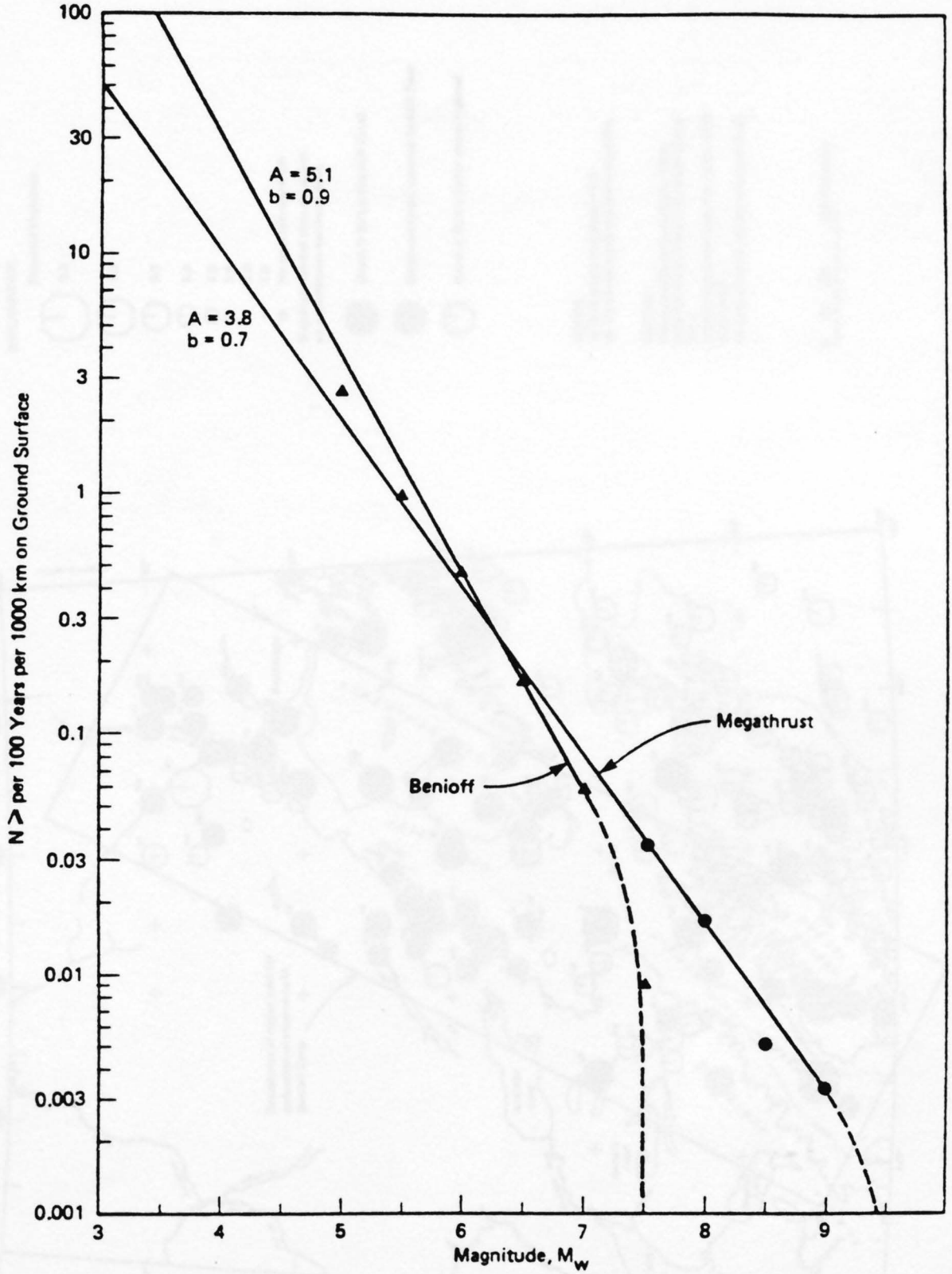

Project GROUND FAILURE POTENTIAL ANCHORAGE, ALASKA Project No. 41966A	EARTHQUAKE RECURRENCE RELATIONS FOR SUBDUCTION ZONE SOURCES	Fig. A-7

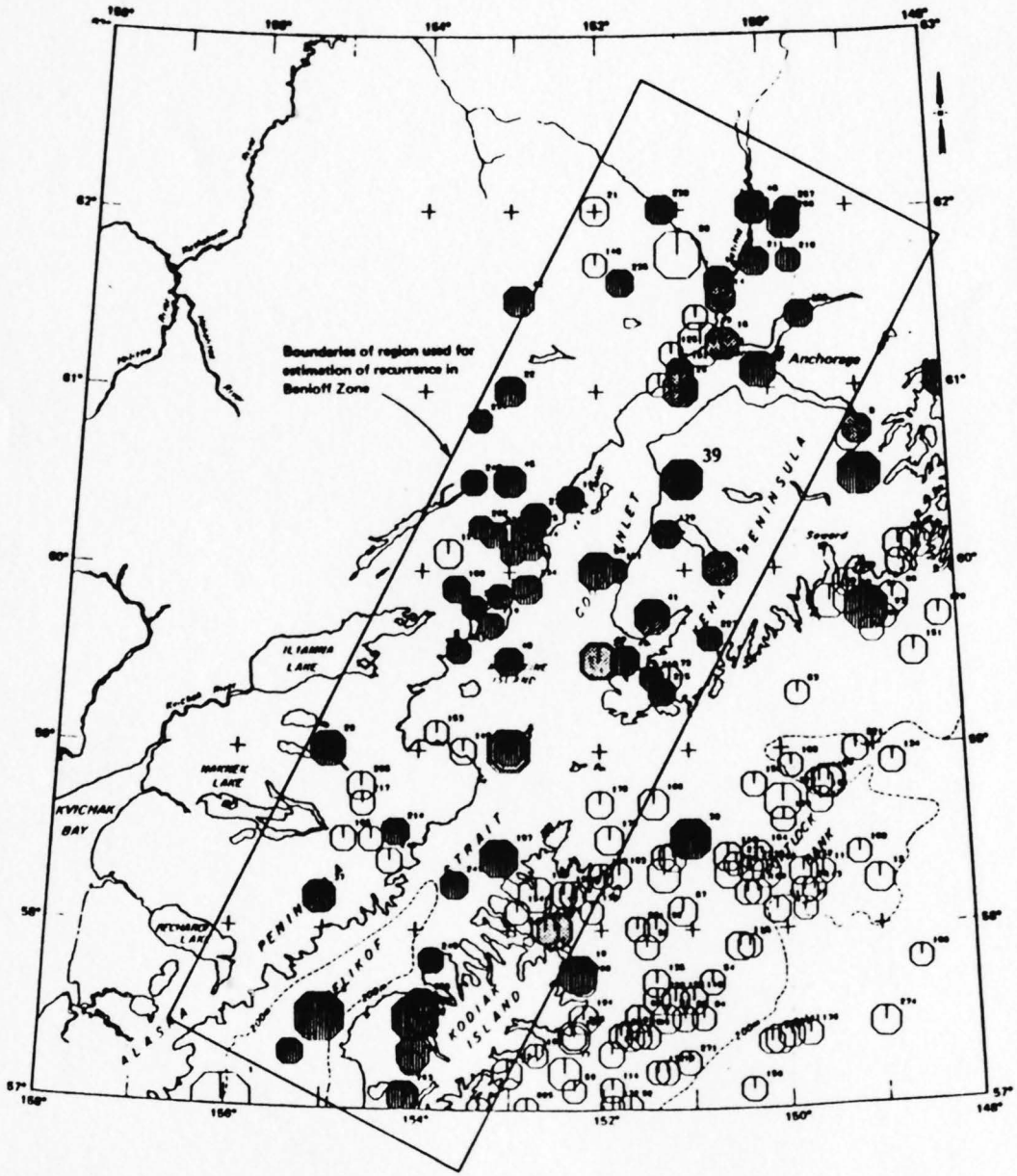

EXPLANATION

Reported Magnitude

8.0

7.0

6.0

5.0

4.0

3.0

2.0

1.0

No reported magnitude

Magnitude symbol sizes are shown on a continuous nonlinear scale.

Depth > 50 km (Benioff Zone)

Depth not know, assumed Benioff Zone

Depth < 50 km (other source regions)

NOTES:

1) Minimum magnitude = 5.0
2) Events are numbered chronologically.

SOURCE:

Woodward-Clyde Consultants, 1978, Offshore Alaska Seismic Exposure Study, Vol. I

NOAA Hypocenter Data File, 1638–1975.

BASE MAP:

Compiled from World Aeronautical Charts.

0 25 50 100 kilometers

Project: Project No.	GROUND FAILURE POTENTIAL ANCHORAGE, ALASKA 41966A	HISTORICAL SEISMICITY OF THE BENIOFF ZONE BENEATH LOWER COOK INLET, 1903 - 1975	Fig. A-8

APPENDIX B

GEOLOGICAL CROSS-SECTIONS

APPENDIX B
GEOLOGICAL CROSS-SECTIONS

This appendix presents seven geological cross-sections in the study area and its vicinity. Figure B-1 shows the locations of these cross-sections: A-A', B-B', C-C', D-D', E-E', F-F', and G-G'. These cross-sections are shown in Plates B-1 through B-7. The facies shown in these cross-sections are discussed in Section 4.2 of the main text. Symbols from the Unified Classification System, such as SM, are also used in these cross-sections to identify various materials. In some cases the type of material, such as peat and silt, is spelled out. It is noted that the symbol "Ls" used in these cross-sections refers to landslide material. Figure B-2 shows the extent of cohesive facies of the Bootlegger Cove formation above sea level.

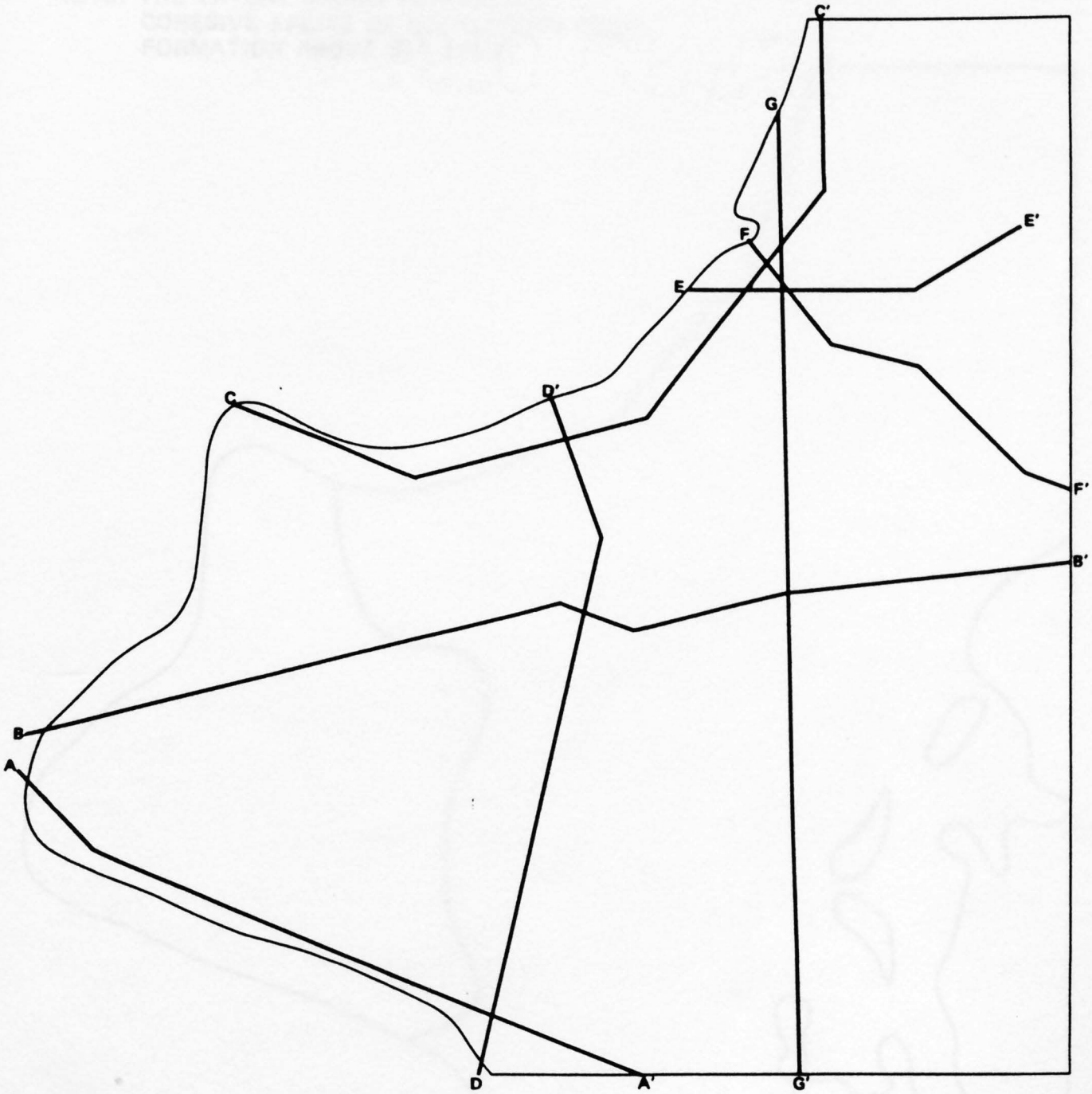

Project GROUND FAILURE POTENTIAL ANCHORAGE, ALASKA Project No. 41966A	LOCATIONS OF GEOLOGIC CROSS SECTIONS	Fig. B-1

NOTE: THE EXTENT SHOWN REPRESENTS
COHESIVE FACIES OF BOOTLEGGER COVE
FORMATION ABOVE SEA LEVEL

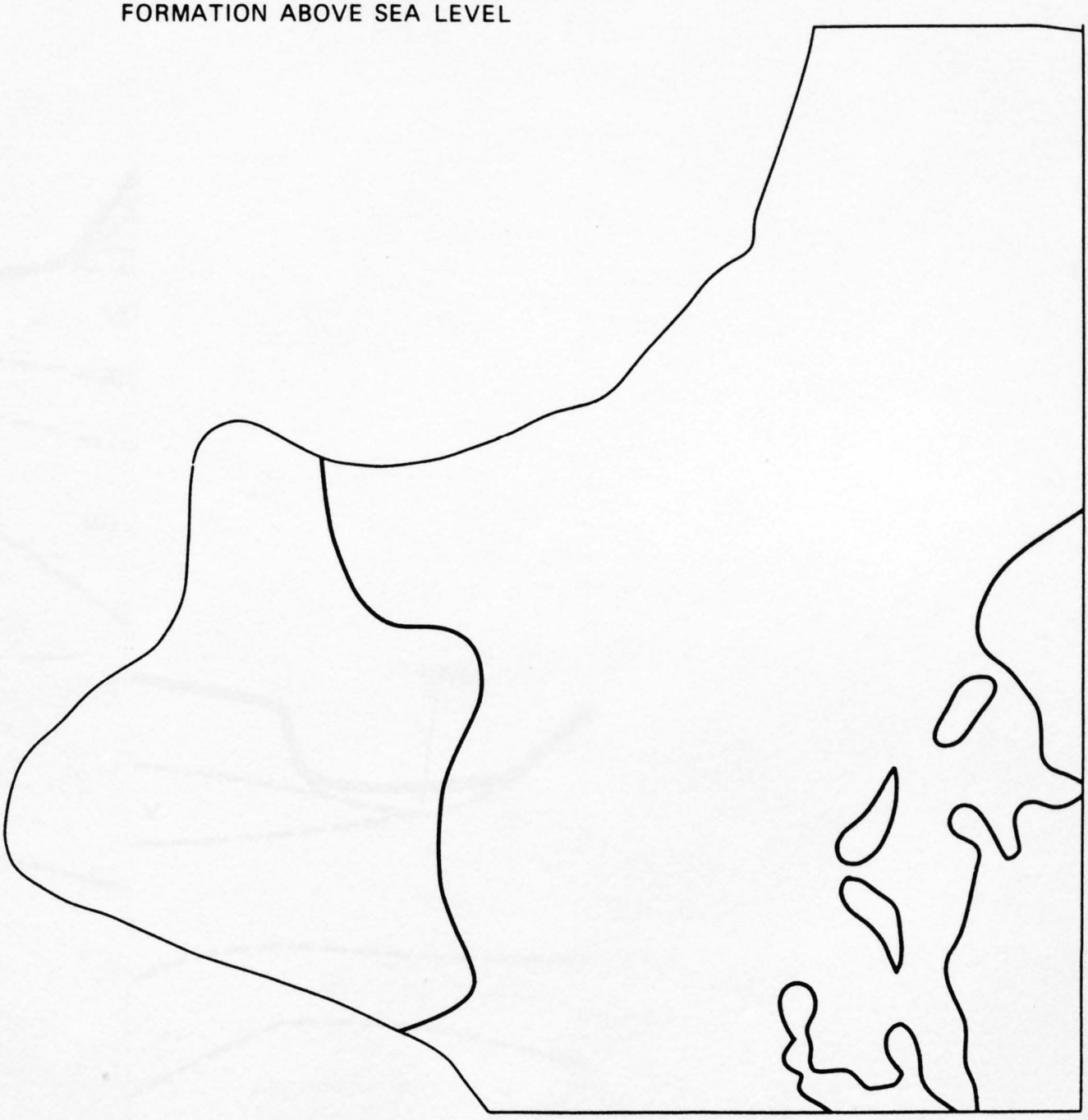

Project GROUND FAILURE POTENTIAL ANCHORAGE, ALASKA Project No. 41966A	APPROXIMATE EXTENT OF BOOTLEGGER COVE FORMATION	Fig. B-2